Quarterly Status Update

Project Title **Scientific evaluation and interpretation of baseline groundwater well testing data available for Alberta**	
Researcher:	**Mayer, Bernhard (University of Calgary)**
Project Technical Champion:	**James Armstrong (ENCANA)**
GL#:	**16-WIPC-01 and 17-WIPC-01**
Final report covering Q1 2016 to Q4 2017 (2 years)	

PTAC
Petroleum Technology
Alliance Canada
Suite 400, 500 Fifth Ave. S.W.
Calgary, Alberta T2P 3L5
phone: (403) 218-7700
fax: (403) 920-0054

Status and technical updates

Please provide brief description on milestones *(in italics)* achieved to date and recent results.

Executive Summary

In this project, the research team investigated three datasets comprising geochemical data for 95,556 water samples (see overview in Table 1). We had access to **data from industry** from five different companies that contained physico-chemical parameters (e.g. field parameters), major ions, some minor ions and trace element concentrations, and usually also microbial parameters and concentrations of selected organic compounds (e.g. BTEX). One industrial data source (D) contained also gas concentration data (i.e. methane and sometimes ethane). None of the industrial data sources reported carbon isotope analyses for methane or other alkanes in dissolved or free gas samples. In the **Alberta Health Services (AHS) database** we evaluated 78,952 different water samples, of which 67,590 are geographically referenced. The database contains physico-chemical parameters (e.g. field parameters), major ions, some minor ions and trace element concentrations, and microbial analyses, but no gas compositional or isotope data for dissolved or free gases. We also evaluated the **BWWT database** that contains physico-chemical parameters (e.g. field parameters), major ions, some minor ions and trace element concentrations, and some organic compounds and microbial analyses, as well as compositional and carbon isotope data for free gases for a subset of samples.

Table 1: Overview of the data sets available for evaluation and interpretation of groundwater well testing data.

Water samples data sources		Sampling time range	Pre-post test info	Coord.	Depth	N-aqueous	N-gas	Parameters					
								PC	M	m&T	O&B	G	I
	A-1	2001 to 2006	Yes	ATS DD	No	804 802*	0	☑	☑	☑	☑	☒	☒
Industrial sponsors	A-2	2001 to 2006	Yes	ATS DD	No	1321 1307*	0	☑	☑	☑	☑	☒	☒
	A-3	2013	No	ATS	No	17 17*	0	☑	☑	☑	☑	☒	☒
	B	2013 to 2015	No	DD ATS	No	16 15*	0	☑	☑	☑	☑	☒	☒
	C	2012 to 2016	No	ATS	No	189 183*	1	☑	☑	☑	☑	☒	☒
	D-1	2011 to 2015	No	ATS UTM	Yes	31 31*	31	☑	☑	☑	☑	☑	☒
	D-2	2012 to 2017	No	UTM	Yes	111 109*	108	☑	☑	☑	☑	☑	☒
	E-1	2013 to 2017	No	ATS DD	Yes	21 21*	0	☑	☑	☑	☑	☒	☒
	E-2	2013 to 2016	No	ATS DD	Yes	42 21*	0	☑	☑	☑	☑	☒	☒
AHS		2001 to 2015	No	ATS DD	Yes	78952 78316*	0	☑	☑	☑	☑	☒	☒
BWWT		2005 to 2014	Yes	ATS DD	Yes	14052 13583*	1698 787*	☑	☑	☑	☑	☑	☑

X* number of samples passing the QA/QC ± 10%
PC: *Physico-chemical parameters (field parameters)*
O& B: *Organic compounds and microbial analyses*
M: *Major ions*
m & T: *Minor ions and Trace elements*
I: *Isotopic analyses*
G: *Gas compounds*
ATS and DD: Alberta Township System and Decimal degree

Project achievements and milestones reached

A summary of all achievements for each milestone is provided in Table 2.

Milestones 1: QA/QC data quality check

For all available aqueous and gas samples a rigorous QA/QC procedure was applied. For aqueous geochemistry data, 2,506 samples of the industry database, 78,316 samples of the AHS database, and

13,583 samples of the BWWT database passed the QA/QC test. For gas geochemistry data, 139 samples from the industry database, and 787 samples from the BWWT database passed the QA/QC test. Only samples passing the QA/QC tests were further evaluated. Milestone 1 was fully achieved.

Milestones 2: Characterization of water types
Analysis of the predominant water types in the AHS, BWWT and industry data sets revealed that sodium-bicarbonate waters comprise the majority of all samples (>52%) followed by sodium-bicarbonate-sulfate waters (~11%). Other important water types include calcium-(magnesium-)bicarbonate waters (~14% of all samples) and Na-SO_4 type waters (<6 % of all samples). In-depth analysis revealed that the deepest groundwater wells are frequently associated with samples characterized by the Na-HCO_3 water type. No major differences were found in dominant water types between groundwater obtained from different geologic units. The three ubiquitous Na-rich water types, Na-HCO_3, Na-HCO_3-SO_4 and Na-SO_4, were dominant in all geologic units from the Belly River Group to the Paskapoo Formation. Milestone 2 was fully achieved.

Milestones 3: Occurrence of methane
The investigation of occurrence of methane in free gas samples is limited to the BWWT database, since the industry and AHS data do not contain information on free gases. QA/QC procedures resulted in 787 free gas samples that contain n-alkane geochemical information including methane concentrations (n= 787) and associated carbon isotope ratios (n= 517), ethane concentrations (n=364) and its carbon isotope ratios (n=253), and propane concentrations (n=106). The median concentrations of methane, ethane and propane were 543,300 (n= 787), 1,007 ppmv (n=364), and 100 ppmv (n=106), respectively. The highest concentrations of methane in free gas samples were observed in groundwaters belonging to Na-HCO_3, Na-HCO_3-Cl and NaCl water types. Sulfate-containing water types were typically characterized by much lower median methane concentrations of <150,000 ppm. The highest methane concentrations were observed in groundwater from the Horseshoe Canyon Formation. Milestone 3 has been reached and the task is fully completed.

Milestones 4: Groundwater redox states and methane occurrence
While investigating aqueous geochemistry trends in samples from the BWWT and some industry databases, it was observed that samples with elevated nitrate and high sulfate concentrations did usually not contain methane. In contrast, samples with negligible nitrate concentrations (<0.1 mM) and sulfate contents below a threshold of 1.0 mM frequently contained methane. This is consistent with the redox ladder concept that states that denitrification and bacterial sulfate reduction must occur first before methanogenic microorganism can generate biogenic methane in-situ in highly reducing aquifers. Using this concept, we developed a classification scheme that uses the results of aqueous geochemical analyses of groundwater samples to determine the redox state of the aquifer from which the groundwater was obtained. To test the accuracy of this approach, we applied the developed redox category concept to 762 groundwater samples of the BWWT database that also had free gas samples passing the QA/QC test. We found that 64% of the groundwater samples indicated a methanogenic groundwater and that 88% of these samples contained methane with elevated concentrations of >150,000 ppmv. Approximately 30% of the groundwater samples belonged to the sulfate reducing redox zone and 83% of these samples contained methane with less than 150,000 ppmv. Groundwater samples belonging to less reducing redox zones (denitrification, Mn-reduction) were usually not characterized by elevated methane concentrations. Hence, the developed methodology appears highly effective in predicting the occurrence of elevated methane in shallow aquifers based on aqueous geochemistry data alone. Using this approach for redox class assignment, we were able to predict that ~48% of the groundwater samples in the AHS database are likely favorable for methane occurrence in the aquifers. Milestone 4 has been reached and the task has been fully completed.

Milestones 5: Carbon isotope fingerprinting to assess methane sources
The investigation of carbon isotope ratios of methane and ethane was limited to the BWWT database, since the industry and AHS data do not contain information about carbon isotope ratios of gases. Methane and ethane in free gas samples had median $\delta^{13}C_{CH4}$ values of -67.3 ‰ (n = 518) and $\delta^{13}C_{CH4}$ values of -49.1 ‰ (n= 395) respectively. Carbon isotope ratios of propane were only determined for 20 samples with a median $\delta^{13}C_{CH4}$ value of -32.1 ‰ (n= 20). It was found that the majority of the methane-containing samples were characterized by $\delta^{13}C$ values of methane < -55 ‰ (n=447) while low to negligible concentrations of higher alkane chain components such as ethane resulted in high gas dryness values (D>500). This, together with water chemistry data indicating highly reducing conditions, is indicative of in-situ formation of biogenic methane in the sampled aquifers for the majority of the samples in the database. For

a smaller number of samples (n=71), methane with elevated $\delta^{13}C$ values of > -55‰ was identified. Some of these samples were characterized by low methane concentrations, which is consistent with the occurrence of methane oxidation. Other samples were characterized by high methane concentrations and elevated $\delta^{13}C$ values of methane suggesting either migration of thermogenic gas into shallow aquifers or "pseudo-thermogenic" gas samples. Milestone 5 has been reached and the task has been fully completed.

Table 2: Overview of milestones, achievements, challenges and tools developed to overcome challenges, and potential further steps.

Milestone	State-of art/achievements
1	**Task: QA/QC data quality check** **Achievement:** Complete **Challenges:** Identification of groundwater wells i.e. non-homogeneity + inaccurate coordinate systems to locate wells, no systematic GIC-ID of the wells, incomplete information such as depth, completion interval + presence of deep groundwater wells (> 300 m) + manual input challenges **Development of tools:** ATS -> DD coordinate system
2	**Task: Characterization of water types** **Achievement:** Complete **Challenges:** No geological information sometimes no depth information provided + no completion interval information to identify if wells are completed in single or mixed units **Development of tools:** PHO matrix to characterize >60,000 groundwater sample data Geospatial software GIS (geological assignment methods/ compilation of AGS data + challenges: layers not always available, geologic layers created from different well groupings, precision varies between sources); Parametric and non-parametric statistical tests (Mann-Whitney, ANOVA, t-test, Kruskal Wallis)
3	**Task: Occurrence of methane** **Achievement:** Complete **Challenges:** No methane concentration and/or isotope ratio information for some datasets **Development of tools:** Development of QA/QC procedure for gas data evaluation (free gas phase samples)
4	**Task**: **Groundwater redox states and methane occurrence** **Achievement:** Complete including tool for predicting methane occurrence **Challenges:** No methane concentration and/or isotope ratio information for some datasets; Lack of redox geochemical speciation characterization (pe) + incomplete redox sensitive species concentrations (i.e. dissolved O_2, Mn); LOQ values sometimes not reported (i.e. analytical precision) **Development of tools:** Geospatial software GIS (geological assignment methods/ compilation of AGS data); Parametric and non-parametric statistical tests (Mann-Whitney, ANOVA, t-test, Kruskal Wallis); Development of a redox category classification to identify redox state of groundwater; assign a redox state to the groundwater samples, evaluate the proportions of redox states in the aquifers, identify favorable redox zones for methane occurrence, predict the potential occurrence of methane in aquifers where gas data are not available.
5	**Task: Carbon isotope fingerprinting to assess methane sources** **Achievement:** Complete **Challenges:** No methane concentration and/or isotope ratio information for some datasets; **Development of tools:** Development of classification of categories differentiating biogenic, thermogenic and mixed gases, and methane occurrences affected by methane oxidation.
6	**Task: Data housing and display** **Achievement:** Complete: distribution of report to stakeholders (PTAC water committee); **Potential further steps:** Results can be made available to PTAC for data housing and display.
7	**Task: Communication of results** **Achievement:** Complete (proposal of simplified summary displays for information sharing) and ongoing (development of manuscripts for peer-reviewed publications). **Potential further steps:** After receiving feedback on the final report, we remain available for developing a communication plan for interested stakeholders.

Milestones 6: Data housing and display

It is important that the results of this study will be made accessible to the stakeholder community. We suggest to achieve this initially by distribution of this detailed report to the industrial stakeholders thereby

delivering on milestone 6. In addition, we are ready to make the data and results available to PTAC for data housing and display.

Milestones 7: Communication of results
The key deliverable of this project is the highly scientific assessment of baseline aqueous and gas geochemistry data for Alberta groundwater in areas of past, current and future hydrocarbon resource development that is summarized in this report. This scientific evaluation is complemented by a simplified summary scheme for water quality data interpretation that may be understandable to non-experts and the public at large. An example of a simplified summary of the redox ladder concept that could provide a guideline for well owners to interpret their water quality data with the occurrence of methane in mind is provided in this report. A further simplification could be a basic traffic light protocol that subdivides groundwater samples from methanogenic aquifers with high potential for occurrence of elevated concentrations of methane (red light) from groundwater samples obtained from aquifers with less reducing redox states and low risk of methane occurrence (green light). The orange traffic light would represent aquifer conditions with bacterial sulfate reduction representing groundwater samples where occurrence of methane predominantly with concentrations <150,000 ppmv in the free gas phase is feasible. After receiving feedback on the final report, we remain available for developing a communication plan for interested stakeholders in close consultation with the funding agency. In addition, we are in the process of developing manuscripts for publishing selected results in the peer-reviewed scientific literature after consultation and approval by the funding organization, thereby delivering on milestone 7.

Conclusions
The objective of this project was to compile, evaluate and interpret all available baseline groundwater testing data on aqueous and gas geochemical compositions across Alberta. The research team delivered a highly scientific assessment of baseline aqueous and gas geochemistry data for Alberta groundwater in areas of past, current and future hydrocarbon resource development. It was found that Alberta groundwater if frequently in a methanogenic redox state that allows for in-situ formation of biogenic methane that frequently occurs with concentrations >150,000 ppmv in the free gas phase. Groundwater samples belonging to the sulfate reducing redox zone contained frequently methane, but predominantly with concentrations of less than 150,000 ppmv. Groundwater samples belonging to less reducing redox zones (denitrification, Mn-reduction) were usually not characterized by elevated methane concentrations. Based on these observations we developed a methodology that appears highly effective in predicting the occurrence of elevated methane in shallow aquifers based on aqueous geochemistry data alone, suggesting that ~48% of the groundwater samples in the AHS database are likely favorable for methane occurrence in the aquifers. Isotopic fingerprinting data revealed that methane in the vast majority of samples is of biogenic origin, while only very few samples appeared consistent with a thermogenic origin of methane. The findings summarized in this report confirm the critical importance of thorough baseline groundwater testing approaches in areas of hydrocarbon resource development above and below the base of groundwater protection. Thorough baseline groundwater testing approaches are a key requirement for a scientifically accurate assessment of the impact of industrial developments on the quality of groundwater, or their lack thereof, especially in areas where natural biogenic methane is ubiquitous in shallow aquifers.

Authors of this report:
Pauline Humez, Leah Wilson, Michael Nightingale & Bernhard Mayer (2018), Applied Geochemistry group, Department of Geoscience, University of Calgary, Calgary, Alberta, Canada T2N 1N4

Corresponding Author: Bernhard Mayer: bmayer@ucalgary.ca or Tel. (403) 220 5389

Table of contents

1. Milestone 1: QA/QC data quality check (e.g. electroneutrality) to assess which results are acceptable for scientific evaluation: Data and methods

Combing the industry, AHS and BWWT databases yields access to geochemical analyses of **95,556** water samples. While some samples were derived from surface water bodies such as springs, rivers, lakes and creeks (n=2,940), the vast majority of samples are groundwater from primarily private and public water-supply wells completed in the shallow aquifers of the province of Alberta. The wells are not evenly distributed (see Fig. 1) with the highest well density in the southeastern part of Alberta. The depth of the wells from which groundwater was obtained is known for the data sources supplied by companies D and E (Fig. 1). The depth information for wells from sources A, B, and C was derived from http://groundwater.alberta.ca/WaterWells/d/ via access to water well drilling reports. However, the ATS coordinates provided by industry sources A, B and C do not permit to identify exactly the individual water well locations. The 7 digit GIC Well ID code would be required to exactly identify the water wells. The geologic formation or lithologic unit of the water-bearing zone is reported only for industry data supplied by company E through water well drilling reports that have been found through http://groundwater.alberta.ca/WaterWells/d/. All the other databases do not provide such information making it challenging to correlate the groundwater geochemistry with specific aquifer units. In Q3 of year 2 we developed two methods of geological formation assignments to overcome this problem and this progress is presented under Milestone 2.

For our evaluation of groundwater chemistry, only analyses that reported pH values and all of the following major dissolved constituents were considered: Ca, Mg, Na, K, HCO_3, CO_3, Cl and SO_4. Most of the provided analytical data also reported dissolved SiO_2, minor ions and trace elements. Using these data, the ionic charge balance as a QA/QC criterium was calculated accepting samples with ionic charge balance values (= electroneutrality) better than ± 10 %. Samples with a higher charge balance error were eliminated from further analysis and interpretation.

For the **industrial databases** between >75 % (data from company E) and >99 % (data from company A) passed the QA/QC electroneutrality test for aqueous geochemistry as follows:
>99 % of the water samples from source A,
>93 % of the water samples from source B,
>96 % of the samples from source C,
>99 % of the samples from source D,
>75 % of the samples from source E.

All industry-derived sample sets are geographically referenced, and sources A1 and A2 contain pre- and post-test sample pairs for aqueous geochemistry. However, depth information for the sampled water wells and gas data were only reported for data sources D and E with median depths ranging from 33.5 to 67.1 m (Fig. 1). Information submitted by company D provided the total depth of the water well (D-1 and D-2) and the screen interval (D-2). Information submitted by company E provided the total depth of the water wells and water well drilling reports associated with well IDs. This additional information includes formation logs and lithology description, a yield test summary, and well completion information. Gas concentration data were only supplied for samples from company D.

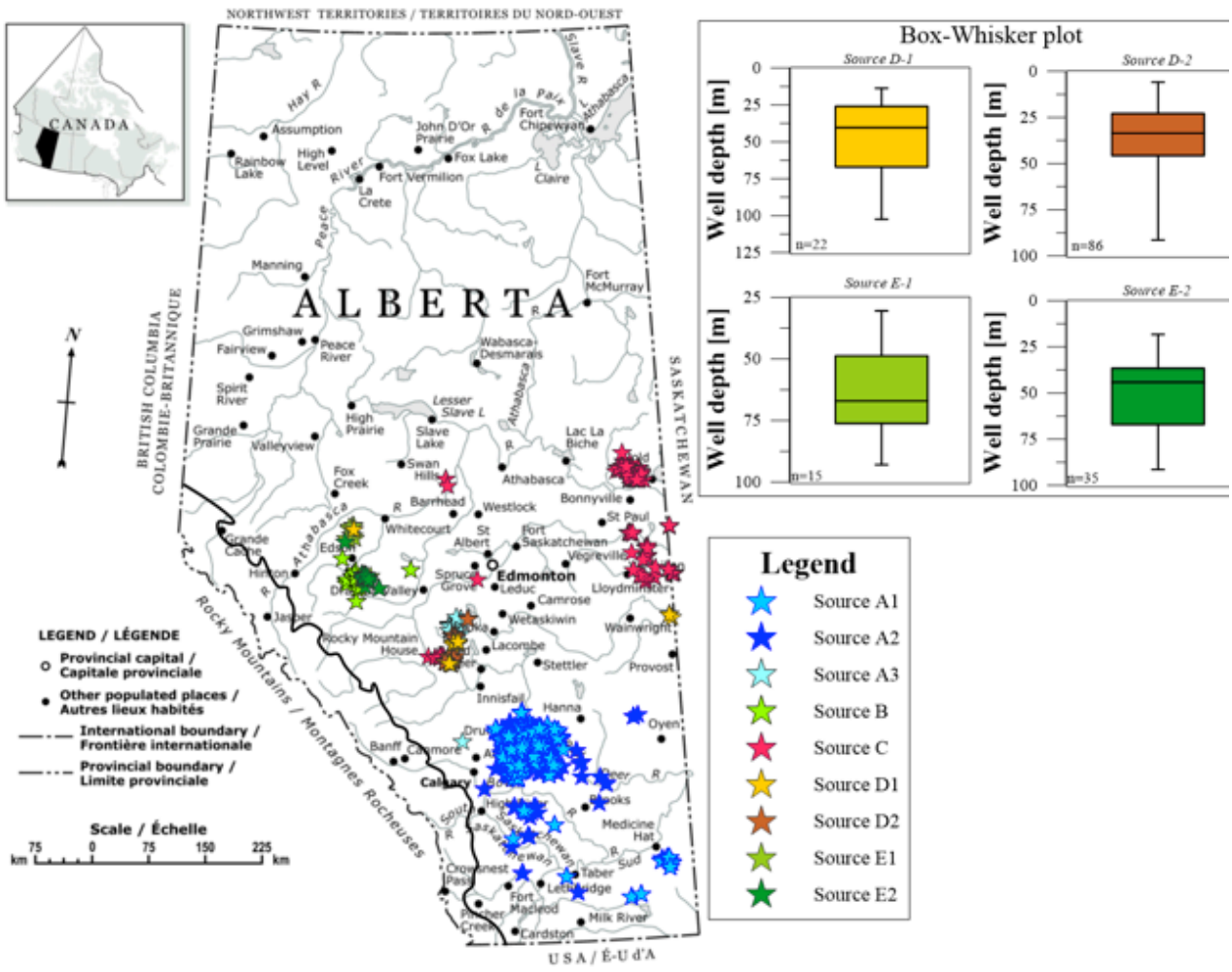

Figure 1: Location of water wells for which geochemical information was provided by five different companies and box and whisker plots showing median, Q1 and Q3 depths as well as shallowest and deepest wells for sources D and E (background map from: atlas.gc.ca).

For the AHS database, 99.2 % of the water samples passed the QA/QC electroneutrality test (n=78,316). The majority of these samples represent groundwater from water wells (n=74,978) with the remainder (n=3,338) representing surface water (springs, rivers, lakes, creeks, cisterns, dugouts, canals) or unknown samples. A total of 67,376 samples passing the aqueous geochemistry QA/QC test are geographically referenced and the well locations are shown in Fig. 2 and Table 3. Well depth information is available. However no gas data have been determined.

Table 3: Overview of type of samples from the AHS database (IB = ionic balance).

	All database			**All samples with location**		**Wells with location**			**Springs with location**		**Surface water with location**		**Unknown with location**	
	Bulk	IB 5%	QA/QC 10%	Bulk	QA/QC 10%	Bulk	QA/QC 10%	QA/QC 10%+ Depth	Bulk	QA/QC 10%	Bulk	QA/QC 10%	Bulk	QA/QC 10%
N	78952	77385	78316	67590	67376	66898	66694	60562	527	520	26	26	139	136
Ratio %		98.01	99.19		99.68		99.70	90.53		98.67		100.00		97.84

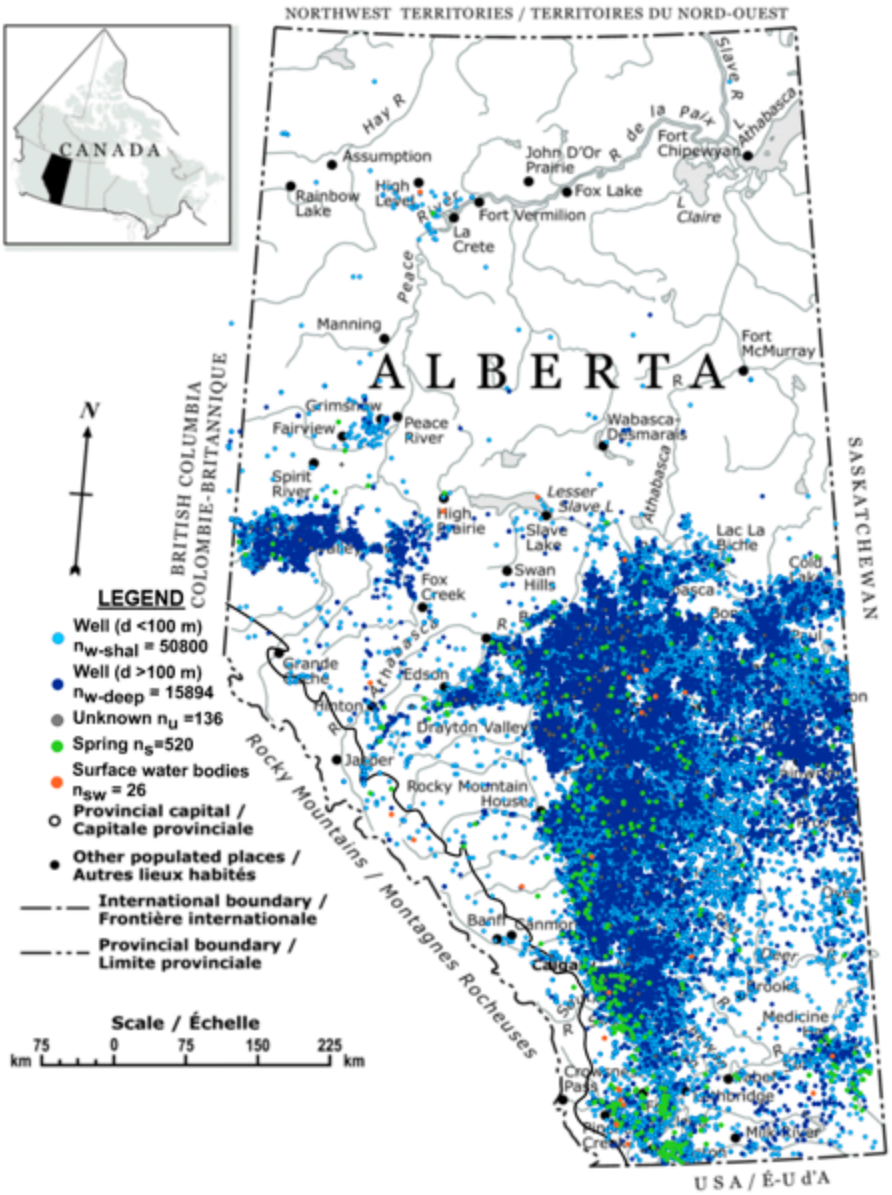

Figure 2: Location of sampling sites of water bodies reported in the AHS database categorized as water wells, springs, and surface water bodies (rivers, lakes, creeks, dugouts, cisterns, canals).

For the BWWT database, 96.6% of the samples passed the aqueous geochemistry QA/QC test representing 13,582 water samples from active water wells used for domestic, pasture, livestock and other purposes. Information on depth, completion interval, and location is available for these wells. The BWWT includes gas data for 1,698 free gas samples. A QA/QC procedure for free gas samples was applied based on three criteria: 1) methane-containing samples with concentration above the reported detection limits (see Table S1 at the end of this document); 2) balanced molecular gas component concentrations within 100 ± 10 %; and 3) air contamination is correctable. We found that 46% of the free gas samples passed this QA/QC test representing 787 free gas samples.

Milestone 1 has been achieved for the industry, AHS and BWWT data.

2 Milestone 2: Broad scale characterization of water types depending on well depth and geological formation in which the groundwater wells are completed

2.1 Creation of a matrix “PHO” dimension 31x15 of water types combinations

2.1.1 Context and objective

Evaluation of the hydrogeochemical processes that control natural groundwater composition is required for water management purposes. The geochemistry of groundwater is partially a function of the mineral composition of the aquifer through which the water flows. Natural water composition is determined by chemical analyses providing a set of concentrations for the different ions present in the sample. This data can then be grouped and statistically evaluated. For example, the water type of a sample can be determined based on the predominant cation and anion concentrations.

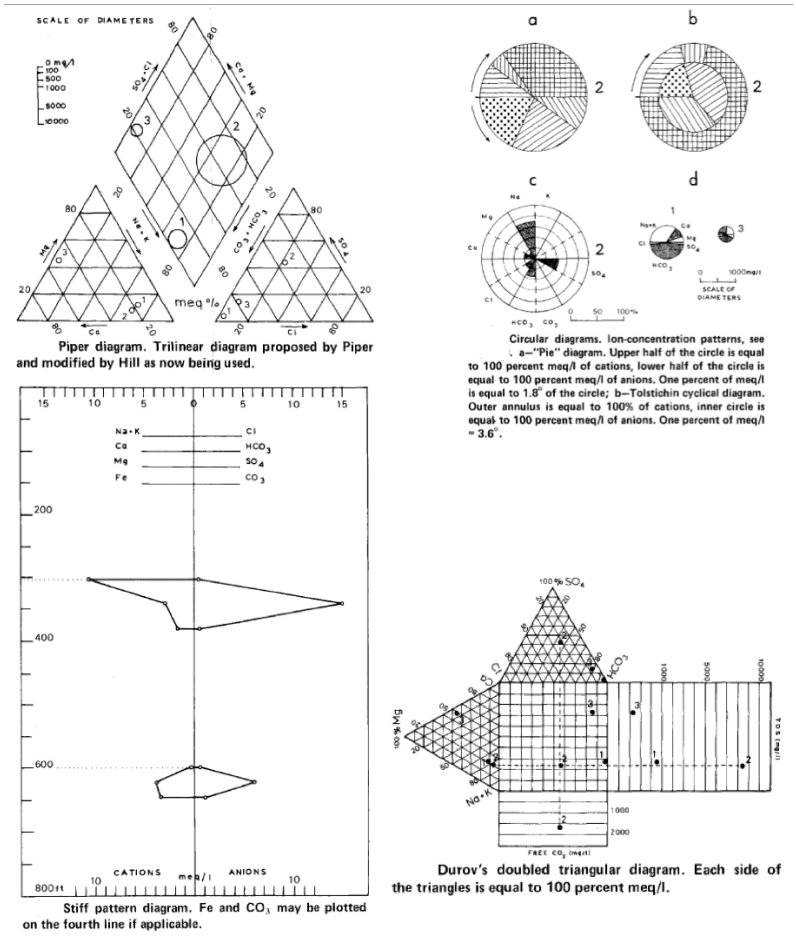

Figure 3: Various graphical interpretations of water quality data (Zaporec, 1972).

Graphical and numerical methods and interpretations of these chemical analyses are needed (i) to decipher relationships between ions or groups of ions characterizing a chemical water type or to evaluate the proportion of ions in comparison to others; (ii) to identify mixing processes involving water of different compositions; (iii) to assess processes that may take place during groundwater circulation, such as redox-processes; and (iv) identify relationships of chemical water compositions to rock types. Tri-linear diagrams (Piper), circular diagrams (Tolstichin), histograms, doubled triangular diagrams (Durov’s) etc. are shown as examples in Fig. 3 and constitute basic tools for hydrochemistry studies to present water quality data.

Each of these graphical representations has limitations when comparing large volumes of data. Usually, Piper diagrams are widely used for displaying water types, but the Piper diagram has serious limitations in separating waters of NaCl and Na-sulfate types, which is of critical importance for this study. Therefore, we developed our own matrix approach to display the water chemistries found in large datasets enabling a clear separation of Na-Cl from Na-sulfate type water, among many others.

2.1.2 Criteria of the "PHO" matrix

Complete chemical analyses are required for most graphical representations and the requirements for the PHO matrix are as follows: Ca, Mg, Na, K for cations and HCO_3, CO_3, SO_4, Cl, NO_3 for the anions. The concentrations of constituents are initially expressed either in milligrams per liter (mg/L), parts per million (ppm) or milliequivalents per liter (meq/L). The objective of the PHO matrix is to differentiate all potential combinations of water types encountered in Alberta and to identify the dominant water types.

The approach consists of four steps:

(1) Convert the concentrations of constituents into meq/L, and then calculate the milliequivalent percentage meq % for cations and anions.
(2) Identify the maximum % of cations and anions respectively, for each water sample x ($Max_{x,meq\%}$)
(3) Determine if any other cation or anion should be considered in the water type assessment. Additional cations and anions are considered if the percentage of the constituent(s) i of the water sample x ($x_{i,meq\%}$) subtracted from the maximum percentage of the sample x ($Max_{x,meq\%}$) does not exceed 20%: $Max_{x,meq\%} - x_{i,meq\%} < 20\%$ with i= 1, 2, 3 or 4 for cations and i=1, 2, 3, 4, 5 for anions. In other words, if the additional cations/anions have a milliequivalent percentage within 20% of the major cation/anion, then they will be considered.
(4) Determine the water type of groundwater based on all the cations and anions considered.

The PHO matrix shows the distribution of a considerable number of potential water types. Each box, as presented with the example in Fig. 4, represents one water type. Each box is associated with a certain combination of cation(s) and anion(s) forming a characteristic water type. The value in the box corresponds to the number of samples belonging to that specific water type.

The main objective of the PHO matrix is to reveal the predominant water types for large datasets.

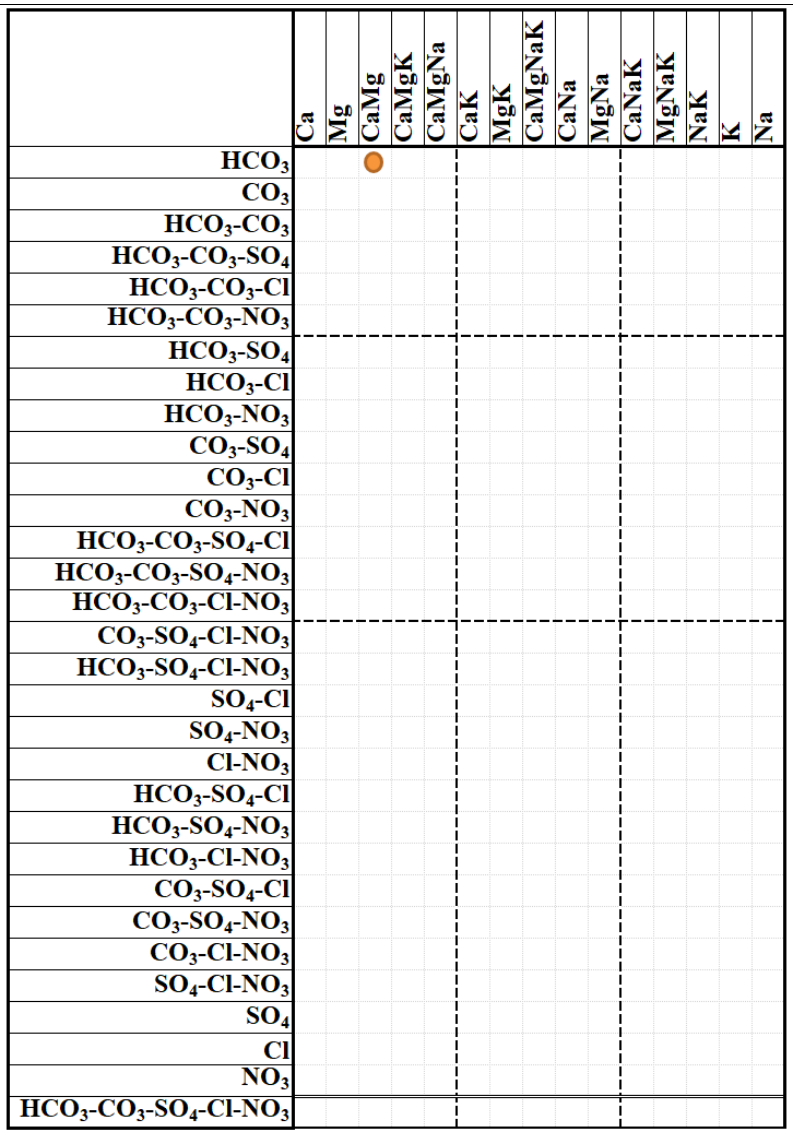

Figure 4: The combinations of water types in the PHO matrix. Dimensions: 31x15. Each box represents a type of water. The orange circle shows that Ca-Mg are the two dominant cations and HCO_3 is the dominant anion leading to a CaMg-HCO_3 water type.

2.2 Characterization of water types and any potential relation with well depth

For water samples from the industry, AHS and BWWT databases passing the QA/QC test (Milestone 1), the water type was determined based on the predominant cation and anion concentrations (see section 2.1). Detailed results for all relevant water types are summarized in Table 4.

Table 4: Water type (WT) distribution and number of samples passing the QA/QC test in each WT for the industrial, AHS (only for water wells with a maximum depth of 300 m) and BWWT data sources. Numbers in bold indicate the predominant water-type.

Water Type (WT)	A-1	A-2	A-3	B	C	D-1	D-2	E-1	E-2	BWWT	AHS
Ca-HCO_3	1	6	3	2	**24**	**10**	**26**	5	7	**210**	**5712**
Ca-Mg-HCO_3	6	7	3	1	**56**	**9**	**18**			**330**	**3474**
Mg-HCO_3					1		1			23	106
Ca-Mg-Na-HCO_3	8	13			11	2	7	1	1	363	2784
Ca-Na-HCO_3	1	5		1	17	2	7	5	3	220	1887
Mg-Na-HCO_3		1								41	97
Na-HCO_3	**269**	**431**	**11**	**10**	**34**	**8**	**49**	**10**	**10**	**6263**	**33613**
Na-HCO_3-CO_3		3								2	9
Na-HCO_3-CO_3-SO_4	6	8								5	3
Ca-HCO_3-SO_4	1	1			2					25	361
Ca-Mg-HCO_3-SO_4	2	4			1					53	265
Ca-Mg-Na-HCO_3-SO_4	7	11			3					146	554
Ca-Na-HCO_3-SO_4	4	6			1					80	365
Mg-Na-HCO_3-SO_4		1								34	41
Na-HCO_3-SO_4	**266**	**431**		1	16		1			**3380**	**5269**
Ca-HCO_3-Cl					1					10	76
Mg-Na-HCO_3-Cl					1						2
Na-HCO_3-Cl	9	13			1					161	849
Na- HCO_3-CO_3-SO_4-Cl		2									
Ca-Na-HCO_3-SO_4-Cl	1	1								4	9
Na-HCO_3-SO_4-Cl	4	4			1					24	91
Ca-SO_4	1	2			1					10	131
Mg-SO_4		1								12	37
Ca-Mg-SO_4	3	7			1					31	148
Ca-Mg-Na-SO_4	11	19								107	375
Ca-Na-SO_4	4	10			1					49	163
Mg-Na-SO_4	1	6								29	84
Na-SO_4	**188**	**301**			6					**1784**	**2328**
Na-Cl	9	12			2					105	810
Others		1			2					82	753
Total	*802*	*1307*	*17*	*15*	*183*	*31*	*109*	*21*	*21*	*13583*	*60396*

The results are also graphically presented in Piper plots (Figs. 5, 7, 11) that classify aqueous geochemical compositions in different water types combinations, but have the severe limitation that Na-Cl and Na-SO_4 type waters can not be graphically separated (Cl+SO_4 plotted on same axis).

While Table 4 comprises a wide range of water types, close inspection of the number of samples associated with each water type reveals that the majority of samples belong to only very few predominant water types including the following:

(1) sodium-bicarbonate waters comprise the majority of all samples (>52% of all samples) followed by sodium-bicarbonate-sulfate waters (>11%); these water types are highlighted in yellow in Table 4. Ion exchange reactions in the subsurface are usually responsible for the increase in sodium concentrations in the groundwater and are not associated with an equivalent increase in chloride concentrations although these samples have often elevated TDS contents;
(2) another important water type is calcium-magnesium-bicarbonate waters (>14% of all samples) that are

highlighted blue in Table 4: Ca-Mg-HCO_3 type waters are typical for recently recharged waters that may have interacted with carbonate minerals and often have comparatively low total dissolved solids (TDS); (3) another less dominant water type is Na-SO_4 (>5.5% of all samples) highlighted in green in Table 4. In these waters the oxidation of sulfide minerals (e.g. pyrite) has usually resulted in highly elevated sulfate concentrations.

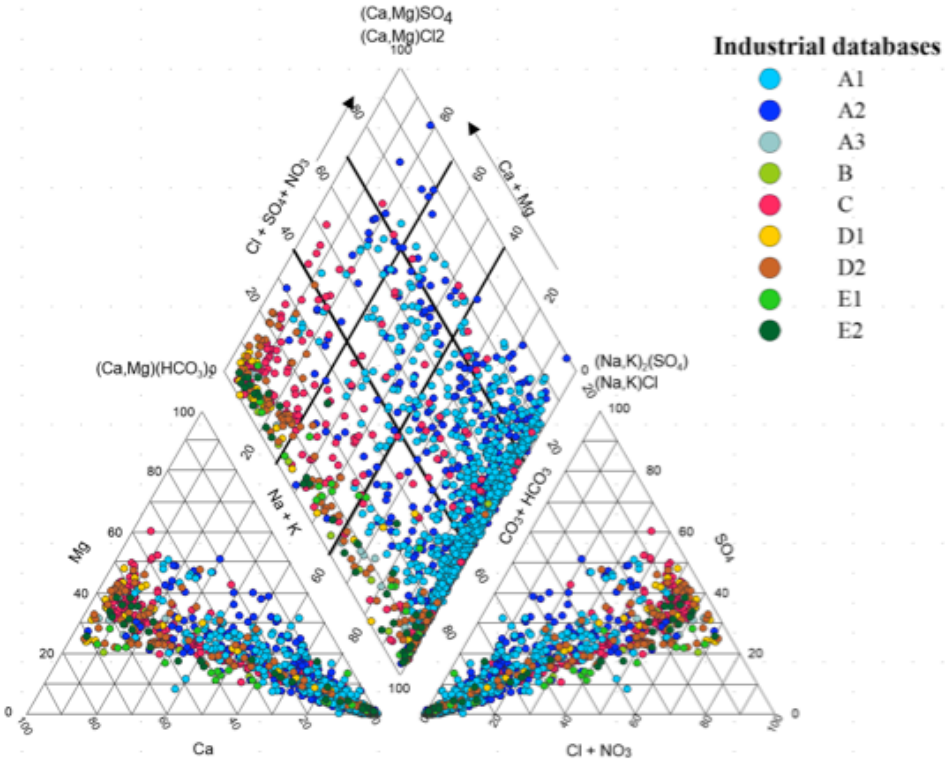

Figure 5: Piper diagram showing water types for industry samples from sources A to E.

In contrast to the three major water types described above, Na-Cl type samples comprise only 1.2% of all water samples and also water types that contain chloride combined with bicarbonate and sulfate constitute only < 1.7 % of all samples (see purple highlights in Table 4).

For the **industry data** we found the following sequence of major water type occurrences in the provided data sets (see Table 4; Fig. 5):
For source A-1: Na-HCO_3 (34%) > Na-HCO_3-SO_4 (33%) > Na-SO_4 (23%),
For source A-2: Na-HCO_3 (33%) = Na-HCO_3-SO_4(33%) > Na-SO_4(23%),
For source A-3: Na-HCO_3(64%) > Ca-Mg-HCO_3(18%) = Ca-HCO_3(18%),
For source B: Na-HCO_3(67%) > Ca-HCO_3(13%),
For source C: Ca-Mg-HCO_3(31%) > Na-HCO_3(19%)> Ca-HCO_3 (13%) > Ca-Na-HCO_3(9%),
For source D-1: Ca-HCO_3(32%)> Ca-Mg-HCO_3(29%)> Na-HCO_3 (26%),
For source D-2: Na-HCO_3(45%)> Ca-HCO_3(24%) > Ca-Mg-HCO_3(17%),
For source E-1: Na-HCO_3(48%) > Ca-HCO_3(24%) = Ca-Na-HCO_3(24%),
For source E-2: Na-HCO_3(48%) > Ca-HCO_3(33%)> Ca-Na-HCO_3(14%).

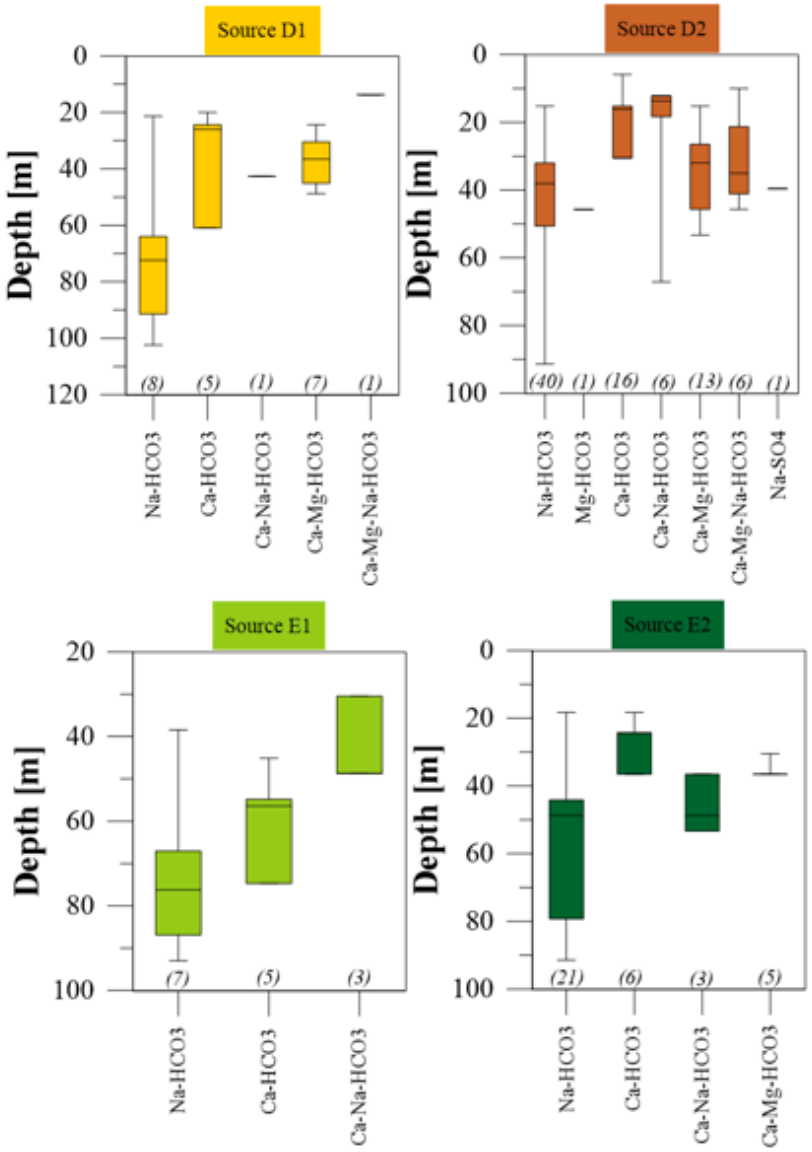

Figure 6: Water well depth versus main water type combinations for the industrial datasets.

Table 4 reveals that samples from sources A and B are predominantly composed of Na-HCO_3 type waters. In contrast, the samples from source C are dominated by Ca-Mg-HCO_3 waters, with Na-HCO_3 representing the 2nd most important water type followed by mixed Ca-Na-HCO_3 waters. The samples from source D-1 are dominated by Ca-(Mg)-HCO_3 waters followed by Na-HCO_3 waters. The samples from sources D-2, E-1 and E-2 were obtained from similar geographical regions and are predominantly composed of Na-HCO_3 type waters followed by Ca-HCO_3 type waters and by mixed Ca-Na-HCO_3 waters. Fig. 5 summarizes the water types in a Piper diagram with data sources from the five different companies separated by color codes.

Fig. 6 shows the relationship between water well depth and water types for D-1, D-2 and E-1 and E-2. For data from D-1, it appears that the deepest wells were predominantly associated with groundwater of the Na-HCO_3 water type. Analysis of variance (ANOVA) was used to compare the different groups with normal distribution for statistical significance to identify any correlation between water types and water well depth. There was a statistically significant difference between groups/water types as determined by one-way ANOVA ($p<0.05$). A Tukey post hoc test reveals that the water well depth was statistically significantly deeper for Na-HCO_3 groundwaters compared to Ca-HCO_3 water types and, statistically significantly deeper for Na-HCO_3 groundwater compared to Ca-Mg-HCO_3 water types. These tests indicate a difference in water well depth among different water types for D-1.

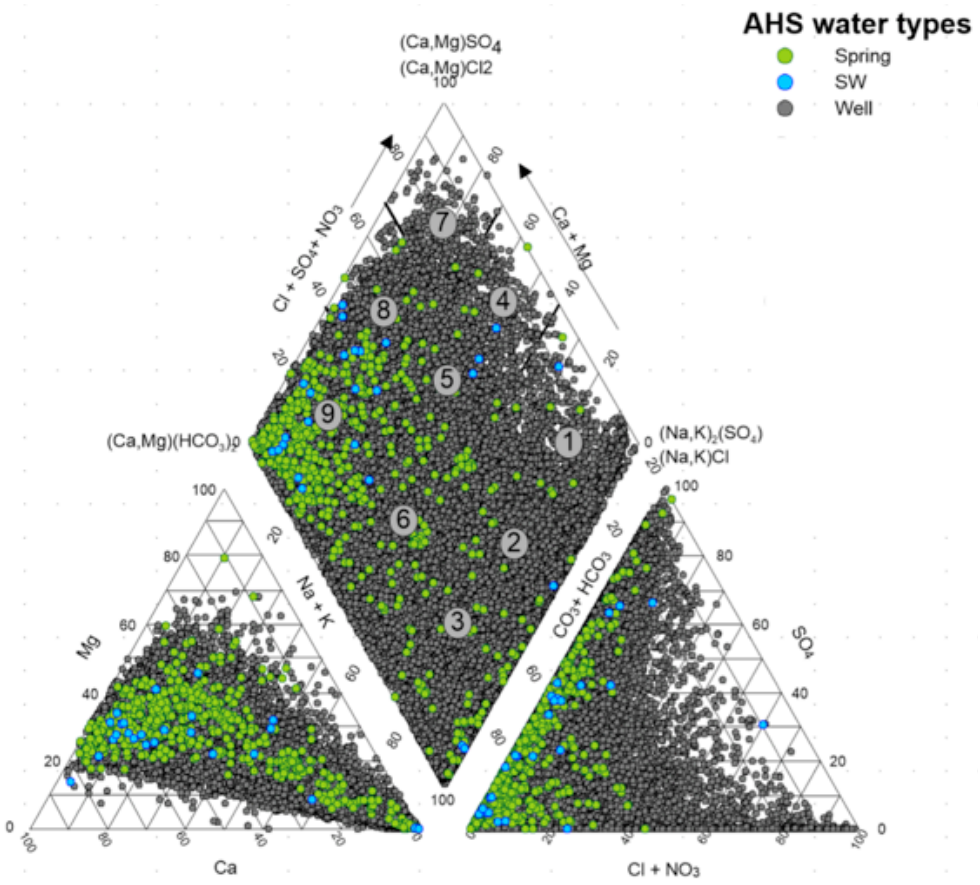

Figure 7: Piper diagram showing water types for 78,316 samples from the AHS database.

For D-2 data, it also appears that the deepest water wells contain predominantly Na-HCO_3 water types. Analysis of variance (non-parametric Kruskal-Wallis, Mann-Whitney tests) was used to compare the different groups with non-normal distribution for statistical significance to identify any correlation between water types and water well depth. There was a statistically significant difference between groups as determined by Kruskal-Wallis ($p<0.05$). A Mann-Whitney test was used to analyze which groups differ from the rest. Water well depth was statistically significantly deeper ($p<0.05$) for groundwater of the Na-HCO_3 type compared to Ca-HCO_3 waters, and statistically significantly deeper ($p<0.05$) for Na-HCO_3 groundwater compared to Ca-Na-HCO_3 water types. These statistical tests indicate a difference in water well depths among these water type pairs.

For E-1 and E-2 data, analysis of variance (non parametric Kruskal-Wallis test and Mann-Whitney test) was used to compare the different groups with non-normal distribution for statistical significance in the water well depth medians among several water types. There was non-statistically significant difference between groups/water types as determined by a one-way Kruskal-Wallis test ($p>0.05$) indicating that no unique water well depth interval can differentiate the water types in the data E-1 and E-2.

For the large **AHS database**, we found the following sequence of water types of water wells samples (see Table 4): Na-HCO_3 (55%) >> Ca-HCO_3 (9.5%) > Na-HCO_3-SO_4 (8.7%) > Ca-Mg-HCO_3 (5.8%) > Ca-Mg-Na-HCO_3 (4.6%) > Na-SO_4 (3.8%) > Ca-Na-HCO_3 (3.1%) > Na-HCO_3–Cl (1.4%) > Na-Cl (1.3%).

Figure 5 shows a Piper plot for all AHS samples passing the QA/QC criteria and reveals that springs and surface water (SW) samples contained in the AHS database are predominantly representing a Ca-HCO_3 water-type. Groundwater samples display a wide variety of water types, with Na-HCO_3 type water being most prominent, followed by Ca-HCO_3 and Na-HCO_3-SO_4 water types. Due to the high number of samples,

the Piper diagram with for the AHS dataset becomes difficult to read and interpret. Hence, we used the "PHO matrix" shown in Fig. 8 for presenting the large database of water types combinations. The PHO matrix groups similar samples into bins and gives the number of samples per bin eliminating the problem of the dataset size (see 2.1). The main water type combinations were extracted and are summarized in Table 4. Fig. 8 reveals the different water type combinations that were not visible in the Piper diagram, and all data (water wells and surface water) from AHS are taken into account.

In Fig. 9, the depths of the groundwater wells in the AHS databases are plotted versus the most predominant water types. There appears to be no clear correlation between water types and the depth of the water wells.

For the **BWWT database**, review of Table 4 reveals that the majority of samples were of Na-HCO_3 (>46%) and Na-HCO_3-SO_4 (>24%) water types. The remaining 29 % are composed of samples belonging predominantly to Na-SO_4 and Ca-Mg-HCO_3 water types, among others. Fig. 10 presents the PHO matrix for the BWWT data and shows the distribution of the various water type combinations that are not recognizable in the Piper diagram (Fig. 11). Only 105 samples belonged to the Na-Cl water type, which represents <1% of all samples passing the QA/QC criteria (Fig. 10).

Well depth information and completion/screen intervals are available for the BWWT dataset. Fig. 12 illustrates the location of the BWWT water wells and the distribution of the main water types versus depth of the water wells. It appears that the sodium-rich water samples e.g. Na-Cl, $NaHCO_3$, Na-SO_4 water types are associated with the deepest water wells whereas Ca-rich water e.g Ca-HCO_3, Ca-Mg-HCO_3 is typically associated with the shallowest water wells. Kruskal-Wallis and Mann-Whitney tests were conducted to identify any correlation between water types and water well depth. The results of these tests revealed that there are significant statistical differences ($p<0.05$) in water well depth between Na-rich water that is found in deeper wells than Ca-rich water. There is no significant statistical difference amongst Ca-rich waters ($p>0.05$) indicating that no specific water well depth can differentiate these Ca-rich waters.

	Ca	Mg	CaMg	CaMgK	CaMgNa	CaK	MgK	CaMgNaK	CaNa	MgNa	CaNaK	MgNaK	NaK	K	Na
HCO_3	5712	106	3474	2	2784	3		7	1887	97	2	1	29	199	33613
CO_3									1	2					1
HCO_3-CO_3															9
HCO_3-CO_3-SO_4										1					3
HCO_3-CO_3-Cl															
HCO_3-CO_3-NO_3															
HCO_3-SO_4	361	10	265	1	554			1	365	41			9	26	5269
HCO_3-Cl	76	11	61	1	46				31	2				2	849
HCO_3-NO_3	16		9		3				1					2	18
CO_3-SO_4															2
CO_3-Cl															1
CO_3-NO_3															
HCO_3-CO_3-SO_4-Cl															
HCO_3-CO_3-SO_4-NO_3															
HCO_3-CO_3-Cl-NO_3															
CO_3-SO_4-Cl-NO_3															
HCO_3-SO_4-Cl-NO_3	5		13		3				3	1					3
SO_4-Cl			2		5				2						11
SO_4-NO_3			1		1										
Cl-NO_3	1														
HCO_3-SO_4-Cl	7		13		23				9	3				1	91
HCO_3-SO_4-NO3	3		11		4				3						8
HCO_3-Cl-NO_3	8		3		1								1	1	2
CO_3-SO_4-Cl															
CO_3-SO_4-NO_3															
CO_3-Cl-NO_3															
SO_4-Cl-NO_3			1												
SO_4	131	37	148		375			1	163	84			5	10	2328
Cl	27		9		19				18	2			1	1	810
NO_3	2		1		1								1		12
HCO_3-CO_3-SO_4-Cl-NO_3															
total	60396														

Figure 8: PHO matrix showing water types for water wells samples from the AHS database with a max depth of 300 m. The value in the box corresponds to the number of samples belonging to that specific water type (e.g. the number 5712 first row and first column corresponds to 5712 samples belonging to the Ca-HCO_3 water type).

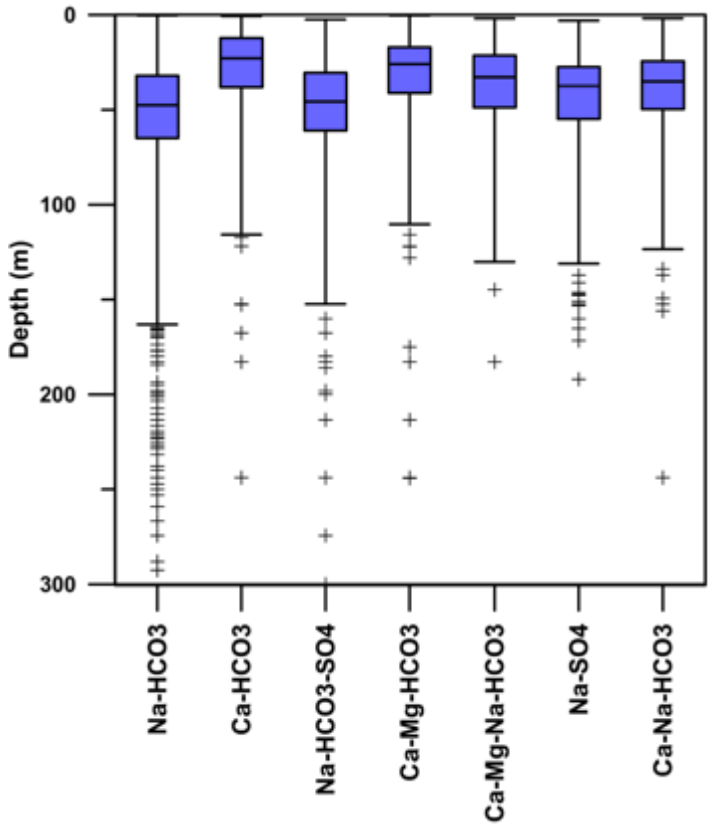

Figure 9: Water well depth versus main water type combinations for the AHS dataset.

	Ca	Mg	CaMg	CaMgK	CaMgNa	CaK	MgK	CaMgNaK	CaNa	MgNa	CaNaK	MgNaK	NaK	K	Na
HCO_3	210	23	330	6	363	3		6	220	41			2	4	6263
CO_3										1					
HCO_3-CO_3															2
HCO_3-CO_3-SO_4															5
HCO_3-CO_3-Cl															1
HCO_3-CO_3-NO_3															
HCO_3-SO_4	25	10	53		146			1	80	34					3380
HCO_3-Cl	10		4		3				2						161
HCO_3-NO_3	3														
CO_3-SO_4															
CO_3-Cl															
CO_3-NO_3															
HCO_3-CO_3-SO_4-Cl															
HCO_3-CO_3-SO_4-NO_3															
HCO_3-CO_3-Cl-NO_3															
CO_3-SO_4-Cl-NO_3															
HCO_3-SO_4-Cl-NO_3	3		1		3				1						
SO_4-Cl									1						3
SO_4-NO_3															
Cl-NO_3															
HCO_3-SO_4-Cl			2		6				4						24
HCO_3-SO_4-NO3		1	1		1				2						5
HCO_3-Cl-NO_3	1				1										
CO_3-SO_4-Cl															
CO_3-SO_4-NO_3															
CO_3-Cl-NO_3															
SO_4-Cl-NO_3															
SO_4	10	12	31		107			1	49	29					1784
Cl					1				1						105
NO_3	1														
HCO_3-CO_3-SO_4-Cl-NO_3															
total	13583														

Figure 10: PHO matrix showing water types for samples from the BWWT database. The value in the box corresponds to the number of samples belonging to that specific water type (e.g. the number 210 corresponds to 210 samples belonging to Ca-HCO_3).

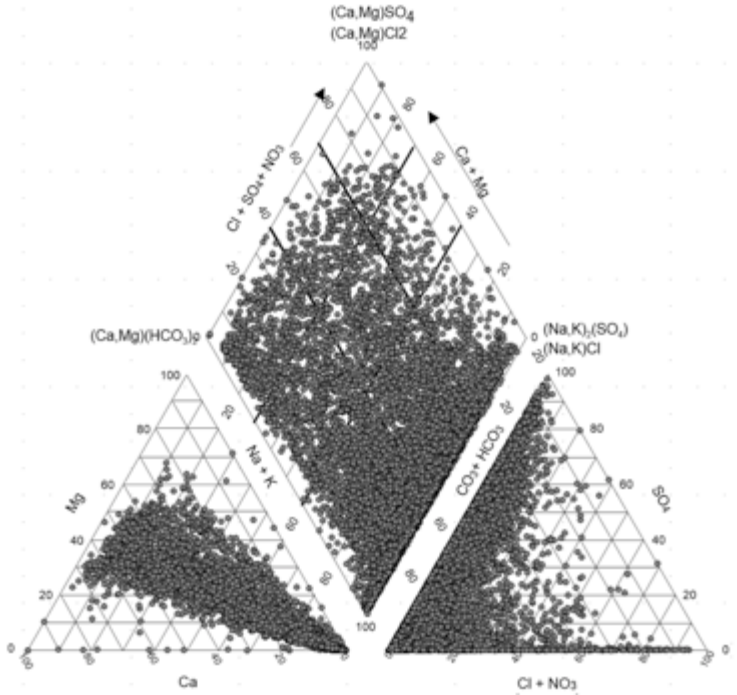

Figure 11: Piper diagram showing water types for samples from the BWWT database.

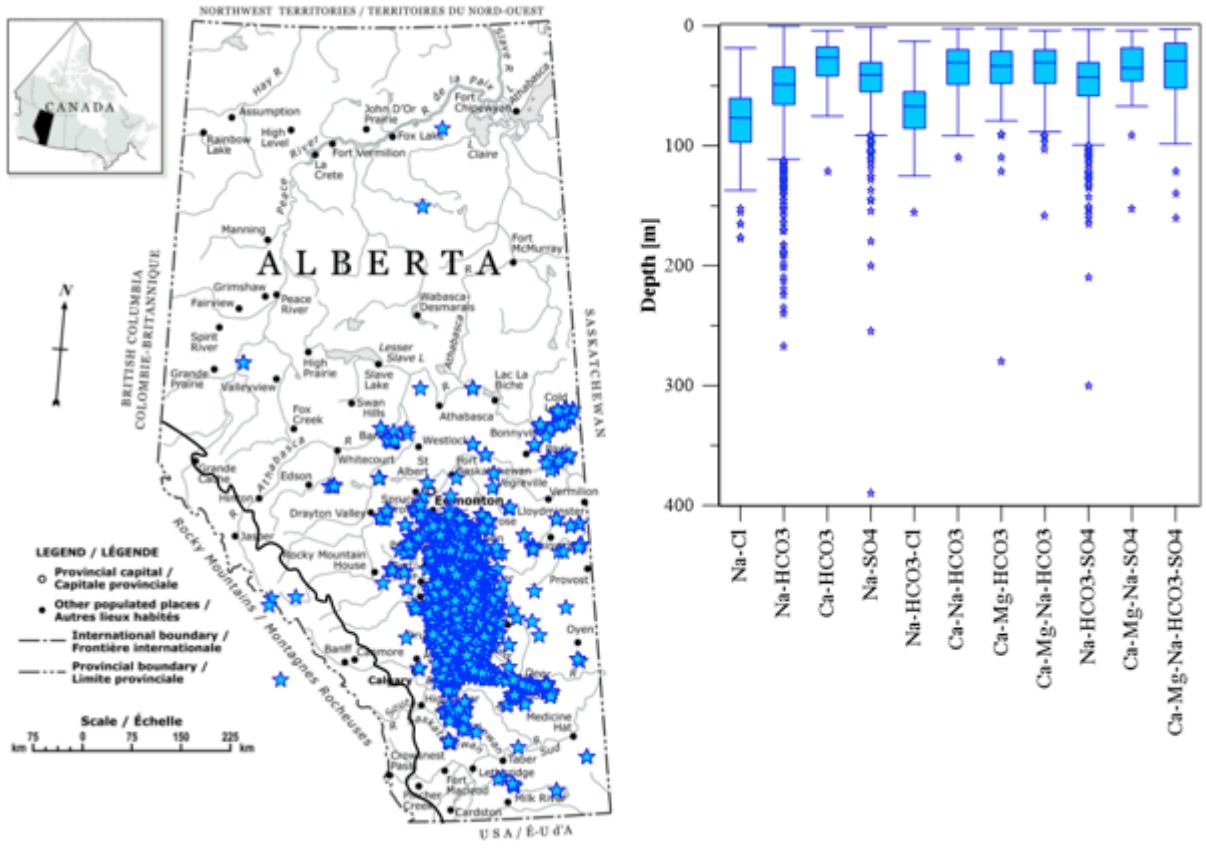

Figure 12: Location of the water wells of the BWWT dataset and relationship between water types and depth (note only the water type combinations with > 50 samples are shown in the plot).

2.3 Development of geospatial methods to assign geological formation in which groundwater wells are completed and investigation of any relation with water types

2.1.1 Description of the methods to assign geological formations

An attempt was made to attribute the geological formation in which each groundwater well was completed and screened, using well coordinates and total well depth for the AHS, BWWT, and industrial (D1, D2, E1, E2) datasets. In addition to total depth, the screened interval(s) was reported for some water wells in the BWWT, D2, E1, and E2 datasets, which allowed for the identification of potential sub-boundaries within the Paskapoo formation and thus potential groundwater mixing between hydrogeological sub-units. When available, wells were assigned to additional geologic units according to their screened interval(s).

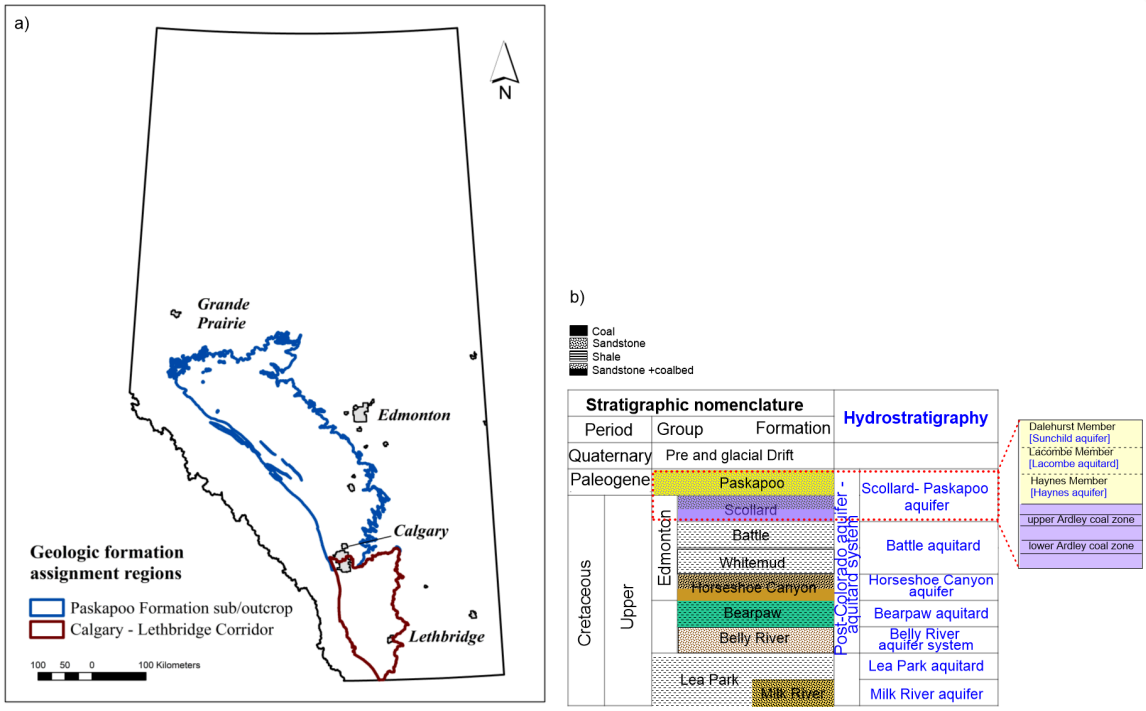

Figure 13: a) Geological formations were assigned to wells in the blue and red regions using method 1 (blue region) and method 2 (red region). Only the Paskapoo Fm. and its internal subdivisions were assigned to water wells within the blue region (limiting factor was the availability of layers from AGS) but within the red region all of the geological formations were assigned based on the hydrostratigraphic 3D model provided by AGS; b) stratigraphic and hydrostratigraphic nomenclatures representative of the geology within west-central and south-western Alberta.

Fig. 13 summarizes the regional Upper Cretaceous to Quaternary stratigraphy of south-western and west-central Alberta which represents the geology of the blue and red regions of the index map in Fig. 13a. Several geologic units comprising coarse-grained clastics (i.e. gravel, sandstone, siltstone) were deposited during this ~100 million year time period including, from oldest to youngest, the (i) early Campanian Milk River Formation (Fm.) (and equivalents), (ii) middle to late Campanian Belly River (Judith River) Group (Gp.) (and equivalents), (iii) late Campanian to early Maastrichtian Horseshoe Canyon Fm. (and equivalents), (iv) late Maastrichtian to early Paleocene Scollard Fm. (and equivalents), and (v) the middle to late Paleocene Paskapoo Fm. (and equivalents), which comprises the major shallow aquifers in the study area. Additionally, four sedimentary units with a greater proportion of fine-grained materials (i.e. mudstones, shales) were deposited during this period including, from oldest to youngest, the (i) the early

Campanian Pakowki Fm. (equivalent to Upper Lea Park Fm.), (ii) the middle Campanian Bearpaw Fm., (iii) the Maastrichtian Battle Fm., and (iv) the early Paleocene Upper Scollard Fm. (Dawson et al., 1994), which are typically classified as aquitards (Fig. 13b). Overlying Quaternary deposits include formations composed of silt, sand, and gravel of glacio-fluvial origin and glacial tills. Among the stratigraphic intervals containing coal zones with CBM potential are the Lower Cretaceous Mannville Gp. (e.g. Mannville Gp. coals), and the Belly River (e.g. McKay, Taber, and Lethbridge Coal Zones), Horseshoe Canyon (e.g. Drumheller Coal Zone, a primary CBM target), and Scollard Fms. (e.g. Ardley Coal Zone). Thin coal seams also occur throughout the Paskapoo Fm. More information about these geological formations can be found in Meyboom (1960), Rosenthal et al. (1984), Hamblin (1998), Hamblin (2004), Dawson et al. (1994), Lyster and Andriashek (2012), Grasby et al. (2008), and Prior et al. (2013).

The regional geology of south-western and west-central Alberta differs only slightly. Although Upper Cretaceous units have been assigned dissimilar names in different regions, on a large scale they are lithologically very similar and we have chosen to use the west-central stratigraphic nomenclature for continuity. An important geological variation is the presence of the up to 800 m thick Paskapoo Fm. in west-central Alberta and conversely the limited extent of the Paskapoo Fm. equivalent, Porcupine Hills Fm., in southwestern Alberta. Wells drilled in the red area of Fig. 13a largely do not encounter the Paskapoo Fm. and therefore groundwater wells from the same area are mostly completed in other geologic units.

The attribution of a geological formation to well samples was based on **Methods 1 and 2,** representative of the blue and red areas respectively (Fig. 13):

1) **Method 1 – Paskapoo** Fm. **sub/outcrop extent – (blue area)** is defined as the attribution of a geological formation to well samples located within the Paskapoo Fm. sub/outcrop extent. Attribution in the blue area was constrained to the Paskapoo Fm. and its internal hydrostratigraphic subdivisions i.e. Dalehurst (Sunchild), Lacombe, and Haynes Members (Mbr.) due to the limiting factor of layer availability from the Alberta Geological Survey (AGS). A geological attribution including post-Paleocene deposit; Paskapoo Fm.; and Sunchild, Lacombe, or Haynes Mbr., was assigned to water wells by utilizing (i) the elevation difference between the topographic elevation (m asl), (ii) structural top of the Paskapoo Fm. and its three members (m asl), and (iii) the isopach of each geologic unit (m), based on the water well coordinates and (iv) total water well depth. Some of the datasets have their screen (completion) intervals reported. Thus, based on the screen interval(s) provided, it was possible to identify if the water wells were screened within a single geological formation, or across multiple geologic units.

2) **Method 2 – CLC – (red area)** is defined as the attribution of a geological formation to groundwater well samples located within the Calgary-Lethbridge corridor (CLC). The groundwater wells present in this red area of Fig. 13a were assigned one of the following geological formations: post-Paleocene deposits, Paskapoo, Scollard, Battle, Horseshoe Canyon, Upper Bearpaw, Lower Bearpaw, Belly River, Foremost, or Pakowki (Fig. 13b). A comprehensive geological formation attribution was possible for the CLC as the AGS has allowed the general public access to the data used in creating their 3D hydro-stratigraphic model of this region. The CLC samples were attributed to geologic formations by using a methodology similar to the elevation difference and isopach method used for geologic attribution in method 1 for the blue region (Paskapoo Formation extent) in Fig 13a. Layers available for the geological attribution in CLC wells included (i) sediment thickness (m), (ii) top of bedrock (m asl), and structural tops (m asl) of all formations listed previously. Combining the sediment thickness (m) and top of bedrock (m asl) provided a measure of topographic elevation (m asl). Using the elevation difference between the calculated topographic elevation (m asl) and the structural top of the formations (m asl) allowed for a geologic formation attribution based on a water well's coordinates and total well depth or completion interval, when this additional information was available.

2.1.2 Geological Fm. attribution for AHS, BWWT, sources D1, D2, E1 and E2

2.1.2.1 Multi-aquifer involvement using total well depth as the input parameter for Methods 1 and 2

a) Overview of the descriptive statistics across the different datasets

This section reports the geological formation in which the water wells were completed based on the total depth criteria and coordinates while using Method 1 and/or 2 respectively. The results indicate that water wells from the different datasets are completed in multiple aquifers varying from the Upper Cretaceous Belly River Gp. to post-Paleocene deposits (Table 5). The aquifer lithologies vary considerably, comprising mostly fractured mudstone, sandstone and siltstone beds, coal seams or lenses, pre-glacial sand, or surficial sandy and gravelly lacustrine or moraine deposits (Dawson et al., 1994).

Table 5: Attribution of geological formations in percent (%) for AHS, BWWT, sources D1, D2, E1 and E2 in the blue and red areas.

	BWWT*[1]	**D1***	**D2*[1]**	**AHS***	**E1[1]**	**E2[1]**
Post-Paleocene deposits	7.0	10.5	38.8	1.1	7.1	
Paskapoo Fm.	70.4	89.5	61.2	54.9	92.9	100
Scollard Fm.	14.1			34.1		
Battle Fm.	0.6			0.3		
Horseshoe Canyon Fm.	8.0			8.5		
Upper Bearpaw Fm.				0.1		
Lower Bearpaw Fm.	0.04			0.7		
Belly River Gp.				0.3		
Pakowki Fm.				0.1		
*Only a subset of water wells is present in the blue and red areas [1]Completion interval information						

All the studied datasets reveal that >50% of water wells are completed in the Paskapoo Fm. (Table 5). The Paskapoo and Scollard Fm. aquifer systems support more groundwater wells than any other aquifers.

b) *Subdivision of the Paskapoo Fm. into its internal hydrostratigraphic units*

The mid to late Paleocene Paskapoo Fm. is one of the largest and most intensely used bedrock aquifer systems in Alberta. The Paskapoo Fm. comprises dominantly alluvial fan and fluvial floodplain facies. A succession of non-marine mudstone, siltstone, and minor coal together with thick and often stacked sandstone units constitute the main lithologies. Three internal lithostratigraphic divisions have been suggested: (1) the lowermost Haynes member characterized by thick, conglomeratic sandstone; (2) the Lacombe Mbr. comprising the bulk of the middle Paskapoo Fm. with interbedded siltstone, mudstone with thin coal or carbonaceous beds and minor sandstone; and (3) the uppermost Dalehurst Mbr. composed of interbedded sandstone, siltstone, mudstone, shale and coal but dominated by sandstone and siltstone layers (Demchuk and Hills, 1991). The Paskapoo Fm. can also be divided into three corresponding hydrostratigraphic units namely (1) the lowermost sandstone-dominated Haynes aquifer, (2) the Lacombe aquitard mostly composed of mudstone with minor interbedded sandstone and (3) the uppermost sandstone-dominated Sunchild aquifer contained within the Dalehurst Mbr.

All water wells originally classified as general Paskapoo Fm. wells from the five different datasets were further sub-divided into the three internal Paskapoo hydrostratigraphic units using Method 1 (Table 6). The majority of the water wells (60.5 to 100.0%) from each dataset were classified into one of the three Paskapoo units. When a unit could not be assigned, there were several explanations as to why this was not possible:

- Required layer data (i.e. structural top, isopach) was not available;
- Total well depth fell between the reported depth to the base of a shallower unit and the depth to the top of the deeper adjacent unit;
- Total well depth was shallower than the depth to the top of the first unit and the assignment given was “post-Paleocene deposit”.

The layers provided by AGS are not always created from the same digital data source and therefore a certain amount of disagreement between geological attributions is expected.

Table 6: Subdivision of the Paskapoo Fm. into its three hydrostratigraphic units in which the water wells from BWWT, D1, D2, E1 and E2 were completed [percentage, %].

	AHS	BWWT	D1	D2	E1	E2
Sunchild	12.1	0.6	82.3	50.0	7.7	80.0
Lacombe	83.3	81.1	17.6	50.0	92.3	20.0
Haynes	4.5	18.4				

Nineteen of 31 source D1 water wells with available coordinate and total depth information were located in the blue area and were completed within the Paskapoo Fm. (Table 6) and more specifically in the Sunchild aquifer (Table 6). The source D2 dataset contains both the total depth and well screen interval(s). Source D2 is composed of 111 water samples: 8 samples were collected from surface water, 17 samples from unknown origin, and 86 samples from 73 water wells. All 73 water wells are located in the blue area and 44 of these water wells have reported screen completion intervals. One of the 44 wells has multi-completion intervals while the 43 other water wells target a single unit. 67 of the 73 D2 water wells were completed in the Paskapoo Fm. with 6 water wells completed in post-Paleocene deposits. Subdividing the Paskapoo Fm. into its three internal hydrostratigraphic units shows that 50% of the D2 wells are completed in the Sunchild aquifer with the remaining 50% appear to be completed in the Lacombe aquitard (Table 6). The latter contains some fine- to medium-grained sandstone and conglomeratic interbeds that can act as localized aquifers (Demchuk and Hills, 1991).

In the Edson area, the sandstones of the Paskapoo Fm. are the most important bedrock aquifer. Water well drilling reports for source E1 and E2 wells indicate the depths of the completion intervals and in which lithologies the wells were completed. Most of the water wells from E1 are completed in salt and pepper/grey sandstones. Geological attribution for E1 wells using Method 1 indicates that most of the water wells are completed in the interbedded sandstone layers of the Lacombe Mbr. For the source E2, most of the water wells were completed in the Sunchild aquifer (Table 6).

The water wells in the AHS and BWWT datasets are mostly completed in the Paskapoo Fm. and more precisely in the interbedded sandstone layers within the Lacombe Mbr. (Tables 5 and 6).

No information on water well depth has been provided for sources A1 and A2. However, based on the nature of the water wells (landowner) and the total depth < 50 m it appears likely that most of the water wells are completed in the Paskapoo Fm. (source personal communication James Armstrong). Sources B and C also do not contain information on the water well depths.

2.1.2.2 *Completion interval criteria as an input parameter for Method 1: general descriptive statistics*

As a second step, the screen interval reported for some water wells was used as an input parameter for Method 1 to identify potential sub-boundaries within the Paskapoo Fm. and thus potential groundwater mixing between hydrogeological sub-units (Table 7).

Table 7: Wells from BWWT, D2, E1 and E2 datasets with completion intervals extending across either a single- or multiple hydrostratigraphic unit(s) [percentage, %].

Dataset	Single unit	Multiple unit
BWWT	88.5	11.5
D2	18.8	81.2
E1	81.8	18.2
E2	70.0	30.0

In the subset of wells with completion intervals spanning multiple hydrostratigraphic units, the following geological unit combinations are observed:

- **BWWT (11%)**: Post-Paleocene deposits-Lacombe, Post-Paleocene deposits-Haynes, Sunchild-Lacombe, Lacombe-Haynes
- **D2 (81%):** Post-Paleocene deposits-Lacombe, Post-Paleocene deposits-Sunchild, Sunchild-Lacombe
- **E1 (18%):** Post-Paleocene deposits-Lacombe, Sunchild-Lacombe
- **E2 (30%):** Post-Paleocene deposits-Sunchild

2.1.3 Water type characterization of the bedrock aquifer systems

2.1.3.1 General overview and inter-comparison between BWWT and AHS datasets

The water types were separately characterized for groundwater samples obtained from the Belly River Gp., Bearpaw, Horseshoe Canyon, Scollard, and Paskapoo Fm. aquifer systems.

The AHS dataset was the only source with groundwater wells completed in the Belly River Gp. (Fig. 14). The dominant (>10%) water types for this formation are Na-HCO_3 (41.03%), Na-HCO_3-SO_4 (20.51%), Na-SO_4 (12.82%) and Ca-Mg-HCO_3-SO_4 (10.26%).

The AHS dataset was the only source with enough groundwater wells completed in the Bearpaw Fm. to characterize the water types (Fig. 14). The main water types (>10%) in aquifers of the Bearpaw Fm. are Na-HCO_3 (44.32%), Na-HCO_3-SO_4 (15.91%), and Na-SO_4 (11.36%).

For the Belly River Gp. and Bearpaw Fm. only one source (AHS) was used to characterize the water types without any inter-comparison possible with other datasets. However for Battle, Horseshoe Canyon, Scollard, and Paskapoo Fms., inter-comparisons between data from the AHS and BWWT sources were possible to identify convergence or divergence in the water type characterization (Figs. 15 and 16).

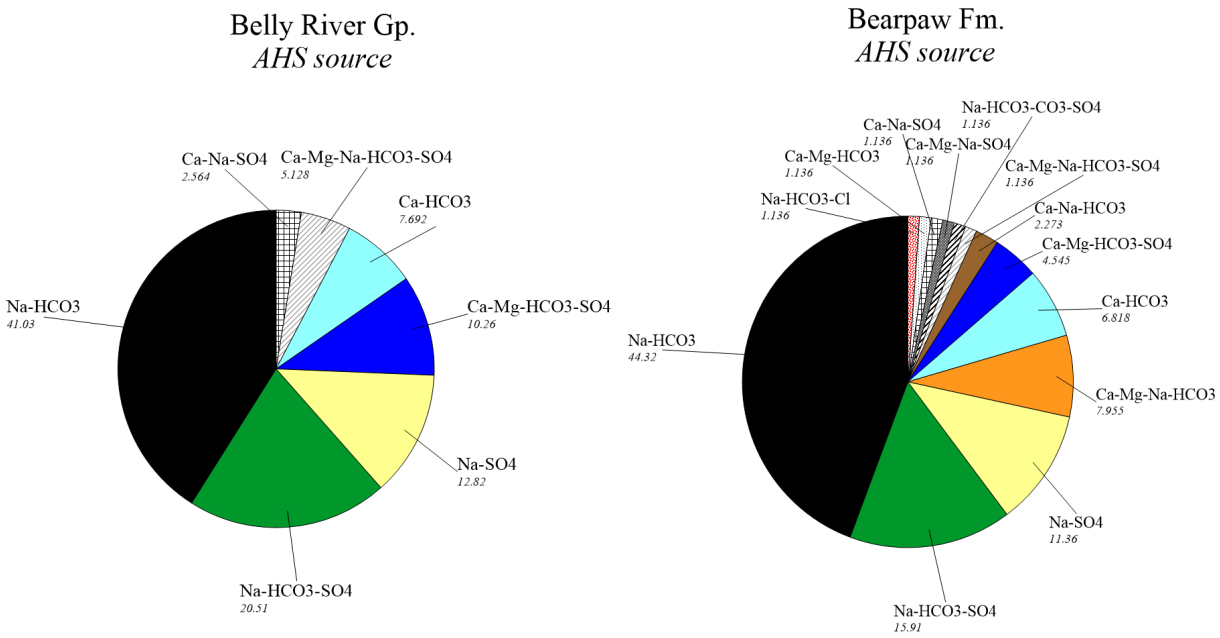

Figure 14: Water type characterization for Belly River Gp. (left, n=39) and Bearpaw (right, n=88) Fm. groundwater samples (AHS data source)**.**

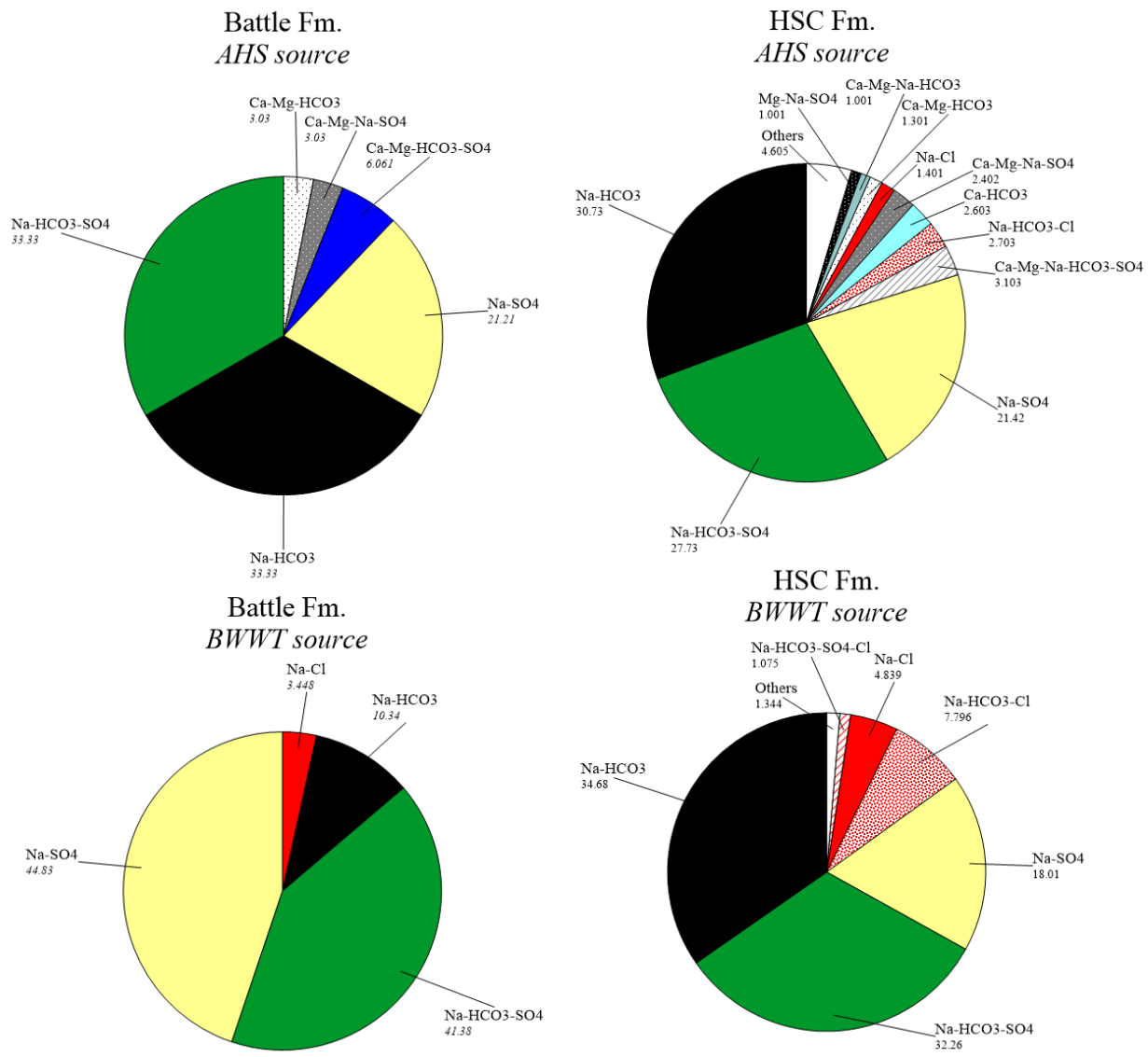

Figure 15: Pie charts of water type characterization for groundwater samples from the Battle (left) (n_{BWWT}= 29, n_{AHS}= 33) and Horseshoe Canyon Fms. (right) (n_{BWWT}= 372, n_{AHS}= 999) and inter-comparison between datasets.

For the Battle Fm., the dominant water types (>10%) are Na-HCO_3, Na-HCO_3-SO_4, and Na-SO_4 in both AHS and BWWT datasets. While there is a good agreement for the identification of the dominant water types, the frequency order differs slightly between BWWT and AHS sources:

- For AHS: Na-HCO_3-SO_4(33.33%) ≥ Na-HCO_3(33.33%) > Na-SO_4(21.21%)
- For BWWT: Na-SO_4(44.83%) > Na-HCO_3-SO_4(41.38%) > Na-HCO_3(10.34%)

For the Horseshoe Canyon Fm., the dominant water types (>10%) are Na-HCO_3> Na-HCO_3-SO_4 > Na-SO_4 in both datasets, which indicates an excellent agreement between results for AHS and BWWT sources.

For the Scollard Fm., the dominant water types are Na-HCO_3, Na-$SO_4$and Na-HCO_3-SO_4 for both AHS and BWWT datasets. Although there is a good agreement for the dominant water types, the frequency order is different between the two datasets.

- For AHS: Na-HCO_3(41.78%) > Na-SO_4(16.55%)> Na-HCO_3-SO_4(13.24%)
- For BWWT: Na-HCO_3-SO_4(45.08%) > Na-SO_4(24.21%) > Na-HCO_3(19.21%)

For the Paskapoo Fm., the dominant water types are Na-HCO_3 (62.12%) for the AHS and Na-HCO_3 (45.81%), Na-HCO_3-SO_4(22.57%) and Na-SO_4(14.35%) for the BWWT dataset.

Based on this geochemical characterization, there are no differences in dominant water types between geologic units with the three ubiquitous Na-rich Na-HCO_3, Na-HCO_3-SO_4 and Na-SO_4 water types dominant in all geologic units from the Belly River Gp. to the Paskapoo Fm.

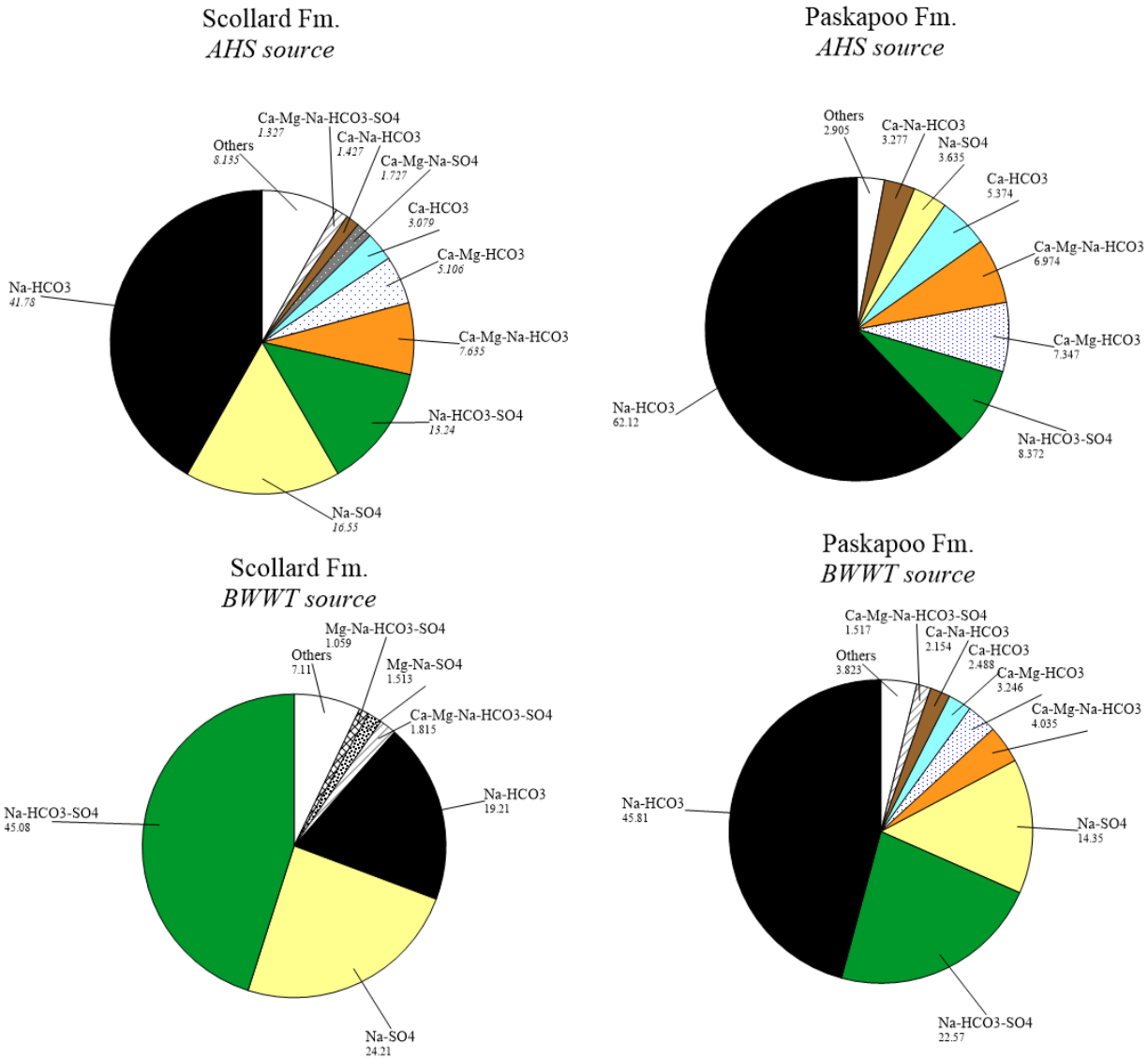

Figure 16: Pie charts of water types characterization for groundwater samples from the Scollard (n_{BWWT}=661, n_{AHS}=3995) and Paskapoo (n_{BWWT}=3296, n_{AHS}=6438) formations and inter-comparison between datasets.

The "minor" (<10%) water types across the datasets permit clustering of some geological formations. The Ca-rich water types such as Ca-HCO_3 and Ca-Mg-HCO_3 occurred in the Belly River Gp., and Bearpaw, Scollard and Paskapoo aquifers in 6-7% of the samples. Some Cl-rich water types such as Na-HCO_3-Cl and Na-Cl were occasionally identified in fine-grained deposits of the Bearpaw (<2%) and Horseshoe Canyon (<5%) Fms., and additionally within the Battle Fm. (<4%) although these findings were observed only in the BWWT dataset.

2.1.3.2 Subdivision of Paskapoo Fm. multi-layer aquifer into internal hydrostratigraphic units and relation with water types characterization

Method 1 permits the subdivision of the Paskapoo Fm. into its three internal stratigraphic units and thus to relate them with water types. Figs. 17 to 19 present the results of water type occurrence in the groundwater samples from the Haynes, Lacombe and Dalehurst (Sunchild aquifer) Mbrs.

The Haynes Mbr. is dominated by the Na-HCO_3 water type for both BWWT and AHS datasets, followed by Na-SO_4 (BWWT) or Na-HCO_3-SO_4 (AHS) (Fig. 17).

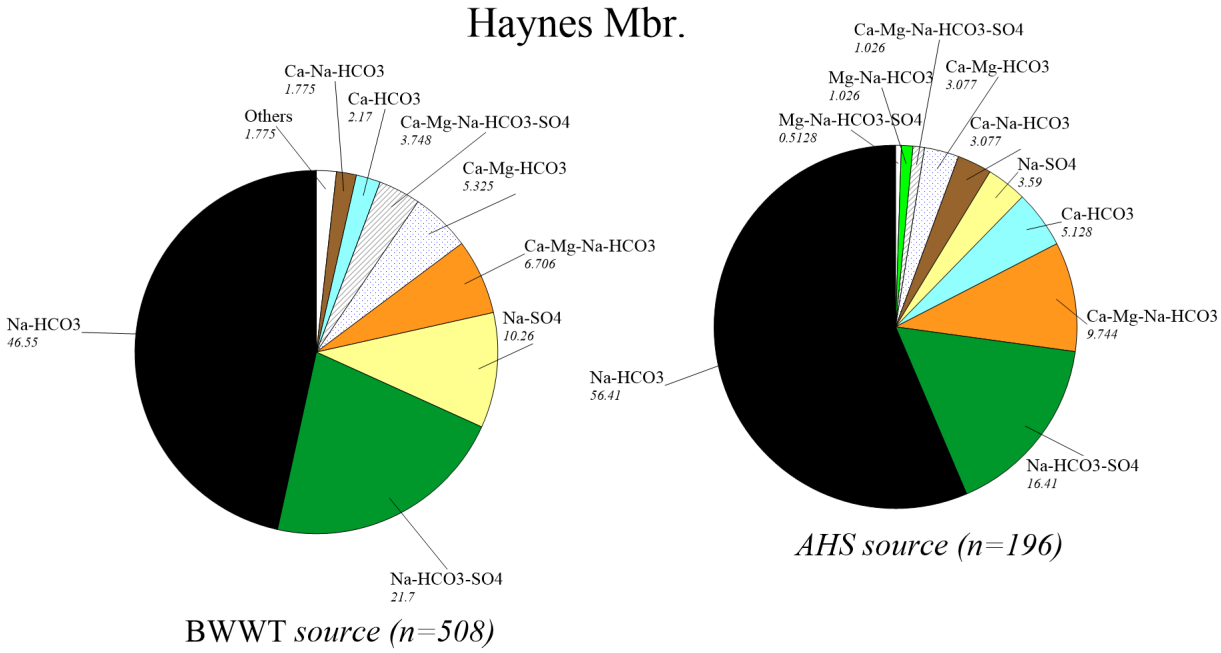

Figure 17: Water type characterization for groundwater samples from the Haynes Mbr. and inter-comparison between BWWT (left) and AHS (right) datasets.

The Lacombe and Haynes Mbrs. share a dominance of Na-HCO_3 groundwater, followed by Na-HCO_3-SO_4 and Na-SO_4 water types. In the Edson area, the pie chart representing the Lacombe Mbr. samples from source E1 seems different from the rest of the datasets represented in Fig. 18 with a dominance of Ca-HCO_3 and Ca-Na-HCO_3 water types. The same pattern was observed by Vogwill (1983) for this area.

The dominant water types in the Sunchild aquifer are Ca-rich and Na-rich (Fig. 19). The three E2, D1 and AHS datasets agree on the dominant water type order with Na-HCO_3 > Ca-HCO_3 followed by Ca-Na-HCO_3(D1), Ca-Mg-Na-HCO_3(D1) or Ca-Mg-HCO_3 (AHS).

Lithology can vary greatly even within hydrostratigraphic units, considerably influencing the geochemistry of the waters residing within the various lithological zones. Additional information on completion interval lithology would allow for optimization with regard to constraining water types to sub-units within geologic or hydrostratigraphic units.

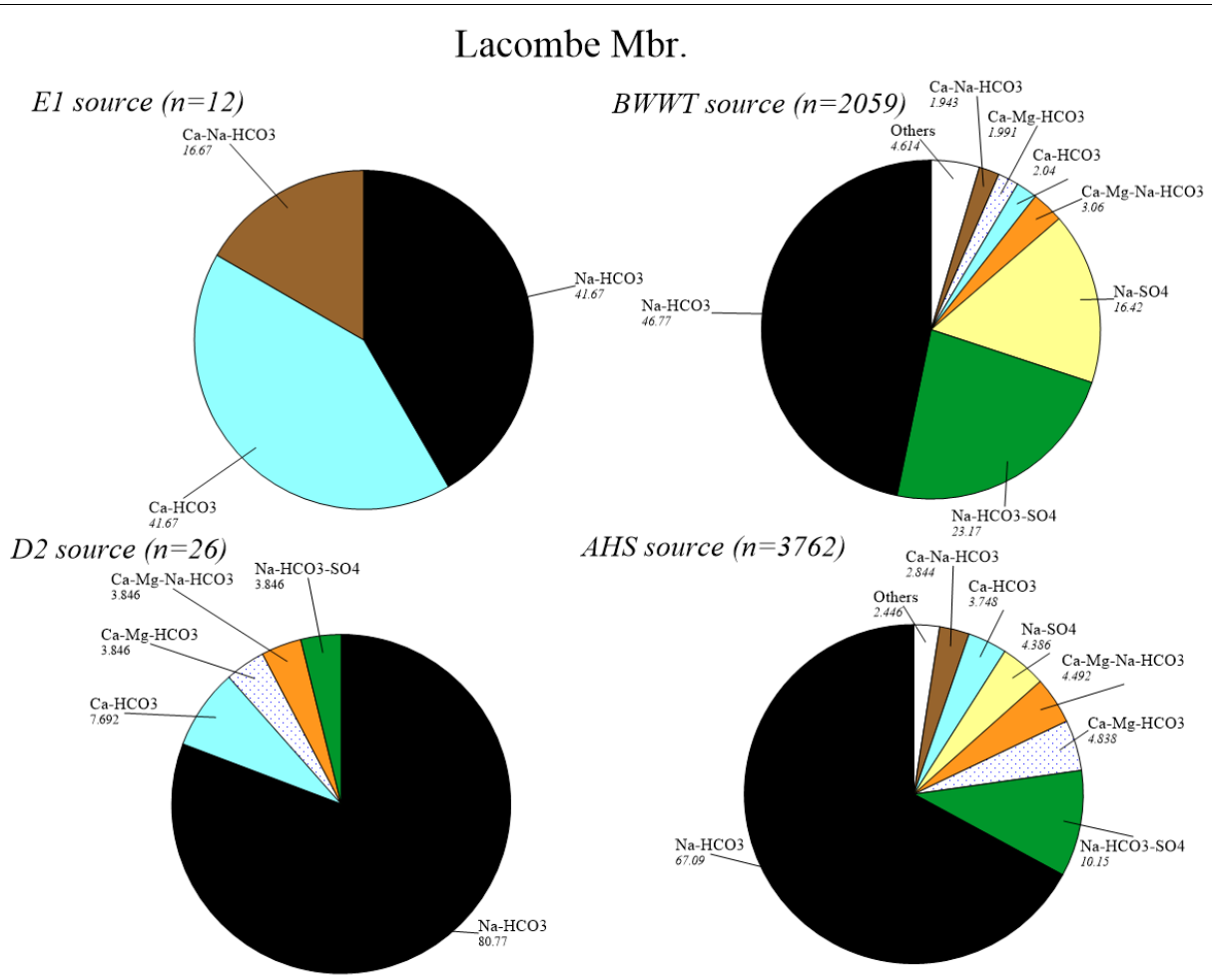

Figure 18: Pie charts of water type characterization of groundwater for the Lacombe Mbr. and inter-comparison between E1, D2, BWWT and AHS datasets.

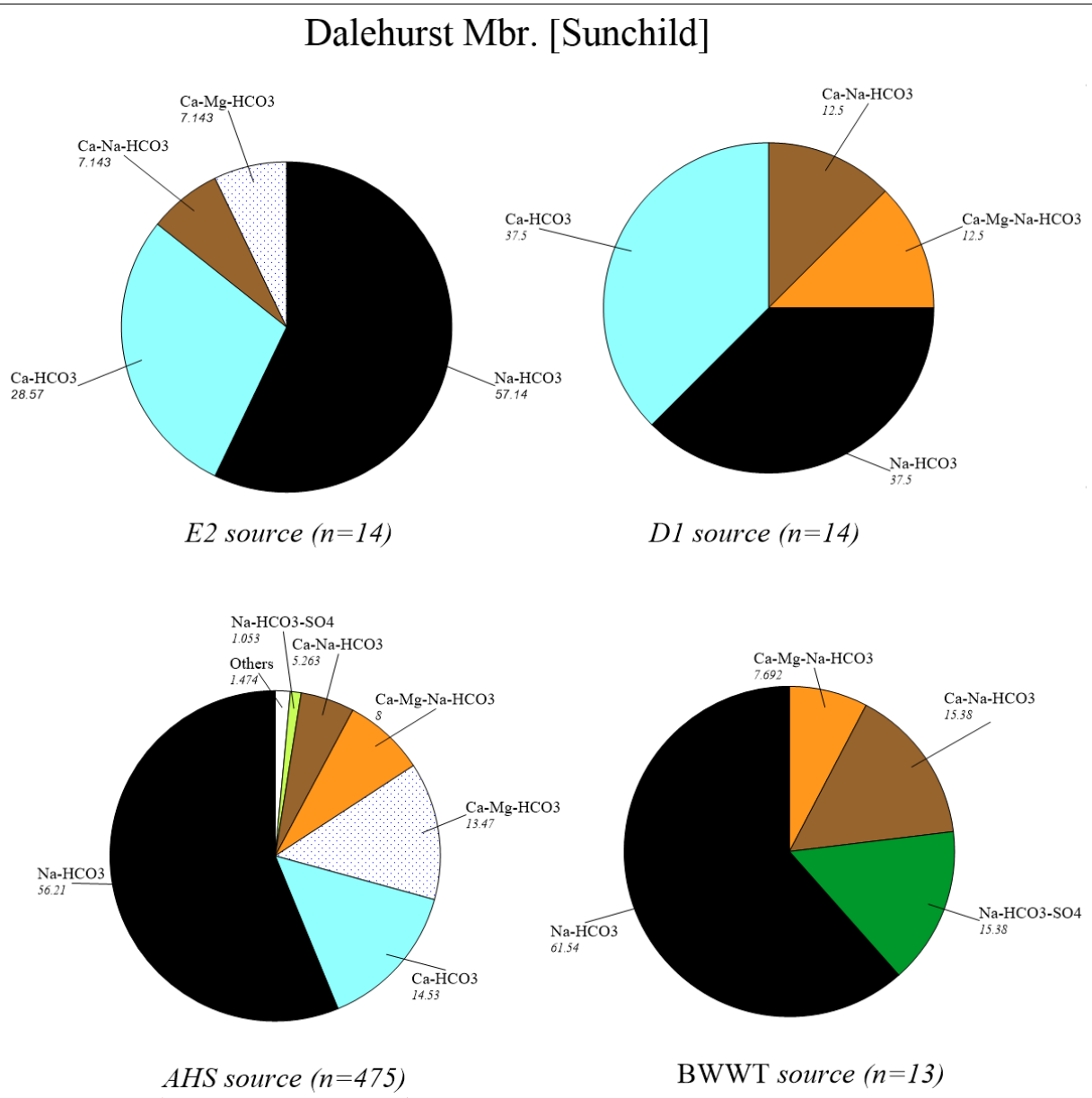

Figure 19: Pie charts of water type characterization for groundwater from the Dalehurst Mbr. (Sunchild aquifer) and inter-comparison between E2, D1, AHS, and BWWT datasets.

A characteristic pattern of water types has been identified for most of the geological formations in which groundwater wells are completed and weak variations of chemical compositions with depth have been found. In the following section a hydrochemical assessment was carried out in order to investigate the variation in chemical compositions of groundwater systems related to hydrogeological settings.

2.4 Relation to hydrogeological settings

2.4.1 Potentiometric surface and geospatial analysis

A potentiometric surface represents the height to which water in a confined aquifer would rise if a well was placed into the aquifer and provides a basis to predict groundwater flow direction. Groundwater generally flows from areas of high elevation (or potential) to areas of low elevation. The potentiometric surfaces of the Scollard and Horseshoe Canyon Fms. were available for download from the AGS digital data resource as part of the Calgary-Lethbridge corridor hydrostratigraphic model. The Paskapoo potentiometric surface is not yet available through the AGS and therefore could not be incorporated into these maps. The overlain red arrows indicating groundwater flow direction were adapted from a report by Bachu and Michael (2002) on the hydrogeology of the Upper Cretaceous – Tertiary strata of Alberta. Groundwater flow direction in the Paskapoo Fm. was inferred solely from Bachu and Michael (2002). The direction of groundwater flow in the Horseshoe Canyon Fm. was mainly interpreted from Bachu and Michael (2002) although a comparison was also made to the limited potentiometric surface extent available from the AGS. For the Scollard Fm., the potentiometric surface was utilized to best deduce groundwater flow direction. Mapping of groundwater type distribution by hydrogeological zone was carried out using ArcGIS.

2.4.2 AHS dataset case study

Figures 20 a) and c) show the potentiometric surface for the Scollard and Horseshoe Canyon Fms., respectively, provided by the AGS with overlain red arrows indicating the general groundwater flow direction (from Bachu and Michael, 2002).

Horseshoe Canyon Formation

In general, the regional groundwater flow in the Horseshoe Canyon Fm. (Edmonton Group) appears to be toward the east-northeast according to Bachu and Michael (2002). The potentiometric surface map from AGS reveals high elevations (>1300 m asl) in the south and in the west and lower elevations (around 790 m asl) in the northeast of the map. Horseshoe Canyon Fm. discharge seems to take place at lower elevations at the subcrop and outcrop of the Horseshoe Canyon Fm. General agreement in terms of hydraulic heads and groundwater flow have been found between the Bachu and Michael (2002) and AGS sources. However, certain local potentiometric surface highs were found especially in the southern part of the map, south of the Lethbridge area that were not identified in Bachu and Michael (2002) due to lack of data.

The groundwater wells completed in the Horseshoe Canyon Fm. show very few Ca-rich groundwater types that are located west of Lethbridge and east of Calgary (black dots, Figs. 20c and d). The water chemistry profile suggests that the water moving through the shallower portion of the Horseshoe Canyon Fm. has undergone geochemical transformations that have converted Ca-Mg-rich groundwater to Na-rich water types and in consequence Na-HCO_3-SO_4 and Na-HCO_3 water types are dominant in this groundwater system. The occurrence of Na-HCO_3-Cl water type has also been found (purple dots) that indicate perhaps a local flow system with input of Cl through mixing with deeper formation(s) or anthropogenic modifications.

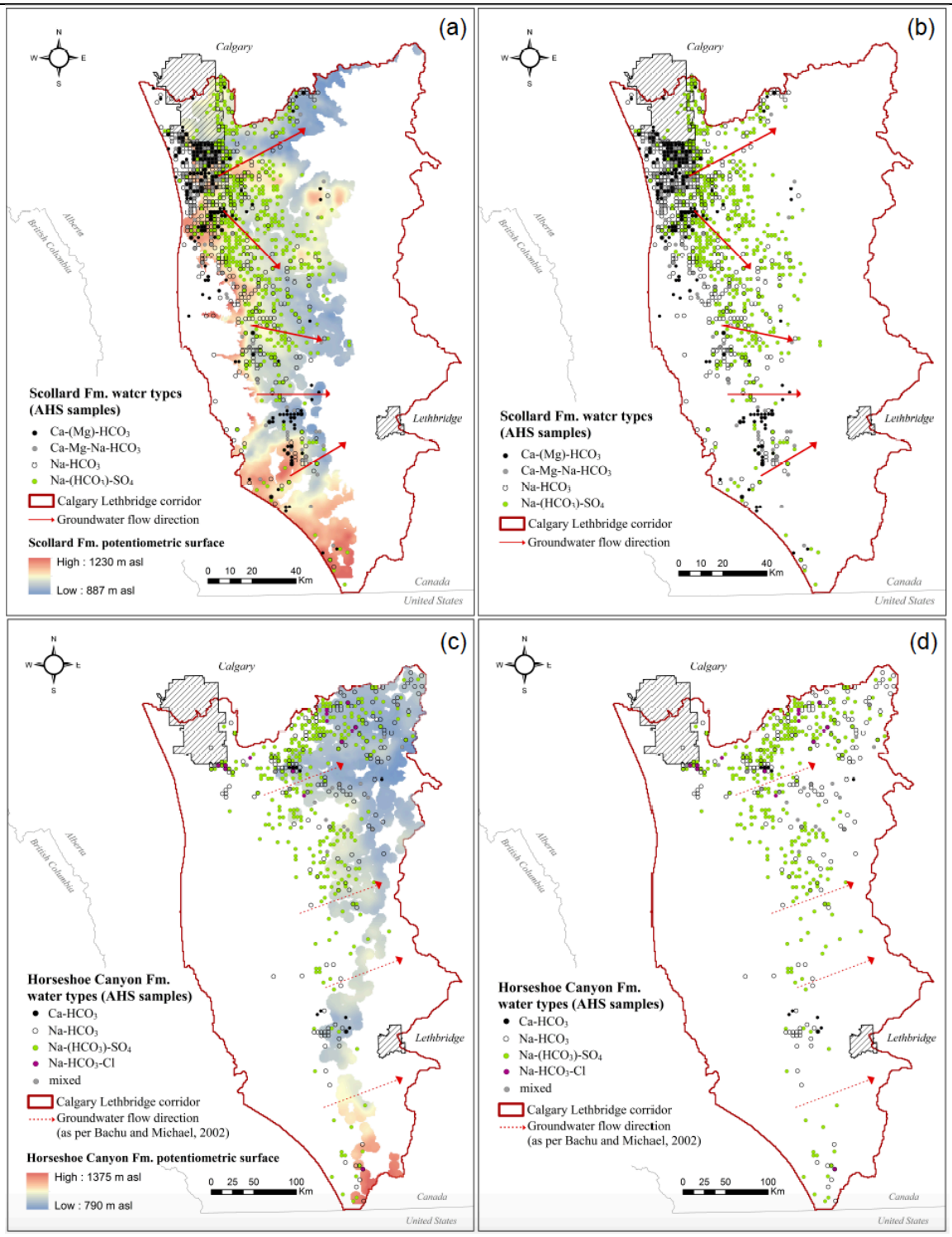

Figure 20: Evolution of AHS groundwater sample water types in the Horseshoe Canyon and Scollard Fms. and potentiometric surface maps from AGS. Overlain red arrows indicate the regional groundwater flow direction as per Bachu and Michael (2002).

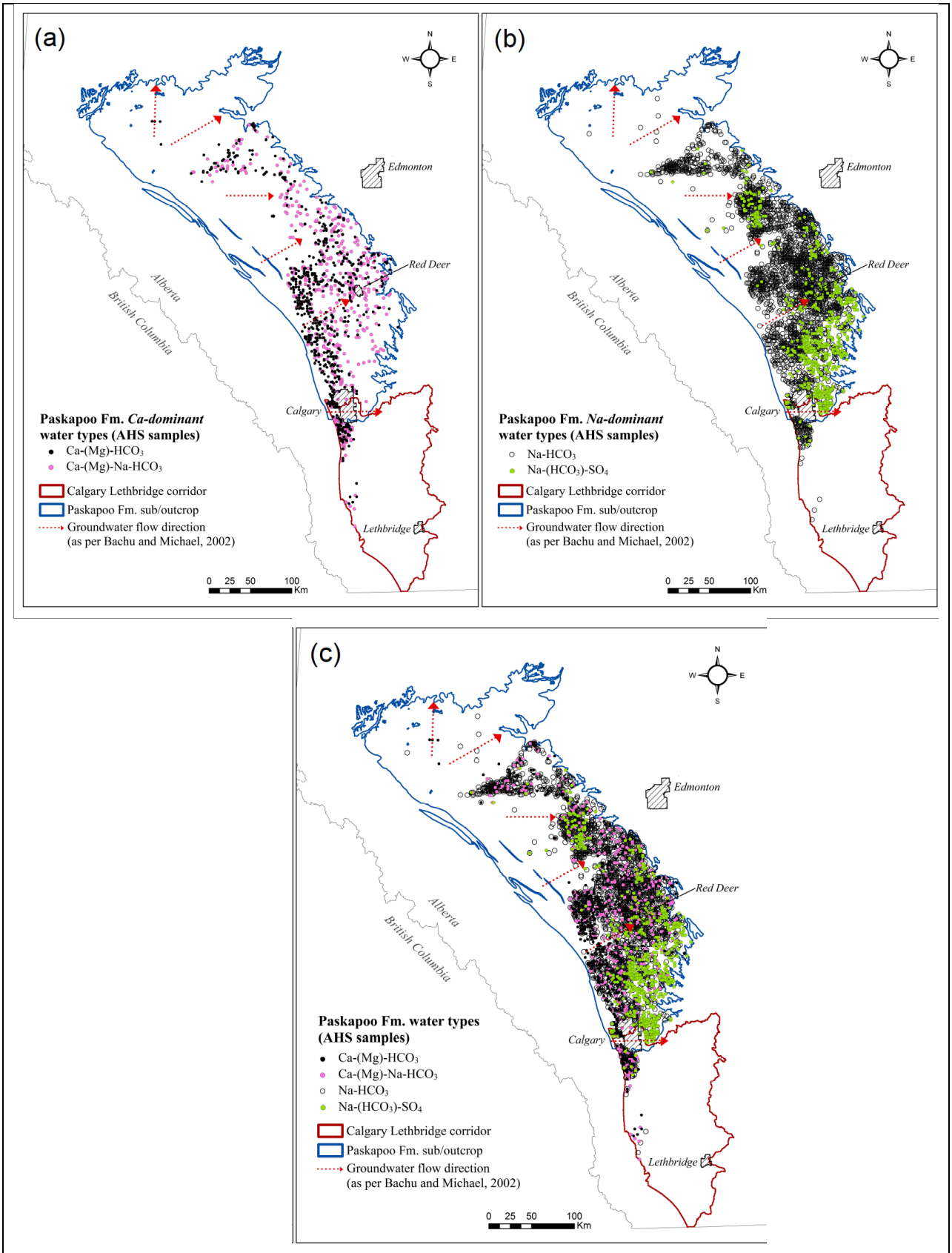

Figure 21: Hydrochemical facies of the Paskapoo Formation subdivided into a) Ca-rich groundwater and b) Na-rich groundwater and c) both for AHS dataset. Groundwater flow directions were reported from Bachu and Michael (2002).

Scollard and Paskapoo formations

The Scollard and Paskapoo hydrostratigraphic units contain most of the data points for the AHS data set. The general groundwater flow direction appears to be toward the northeast according to Bachu and Michael and the potentiometric surface data from AGS (Figs. 20 and 21).

For the Scollard Fm., access to the potentiometric surface allowed for the assessment of groundwater flow within this groundwater system from high elevations (>1200 m) in the west to the lower elevation (around 887 m) along the northeast. This map clearly demonstrates that the chemical compositions of the groundwater evolve along the flow path from a Ca-HCO_3 type towards Na-HCO_3-(SO_4) water types. The hydrogeochemical conceptual model infers that carbonate dissolution during recharge leads to one end-member, a Ca-HCO_3 type water, which further evolves along its flow path. Local higher elevations were found in the southeast of Calgary (>1000 m).

Unfortunately access to the potentiometric surface data for Paskapoo aquifer was not available with AGS. According to Bachu and Michael (2002) flow within the Paskapoo aquifer is in equilibrium with and driven by the topography from recharge areas at high elevation near the thrust and fold belt (deformation front) to discharge area in the east-northeast. Due to the high density of groundwater wells and their associated water types, three maps were generated: a) displaying Ca-dominant groundwater; b) Na-dominant groundwater; c) compiling both a+b maps (Fig. 21). The Figures reveal that the Ca-HCO_3 water type is mostly found close to the recharge area while Na-HCO_3-SO_4 is found along the flow path. Ca-Na rich groundwater types were found along the flow path and can be attributed to the mixing effect between different water types.

2.4.3 BWWT

The groundwater wells from the BWWT dataset are located in a very narrow corridor between Edmonton-Calgary making the interpretation of the hydrochemical maps challenging.

Horseshoe Canyon Formation

According to the potentiometric surface of the Horseshoe Canyon Fm. provided by AGS, Na-HCO_3, Na-SO_4 and Na-Cl water types from the Horseshoe Canyon Fm. correspond to areas of lower potential. The occurrence of a Na-Cl water type in a low potential area requires further investigation in order to understand its origin as no recharge from aquifers below the Horseshoe Canyon Fm. seem to occur based on potentiometric surface data (Fig. 22).

Scollard and Paskapoo formations

The Na-HCO_3, Na-SO_4 and Na-Cl water types from BWWT groundwater samples collected from the Scollard Fm. show that these more mature groundwater types are found in the lower elevation (900 m) aquifers (Fig. 22).

No obvious trend was found regarding the evolution of water types in relation to hydrogeological settings within the Paskapoo Formation. This is likely due to the broad physical heterogeneity of the Paskapoo Fm. that not only impacts water production but the geochemical signature of the Paskapoo Formation groundwater as well (Grabsy et al., 2008; Fig. 23).

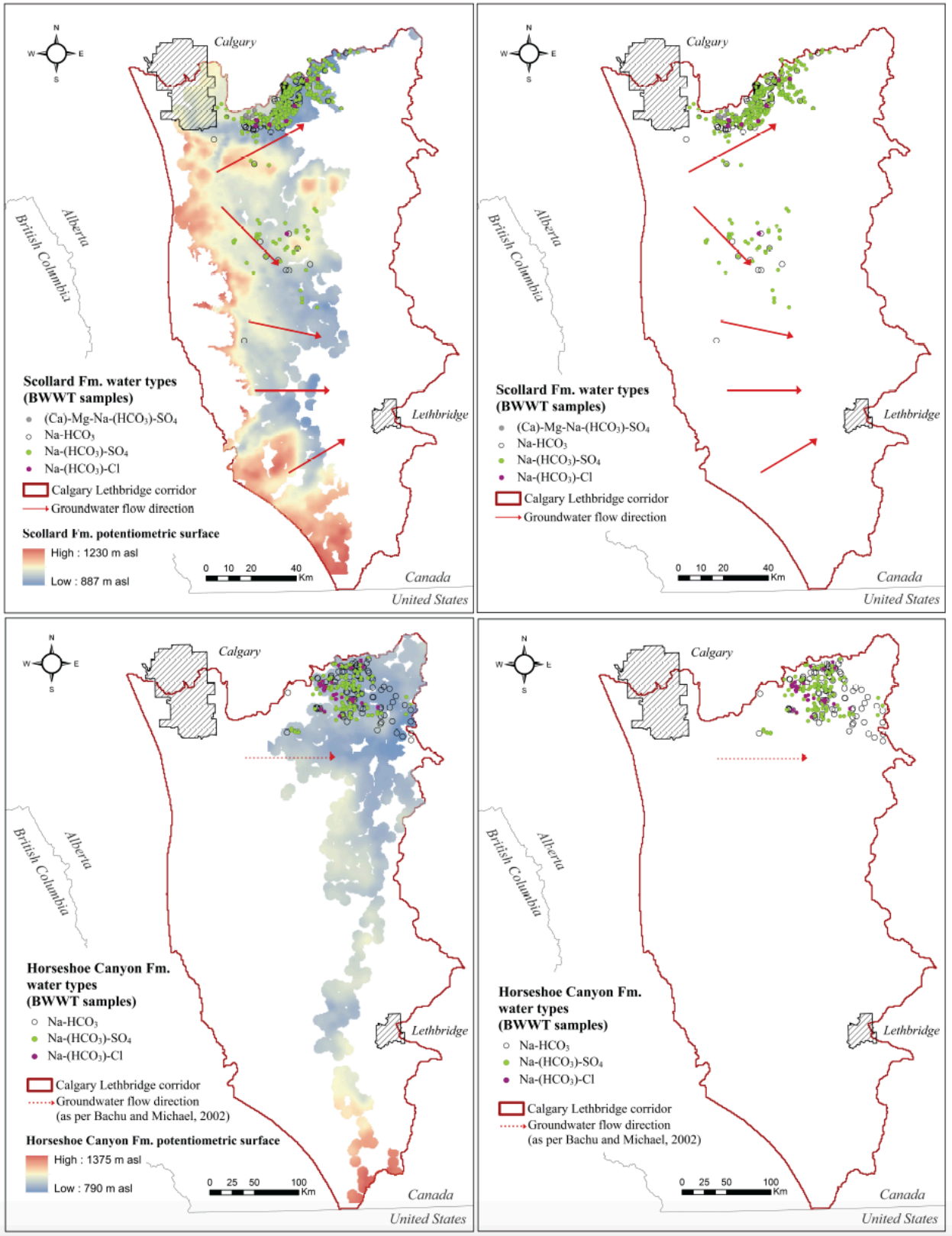

Figure 22: Evolution of the BWWT groundwater sample water types in the Horseshoe Canyon and Scollard formations and potentiometric surface maps from AGS. Overlain red arrows indicate the regional groundwater flow direction as per Bachu and Michael (2002).

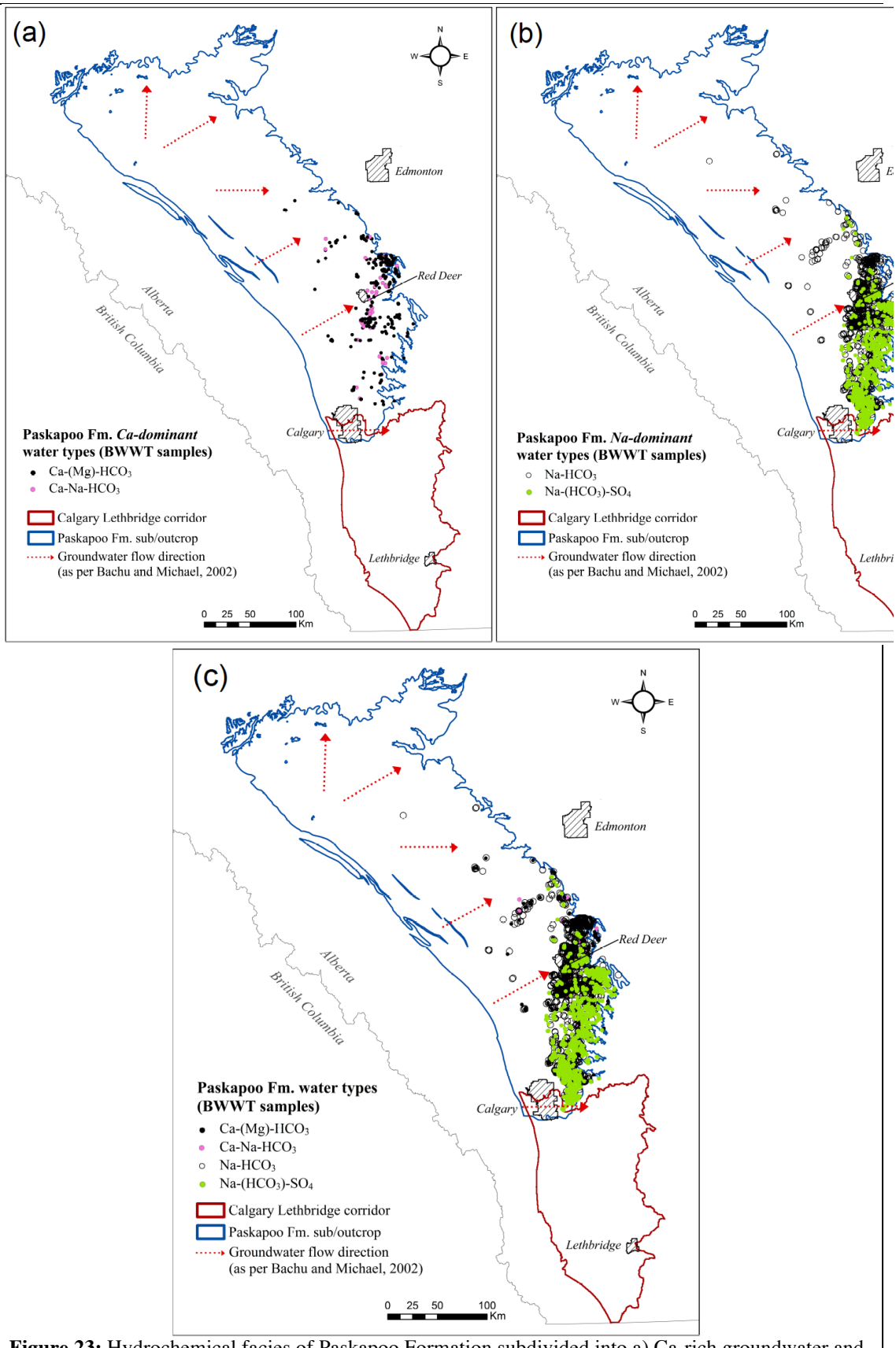

Figure 23: Hydrochemical facies of Paskapoo Formation subdivided into a) Ca-rich groundwater and b) Na-rich waters and c) both for BWWT dataset. Groundwater flow directions were reported from Bachu and Michael (2002).

Milestone 2 has been achieved for the industry, AHS and BWWT data. Realizing the importance of sulfate in classifying water types and the ability to distinguish Na-SO_4 from Na-Cl water types, we developed a refined classification model called "PHO matrix" presented in section 2.1 to provide a detailed list of potential water type combinations that describe groundwater chemistry of the different samples investigated in this project. In-depth analysis revealed that the deepest groundwater wells are frequently associated with samples characterized by Na-HCO_3 water types. We found no major differences in dominant water types between groundwater obtained from different geologic units. The three ubiquitous Na-rich water types Na-HCO_3, Na-HCO_3-SO_4 and Na-SO_4 were dominant in all geologic units from the Belly River Gp. to the Paskapoo Fm. Hydrogeochemical maps for AHS and BWWT were also generated to identify the relationship between water types and groundwater flow and recharge/ discharge zones for the main geological formations from which the groundwater samples were collected.

3 Milestone 3: The data evaluation will subsequently focus in particular on the occurrence, variability and source of methane in shallow groundwater.

3.1 Methane and higher alkane chain occurrences in groundwater samples

The investigation of occurrence of methane in free gas samples is limited to the BWWT database, since the industry and AHS data do not contain information on free gases. The gaseous data from the BWWT database were subjected to QA/QC procedures (Tables 1 and 8). The QA/QC criteria consist of (i) methane-containing-gas concentrations are above their respective detection limits of 0.0001, 5, 10 and 100 ppmv respectively (n=1610). (ii) gas concentration balanced e.g. the sum of the gas components in the free phase is 100 ± 10 % and thus the total gas concentration varies from 900,000 to 1,100,000 ppm (v/v) (n=1250); (iii) to minimize the risk of biased data due to air contamination, samples with >4% of oxygen content were discarded. These QA/QC procedures resulted in 787 free gas samples that contain n-alkane geochemical information including methane concentration (n= 787) and associated carbon isotope ratios (n= 517), ethane concentration (n=364) and its carbon isotope ratios (n=253), propane concentration (n=106) and higher alkane concentration such as butane (n=7). The gas dryness parameter defined as the ratio between concentrations of methane / higher n-alkanes was also determined. Further information on free gas samples in the BWWT database is summarized in Table 8.

Table 8: Inventory of wells and aqueous and free gas samples contained in the BWWT database.

	Total	Free Gas bulk	Free Gas QA/QC with CH_4 data	Aqueous bulk	Aqueous QA/QC
# of samples in total	14252	1705 total including 1697 with CH_4	787 with $conc_{CH4.} > DL$ 15 with $conc_{CH4.} = DL$ 6 with $conc_{CH4.} < DL$	14052	13583
# of samples with well identification number	7237	922	419	7153	6957
# of samples with isotopic data		541-1015	281-518		
# of wells sampled once	4265	691	354	4239	4149
# of wells sampled more than once	Duplicates (1125) Triplicates (183) 4-replicates (42) 5-replicates (1)	Duplicates (86) Triplicates (17) 4-replicates (2)	Duplicates (29) Triplicates (1) 4-replicates (1)	2914	2792
# of wells with pre test samples (= baseline)		Single (269) Duplicates (17) Triplicates (1)	Single (93) Duplicates (4)	2545	2494
# of wells with post test samples		7	6	19	19
# of wells with pre and post tests samples		1	0	5	5

Evaluation of data from the BWWT database revealed that methane is ubiquitous in free gas samples obtained from groundwater sampled predominantly in the Edmonton-Calgary corridor. Methane concentrations in free gas samples ranged from <10 ppmv to >1,000,000 ppmv. A limited number of repeat analyses of the composition of free gas samples obtained from the same wells (n=31, Table 8)

enabled the assessment of temporal variabilities of methane concentrations. Methane concentrations in the replicate samples were found to be quite variable with coefficients of variation from 0.3 to 129 %.

Methane was detected in 787 of 808 free gas samples (97.4 %) with concentrations above the detection limit. Only 15 QA/QC free gas samples with methane data had concentrations equal to the detection limits and 6 QA/QC free gas samples with methane data showed methane concentrations below the detection limits. These 21 QA/QC free gas samples with concentration below the detection limits for methane were discarded from the dataset. Box-Whisker plots summarizing the distribution of concentrations of methane and higher alkanes are provided in Fig. 24a.

The methane concentrations in free gas samples have median and mean values of 543,300 and 454,699 ppmv (n= 787). The first (Q1) and third quartile (Q3) values for methane concentrations are 2,625 and 837,050 ppmv respectively. This variable has a non-normal distribution (p< 0.05).

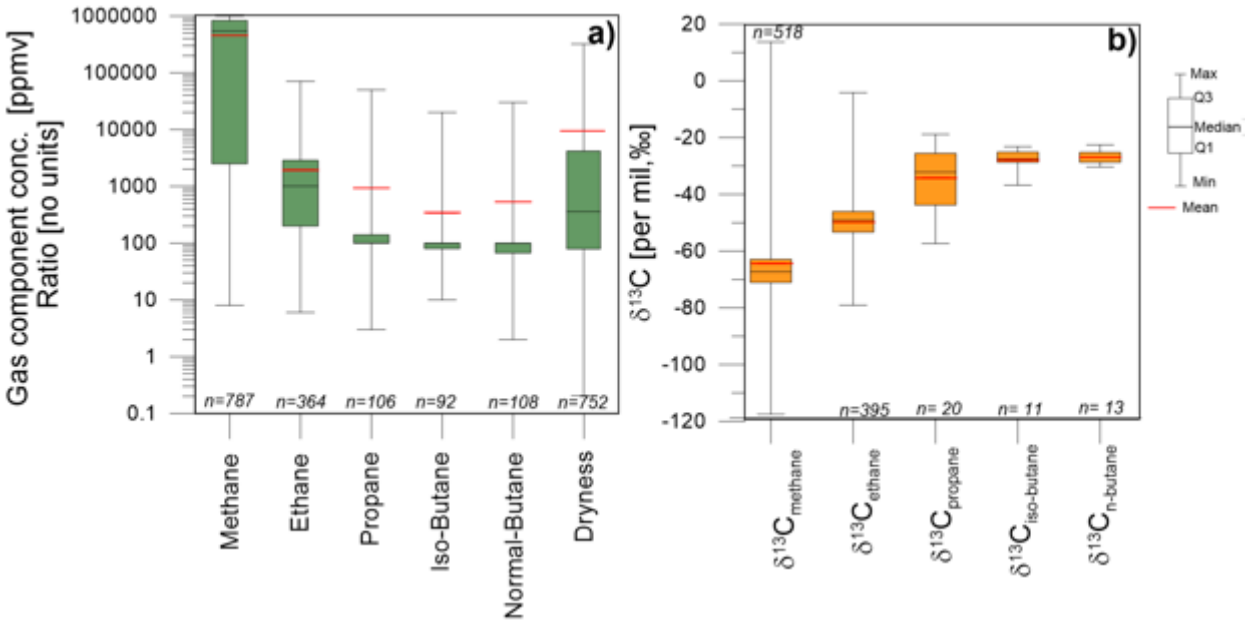

Figure 24: a) Box-Whisker plots displaying concentrations of methane and higher alkane chain components and the dryness parameter with Q1, Q2, and Q3 values shown in the box; arithmetic mean values are shown as red lines; b) Box-Whisker plots depicting $\delta^{13}C$ values of methane and higher alkanes chain components with Q1, Q2, and Q3 values shown in the box; arithmetic mean values are shown as red lines.

Ethane was detected in 364 free gas samples with reliable concentration data above the detection limits, while 444 free gas samples had reported ethane concentrations equal or below the detection limits and these samples were not considered in the descriptive statistics. Ethane concentrations in free gas samples have median and mean values of 1,007 and 1,928 ppmv (n=364). The first (Q1) and third quartile (Q3) values for ethane concentrations are 200 and 2,861 ppmv respectively (Fig. 24a). The highest reported ethane concentration was 70,500 ppmv. This variable has a non-normal distribution (p< 0.05).

Propane was detected in 106 free gas samples with concentrations above the detection limits while 702 free gas samples had reported propane concentrations equal or below the detection limits and hence these samples were not included in the descriptive statistics. Propane concentrations in free gas samples have median and mean values of 100 and 931 ppmv, respectively. The first (Q1) and third quartile (Q3) values for propane concentrations are 100 and 132 ppmv, respectively (Fig. 24a). The highest reported propane concentration was 50,000 ppmv. This variable has a non-normal distribution (p< 0.05). Iso-butane was detected in 92 free gas samples with concentrations above the detection limits, while 716 free gas samples had reported iso-butane concentrations equal or below the detection limits and hence these samples were not included in the descriptive statistics. The median and mean iso-butane concentrations are 100 and 345 ppmv, respectively (n=92). The first (Q1) and third quartile (Q3) values for iso-butane concentrations are 87 and 100 ppmv respectively (Fig. 24a). This variable has a non-normal distribution (p< 0.05). Normal butane was detected in 108 samples with concentrations above the detection limits, while 700 free gas samples had reported normal butane concentrations equal or below to the detection limits and were thus

not included in the descriptive statistics. The median and mean normal butane concentrations are 532 and 100 ppmv, respectively (n=108). The first (Q1) and third quartile (Q3) values for normal butane concentrations are 69 and 100 ppmv respectively (Fig. 24a). This variable is has a non-normal distribution ($p < 0.05$).

The dryness parameter was calculated for 752 samples. For free gas samples with concentrations of higher alkanes at or below the detection limit, the detection limit value was used for this calculation. Therefore, the reported dryness parameters may be underestimated in many cases and additional variability is introduced due to different detection limits reported by different laboratories. The dryness parameter in free gas samples has median and mean values of 350 and 9,274 respectively (n=752). The first (Q1) and third quartile (Q3) values for the dryness parameter are 77 and 4,029. A total of 338 free gas samples had a dryness parameter > 500 (Fig. 24a).

3.2 Methane occurrence versus water types

Combining the gaseous data passing the QA/QC tests with aqueous geochemistry data results in 762 groundwater samples containing methane. Table 9 shows that the highest concentrations of methane in free gas samples were observed in groundwaters belonging to Na-HCO_3, Na-HCO_3-Cl and NaCl water types. In these water samples, the average methane concentrations varied between 502,337 and 901,878 ppmv and the median methane concentrations ranged between 634,100 and 920,000 ppmv, respectively. Sulfate-containing water types were characterized by much lower mean and median methane concentrations (<150,000 ppm) and the lowest concentrations of methane belong to Na-SO_4, Ca-(Na)-HCO_3 or a mixture of these water types.

For the industrial data, only source D provided methane concentrations, however for dissolved methane rather than methane in free gas. Methane was detected in 7 samples comprising 22% of all samples from source D-1 with concentrations above the detection limit. The methane concentrations varied from 0.007 mg/L ($0.44*10^{-3}$ mmol/l) to 6.34 mg/L (0.39 mmol/l). Six of the 7 methane-containing samples (>85%) belong to a Na-HCO_3 water type, whereas the only other methane-containing sample was associated with a Ca-Na-HCO_3 water type. Source D-2 contains 23 water samples with detected methane concentrations representing 21% of all samples from this source (D-2). The concentration of dissolved methane varied from 0.02 mg/L ($1.24*10^{-3}$ mmol/l) to 4.39 mg/L (0.27 mmol/l). Eighteen of the 23 methane-containing samples (>78%) belong to a Na-HCO_3 water type, whereas the other methane-containing samples were associated with Ca-Na-HCO_3 and Ca-Mg-HCO_3 water types.

Table 9: Relationship between water types, methane concentrations in free gas samples, and TDS of groundwater samples in the BWWT dataset (n=762).

Water type combination	N	%	CH4 Median [ppmv]	CH4 Mean [ppmv]	TDS Mean [mg/L]	TDS Median [mg/L]
Na-HCO_3	**519**	**68**	634,100	502,337	760	735
Na-HCO_3-SO_4	97	**13**	750	92,637	1,104	957
Na-HCO_3-Cl	52	**7**	838,250	802,622	876	885
Na-Cl	31	**4**	920,000	901,878	1,193	1,100
Na-SO_4	33	**4**	320	95,363	2,088	1,680
Ca-Na-HCO_3	8	**1**	186	373	561	474
Ca-HCO_3	1	**0**	31	31	807	807
Others*	21	**3**				
Total	762	**100**				

*Ca-Mg-Na-HCO_3 (4), Ca-Mg-HCO_3 (4), Ca-Na-HCO_3-SO_4(1), Na-HCO_3-SO_4-Cl (3), Ca-Mg-Na-SO_4(3) etc.

3.3 Is there any relation between methane concentrations and geological formations in which the water wells are completed?

3.3.1 Total depth criteria

The geological formation assignment methods permit to establish potential relations between methane concentrations and geological formation for the BWWT, D1 and D2 datasets (Fig. 25). For BWWT, Fig. 25a shows that the highest methane concentrations were observed in groundwater from the Horseshoe Canyon Fm. with a median of 744,000 ppmv (n=24), followed by Lacombe Mbr. with a median of 345,720 ppmv (n=99), the Haynes Mbr. with a median of 21,170 ppmv (n=35) and the Scollard Fm. with a median of 310 ppmv (n =41) and Post-Paleocene deposits with a median of 320 ppmv (n=19). However, the methane concentrations obtained for D1 and D2 do not show any trend or cluster when compared with the internal hydrostratigraphic units of the Paskapoo Formation (Fig. 25b and c).

A Kruskal Wallis test showed that there was a statistically significant difference in methane concentrations between groundwaters from different geological formations for the BWWT dataset $\chi^2(4) = 40.002$, $p<0.05$. A post hoc test was performed to determine where any difference lies between geological formations/ members (Table 10).

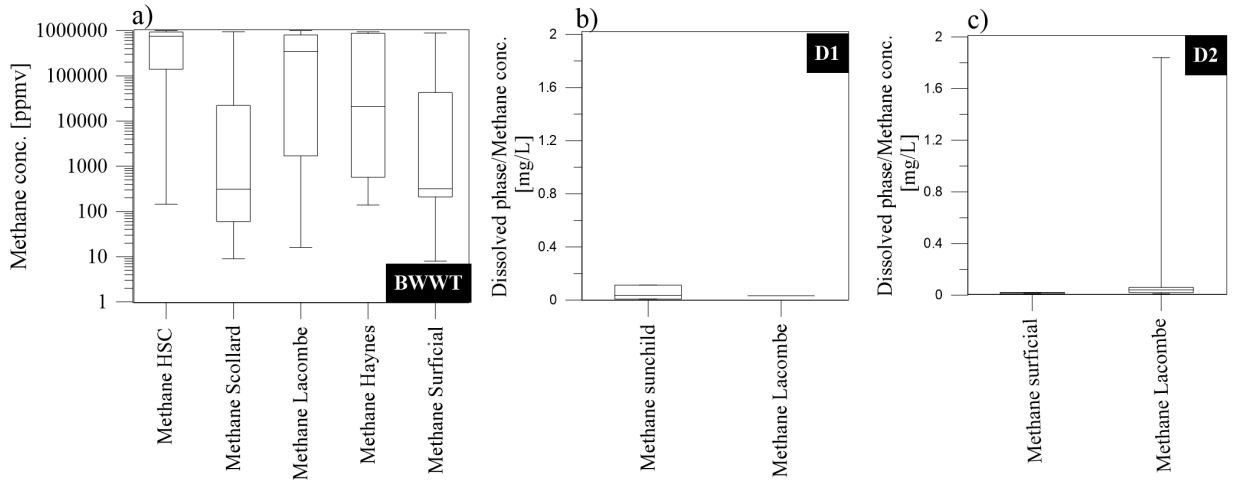

Figure 25: Occurrence of methane in groundwater depending on the different geological formations based on total depth a) methane concentrations in the free gas phase [ppmv] from BWWT b) methane concentrations in the dissolved gas phase from D1 and D2.

A Mann-Whitney test indicated that there are statistical differences in methane concentrations in groundwater obtained from: Horseshoe Canyon Fm. and Scollard Fm.; Horseshoe Canyon Fm. and Lacombe Mbr.; Horseshoe Canyon Fm. and Post-Paleocene deposits. In all these binary relations the groundwater from the Horseshoe Canyon Fm. shows statistically significantly higher methane concentrations.

Table 10: Non-parametric Mann-Whitney tests results to assess statistical differences between methane occurrences within different geological formations based on total depth criteria from BWWT dataset. In bold the statistical difference between two geological formations ($p<0.05$)

	HSC	Scollard	Lacombe	Haynes	Post-Paleocene
HSC					
Scollard	**<0.05**				
Lacombe	0.014	**<0.05**			
Haynes	0.061	**<0.05**	0.929		
Post-Paleocene	**<0.05**	0.404	**<0.05**	0.014	

Statistical differences in groundwater methane concentrations have been observed between: Lacombe Mbr. and Scollard Fm.; Lacombe Mbr. and Post-Paleocene deposits with the Lacombe Fm. having groundwater with higher methane concentrations in the geological formation pairs. Finally, a statistical difference in methane concentration was observed between Haynes Mbr. and Post-Paleocene deposits with higher methane concentration reported in groundwater from the Haynes Mbr. compared to the Post-Paleocene deposits.

There are no significant statistical differences for methane concentrations in groundwater between Lacombe Mbr. and Haynes Mbr., Scollard Fm. and Post-Paleocene deposits with p=0.929 and p=0.404 respectively.

3.3.2 Completion interval criteria

Although groundwater wells with completion interval information are scare, some information from BWWT was extracted and the distribution of methane concentration was investigated (Fig. 26). A K-Wallis test was performed to assess if any statistical difference exists in methane concentration distribution and geological formation based on completion intervals. The test indicates that there was a statistically significant difference in methane concentration between the different geological formation $\chi^2(4) = 16.691$, $p < 0.05$ (Table 11).

Table 11: Non-parametric Mann-Whitney tests results to assess statistical difference between methane occurrences within different geological formations based on completion intervals from BWWT dataset. In bold the statistical difference between two geological formations ($p<0.05$)

	Post-Paleocene	Lacombe	HSC	Haynes	Scollard
Post-Paleocene					
Lacombe	0.047				
HSC	**<0.05**	0.224			
Haynes	0.354	0.072	0.03		
Scollard	0.562	**<0.05**	**<0.05**	0.05	

A Mann-Whitney test reveals that there is a statistical difference between Post-Paleocene and HSC, Scollard and Lacombe, HSC and Lacombe. The statistical results based on completion interval criteria are in agreement with those based on total depth criteria. Based on the completion intervals, some groundwater collected from the wells were mixed between different geological formations highlighted in grey in the Fig. 26 but were not present in a large enough numbers to be integrated in the statistical tests.

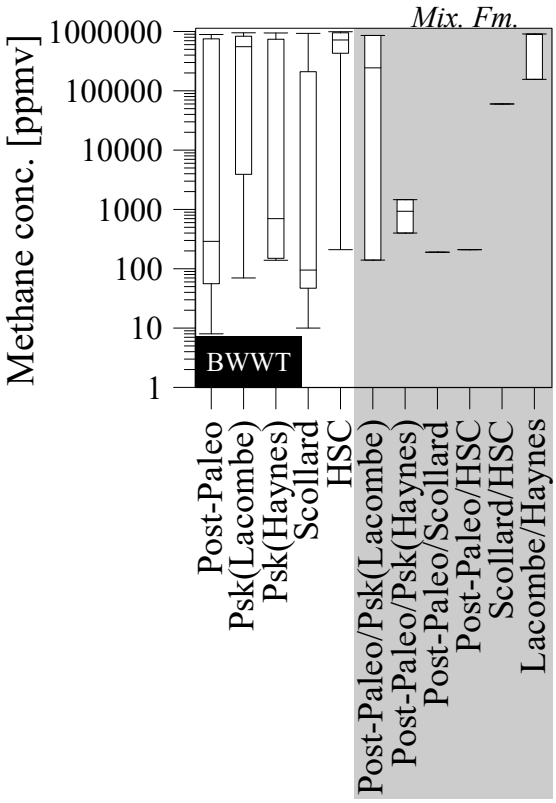

Figure 26: Occurrence of methane within the geological formations based on completion intervals from the BWWT dataset. In grey the mixture of different geological formations.

For the BWWT and the industrial databases D, milestone 3 has been achieved.

4 Milestone 4: Aqueous geochemistry data will be used to determine whether methane occurring in shallow groundwater was produced microbially in-situ by assessing the groundwater redox conditions. These rather common occurrences will be distinguished from more infrequent situations where methane transport from underlying stratigraphic units must be postulated.

4.1 Occurrence of methane and redox sensitive species in groundwater samples

4.1.1 BWWT and industrial databases (source D)

For the BWWT database, we compared the occurrence of methane in free gas samples with the occurrence and concentrations of terminal electron acceptors (TEAPs) such as O_2, NO_3, Mn, Fe, and SO_4 in the water samples. We found that in most samples (>90 %) the occurrence of elevated concentrations of methane was only identified in water samples where TEAPs such as O_2, NO_3, Mn, Fe, and SO_4 were either not present or occurred only in negligible concentrations (Fig. 27). Threshold concentrations werer selected in this study in order to help interpret geochemical patterns using the 95th percentile background values to detect case-specific limits especially between occurrence of methane concentration and redox sensitive species.

Typically, samples with elevated nitrate and sulfate concentrations did not contain any methane suggesting that elevated concentrations of TEAPs are not suitable for methane formation or preservation. Manganese and iron concentrations are reported as total concentrations and it seems that groundwater

with total elevated concentrations of Mn and Fe did not contain elevated methane concentrations. Geochemical speciation would be needed to associate their oxidation state e.g. Mn(II), Mn(IV), Fe(II), Fe(III) etc. Fig. 27 shows that only groundwater samples with nitrate concentration <0.01 mM contained elevated methane concentrations. Only four samples showed elevated methane concentrations and elevated nitrate concentrations of > 0.01 mM (95th percentile).

Fig. 27 shows that groundwater samples with total manganese concentrations <0.001 mM contained elevated methane concentrations. Only one sample had an elevated Mn concentration in concert with a methane concentration of 900,000 ppmv. The reducing conditions imposed by the elevated concentration of methane would suggest that manganese would occur in its reduced form Mn(II). Geochemical speciation and stability diagrams (pH, pe) would thus be additional parameters needed.

Fig. 27 shows that groundwater samples with total iron concentrations <0.005 mM contained elevated methane concentrations. Only two samples had an elevated Fe concentration in concert with a methane concentration of 700,000 and 900,000 ppmv. In such reducing conditions, it is probable that Fe occurs in its reduced form (Fe^{2+} concentration) due to Fe(III) reduction.

Fig. 27 shows that groundwater samples with sulfate concentrations <2 mM (95th percentile) contained elevated methane concentrations. Only a few samples had elevated SO_4 concentrations in concert with a methane concentration between 700,000 and 900,000 ppmv.

For most of the investigated samples, this is consistent with an in-situ formation of methane within the aquifer. An alternate explanation that also needs to be considered is the potential migration of methane into the aquifer thereby triggering removal of TEAPs via redox buffering reactions.

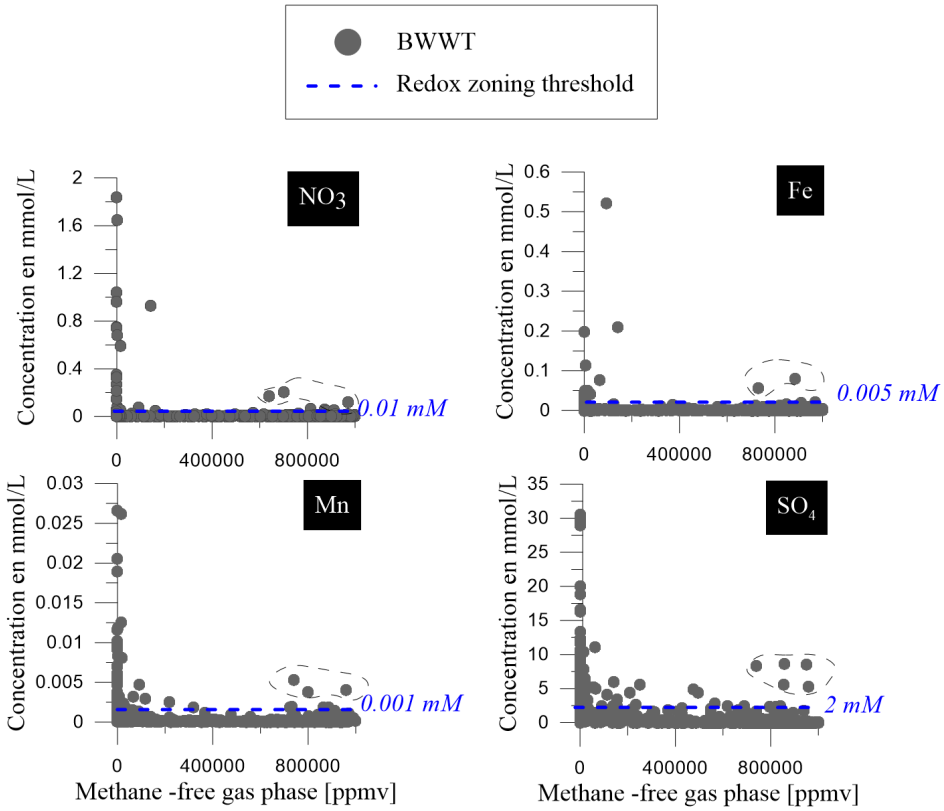

Figure 27: Relationships between concentrations of methane and TEAPs concentrations in BWWT water and free gas samples and identification of redox sensitive species thresholds that enable occurrence of methane (blue dashed lines based on 95th percentile method).

For industry data from source D, it has been found that >80% of the samples containing methane concentrations above the detection limit are associated with a Na-HCO_3 water type. This is consistent with findings from the much larger BWWT dataset. Similarly to the BWWT dataset, an inverse correlation

between methane and TEAPs concentrations is evident in Figs. 28 and 29. Typically, groundwater samples with elevated nitrate, manganese, iron, and sulfate concentrations did not contain any elevated dissolved methane concentrations. Figs. 28 and 29 shows the NO_3, Mn, Fe, and SO_4 redox zoning thresholds found in BWWT as blue dashed lines. For most of the studied TEAPs concentrations, these thresholds from BWWT seem to appear as upper limits and could be re-adjusted to lower limits using the industry data from source D-1. Figs. 28 and 29 show that only groundwater samples with sulfate concentrations < 1 mM contained elevated methane concentrations.

The BWWT and the industry source D databases permit to describe a range of redox zoning limits for groundwater from landowner wells below which the in-situ formation of methane via methanogenesis within the aquifer appears feasible. The redox thresholds or limits in BWWT are higher than those identified using samples from source D. Different hypotheses for variable redox thresholds include mixing of water from different redox zones due to long screen intervals or spatial heterogeneity of redox processes in a given hydrologic system.

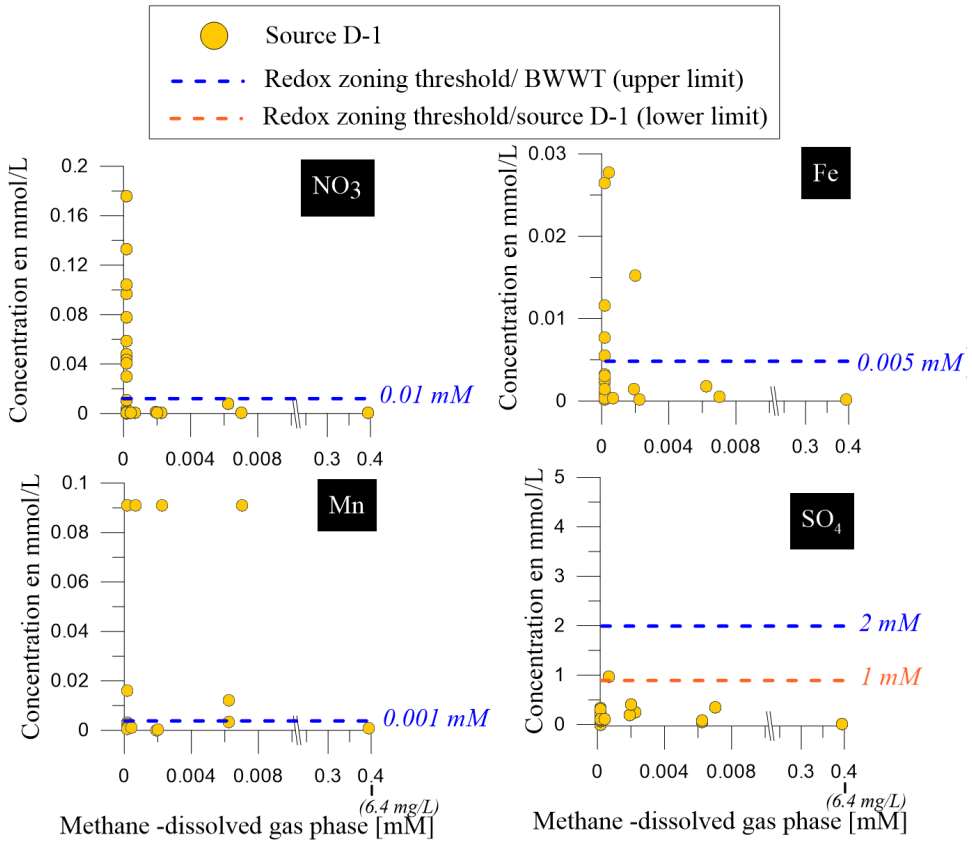

Figure 28: Relationships between redox sensitive species and methane concentrations in Source D-1 water and dissolved gas samples and identification of redox sensitive species thresholds that enable occurrence of methane (orange dashed lines).

4.1.2 AHS database

An assessment of water well samples from the AHS data set was completed to understand the occurrence, distribution, and concentrations of terminal electron acceptors (TEAPs) and to determine the redox classification and distribution for each sample. For the 60,562 groundwater samples, which passed the QA/QC test and had known depths and locations, TEAP concentration values (e.g. NO_3, Fe, SO_4) were used to assess the redox conditions. Groundwater samples with unknown concentrations were discarded which represent 127 samples out of 60,562 samples reducing the total number of groundwater samples to 60,435 and only concentrations above the respective limit of quantification (LOQ) were reported in the

descriptive statistics (see Table 12). Limitations of this database include the lack of Eh-measurements, dissolved oxygen data, and there are no methane concentrations. Another limitation is that well coordinates are only specified to the Dominion Land Survey section level. This means many of the samples have non-unique coordinates. Manganese concentrations were evaluated as part of the minor/trace element analysis. Due to the overlap in sample coordinates, it is only possible to link the trace element and major ion analyses in 23 wells (0.04%). For this reason the manganese concentrations reported in the minor/trace elements analyses were not integrated in the redox evaluation for the AHS dataset. The groundwater redox conditions for the AHS dataset were constrained based only on the NO_3, Fe, and SO_4 concentrations provided within the routine analysis data set.

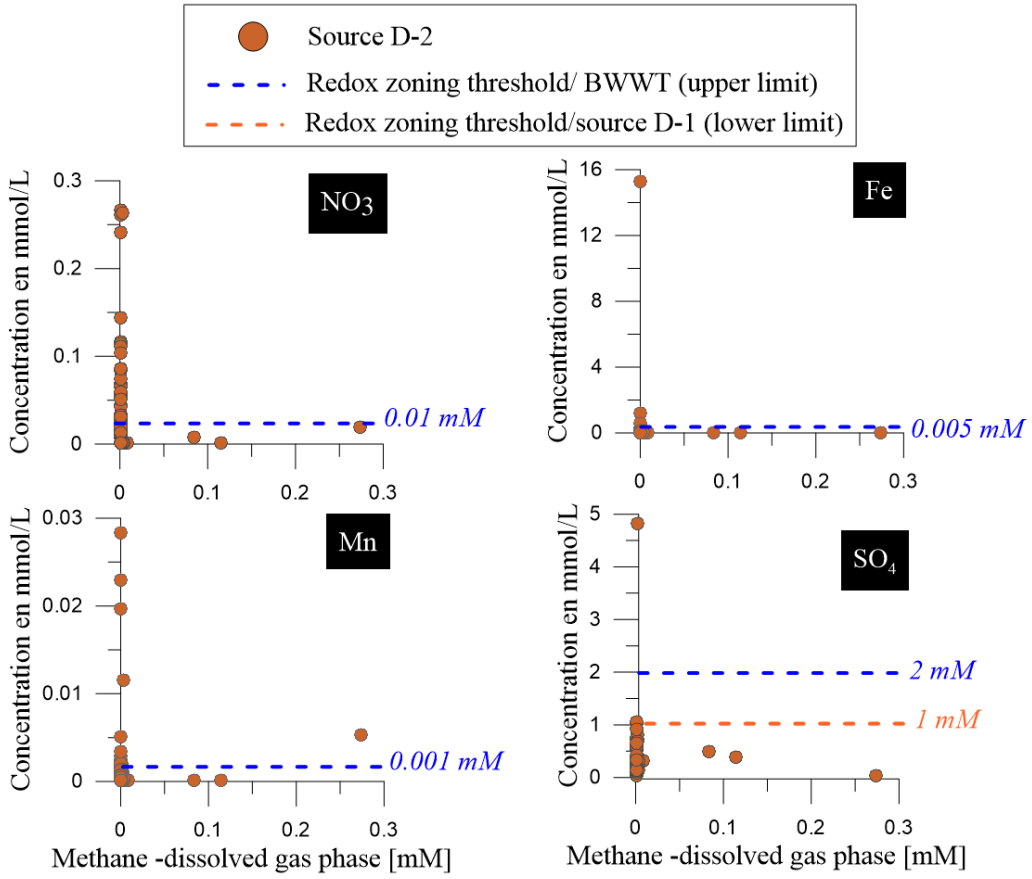

Figure 29: Diagrams showing relationships between concentrations of methane/nitrate, methane/manganese, methane/iron and methane/sulfate in industry source D-2 water and dissolved gas samples. Redox sensitive species thresholds that enable occurrence of methane from BWWT and Source D-2 are reported in blue/orange dashed lines

Table 12: The limit of quantification (LOQ) as reported for NO_3, Fe, and SO_4 and the number of samples less or greater than each TEAP's respective LOQ.

	LOQ		**N**	
	Reported value (mM)	*Reported value (mg/L)*	*≤LOQ*	*>LOQ*
NO_3	1.61×10^{-2}	1	51948	8487 (14.0%)
Fe	1.79×10^{-4}	0.01	13054	47381 (78.4%)
SO_4	1.04×10^{-2}	1	4992	55443 (91.7%)

Of the samples evaluated, 14.0% have a NO_3 concentration >LOQ with a minimum concentration value of 7.14 $x10^{-2}$ mM and a maximum concentration value of 21.4 mM (Table 12, Fig. 30).

Fe concentration values range from a minimum of $1.79x10^{-4}$ mM to a maximum of 1.90 mM with 78.4% of the samples having an Fe concentration >LOQ (Table 12, Fig. 30).

For SO_4, 91.7% of the samples have a concentration >LOQ with a minimum concentration value of $1.04x10^{-2}$ mM and a maximum of $1.71x10^{2}$ mM. The respective mean values for NO_3, Fe and SO_4 are $6.13x10^{-1}$ mM, $1.04x10^{-1}$ mM, and 2.13 mM and their standard deviations are 1.25 mM, $3.39x10^{-2}$ mM, and 3.77 mM (Tables 12 and 13, Figs. 30).

Table 13: NO_3, Fe, and SO_4 concentrations and the minimum, maximum, median, mean, IQR, and standard deviation values for each TEAP.

	Unit	**Min.**	**Max.**	**Mean**	**Median**	**IQR**	**Std. Dev.**
		>LOQ	*>LOQ*	*>LOQ*	*>LOQ*	*>LOQ*	*>LOQ*
NO_3	mM	$7.14x10^{-2}$	21.4	$6.13x10^{-1}$	$2.14x10^{-1}$	$5.14x10^{-1}$	1.25
	mg/L	4.43	$1.33\ x10^{3}$	38.0	13.3	31.9	77.8
Fe	mM	$1.79x10^{-4}$	1.90	$1.04x10^{-1}$	$1.61x10^{-3}$	$5.91x10^{-3}$	$3.39x10^{-2}$
	mg/L	$1.00x10^{-2}$	106	$5.80x10^{-1}$	$9.00x10^{-2}$	$3.30\ x10^{-1}$	1.89
SO_4	mM	$1.04x10^{-2}$	171	2.13	$9.04x10^{-1}$	2.08	3.77
	mg/L	1.00	$1.65x10^{4}$	205	86.8	200	362

Fig. 30 shows the distribution of NO_3, Fe, and SO_4 concentrations in the AHS data set. In the 8487 samples containing NO_3 >LOQ, there are 733 outliers (8.6%) defined as IQR x 3. Within the 47,380 samples containing Fe > LOQ, there are 6057 outliers (12.8%) and of the 55,441 samples containing SO_4 >LOQ, 4304 samples are outliers (7.8%)

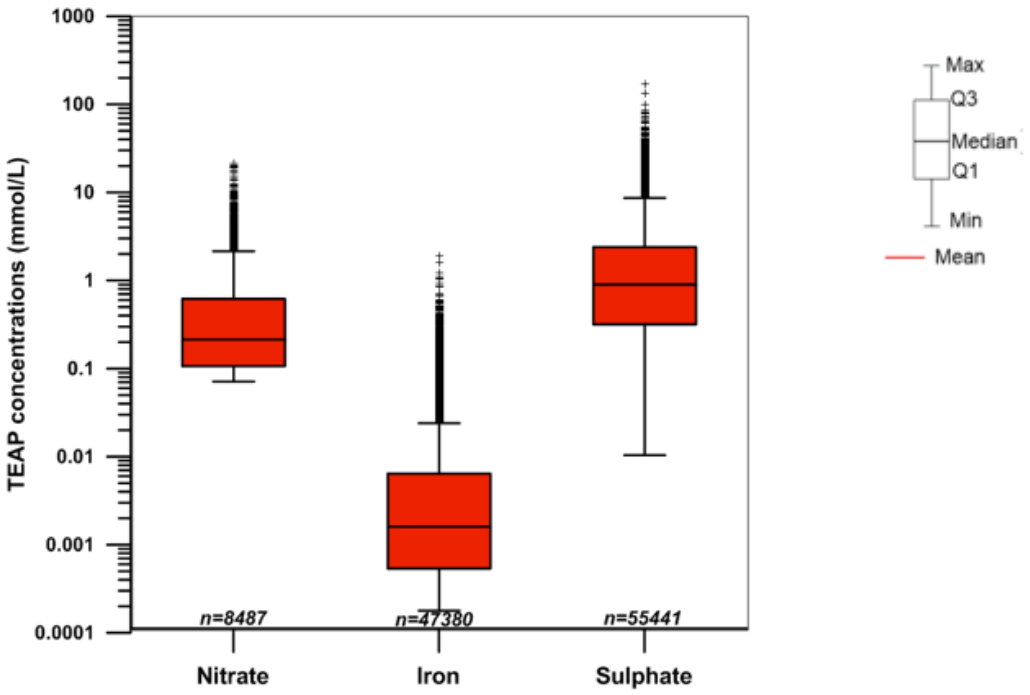

Figure 30: Box plots of distribution of TEAP concentrations in AHS groundwater samples.

Fig. 31 shows the spatial distribution of NO_3, Fe and SO_4 concentrations in groundwater across Alberta. The highest NO_3 concentration (1.33×10^3 mg/L or 21.4 mM) was observed in southwestern Alberta, in groundwater near the town of High River. Additional samples exceeding 1.20×10^3 mg/L (19.0 mM) NO_3 were found in the vicinity of Vegreville (1.20×10^3 mg/L or 19.4 mM and 1.27×10^3 mg/L or 20.5 mM), north of Edmonton (1.31×10^3 mg/L or 21.2 mM), and near Burstall, Saskatchewan (1.23×10^3 mg/L or 19.9 mM). On a provincial scale, elevated NO_3 concentrations are found in groundwater north and east of Edmonton, in the Red Deer to Lethbridge corridor, and surrounding Medicine Hat.

The highest Fe concentrations (1.06×10^2 mg/L or 1.90 mM) were found in groundwater west of Edmonton, near the town of MacKay. Very high Fe concentrations (90.0 mg/L or 1.61 mM) were also found in groundwater west of Bonnyville. High Fe concentrations in groundwater appear to occur mainly around the Edmonton area and Cold Lake.

The highest SO_4 concentrations (1.64×10^4 mg/L or 1.71×10^2 mM) in groundwater were observed near Burstall, Saskatchewan, and near High River, Alberta (1.28×10^4 mg/L or 1.33×10^2 mM). The highest SO_4 concentrations appear to be concentrated in groundwater in the Red Deer to Lethbridge corridor and surrounding Medicine Hat.

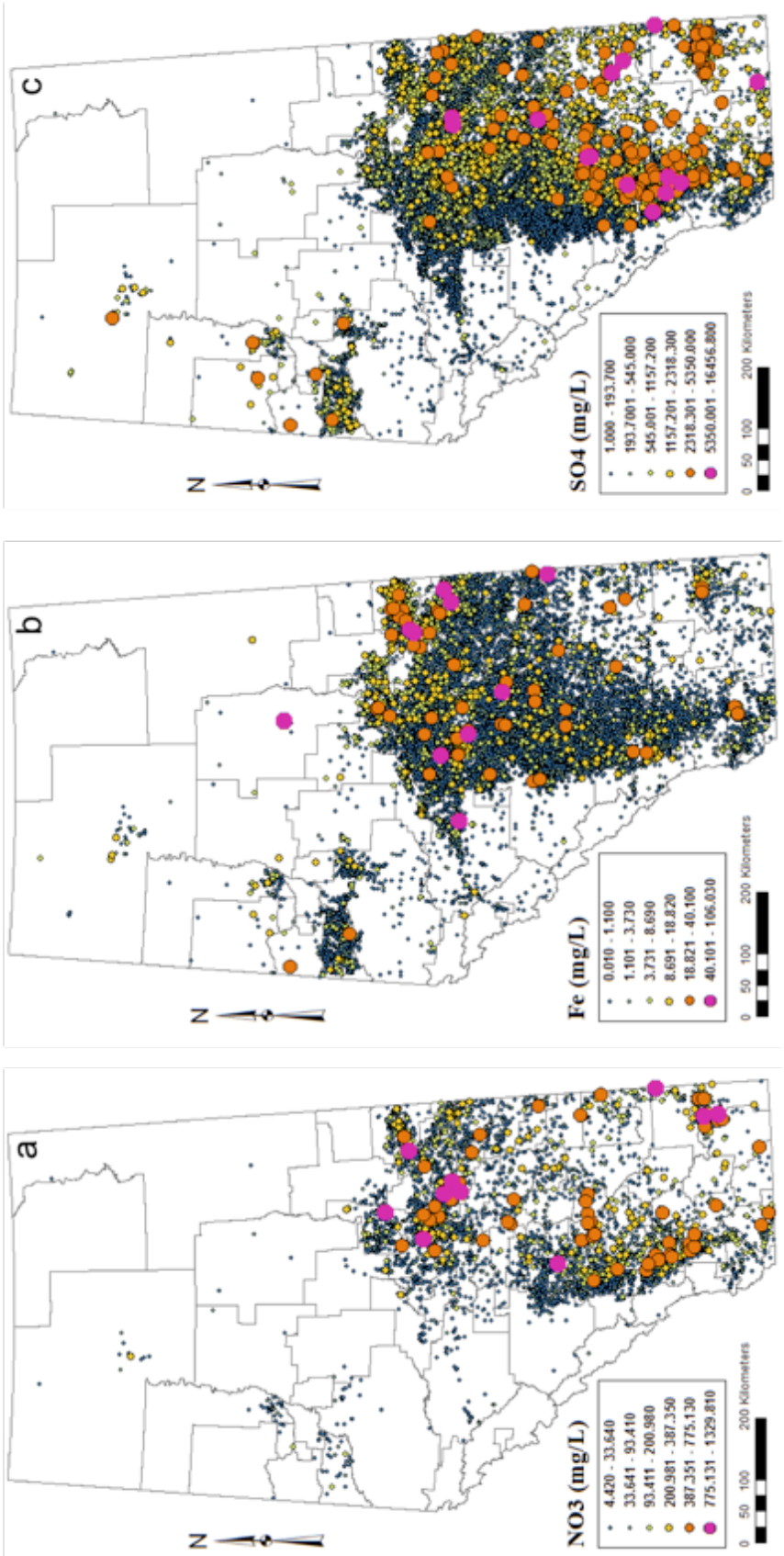

Figure 31: Spatial distribution of TEAP concentrations in mg/L. a) NO_3 b) Fe c) SO_4.

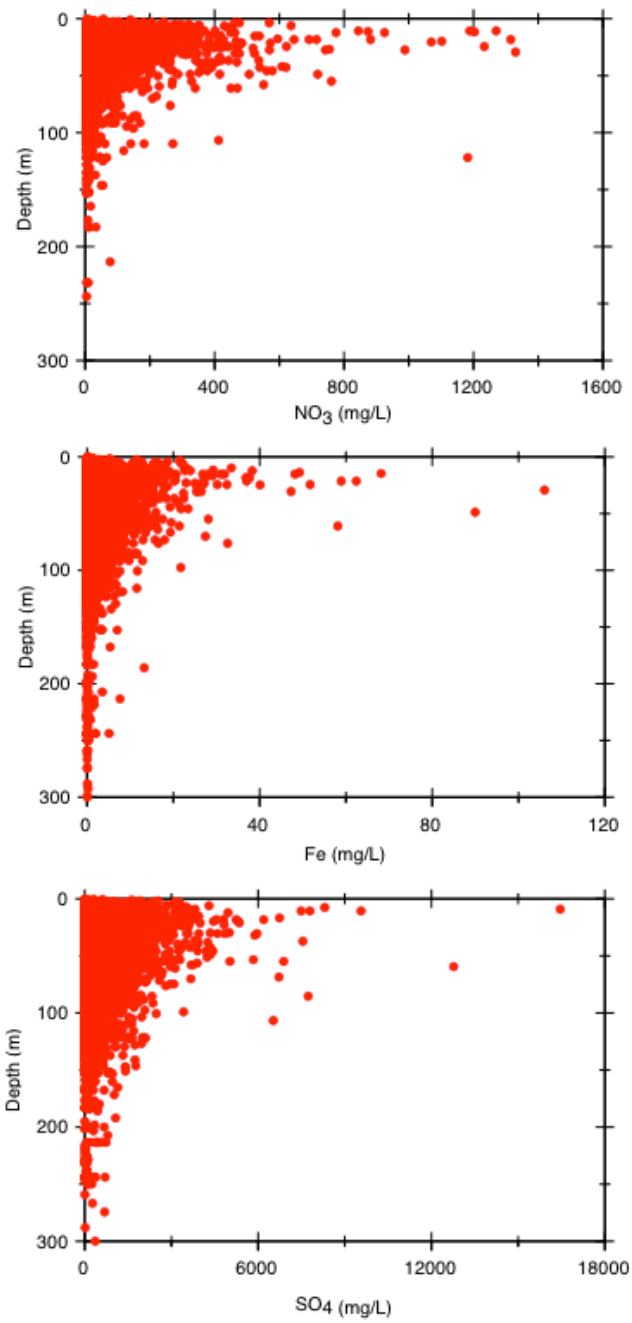

Figure 32: Well depth vs. concentration of NO_3, Fe, and SO_4 in groundwater.

The reported depth of the residential water wells varies from 0.3 to 2195 m below ground level. While all groundwater samples from wells with a reported depth were analyzed, only the water chemistries from samples with a reported depth of 300 m or less were evaluated here (n= 60396). This allows for a better comparison of the AHS data against BWWT and the various industry data, which report well depths of less than 300 m. Fig. 32 shows a profile of the select water chemistry parameters versus water well depth revealing that the concentration for NO_3, Fe, and SO_4 in groundwater decreases with depth. The variability of NO_3, Fe, and SO_4 concentrations decreases significantly for water well depth > 100 m. Decreases in NO_3 and SO_4 concentrations at these greater depths is consistent with denitrification and bacterial sulfate reduction progressing towards completion. If so, the conditions suitable for in-situ methane formation would be favorable.

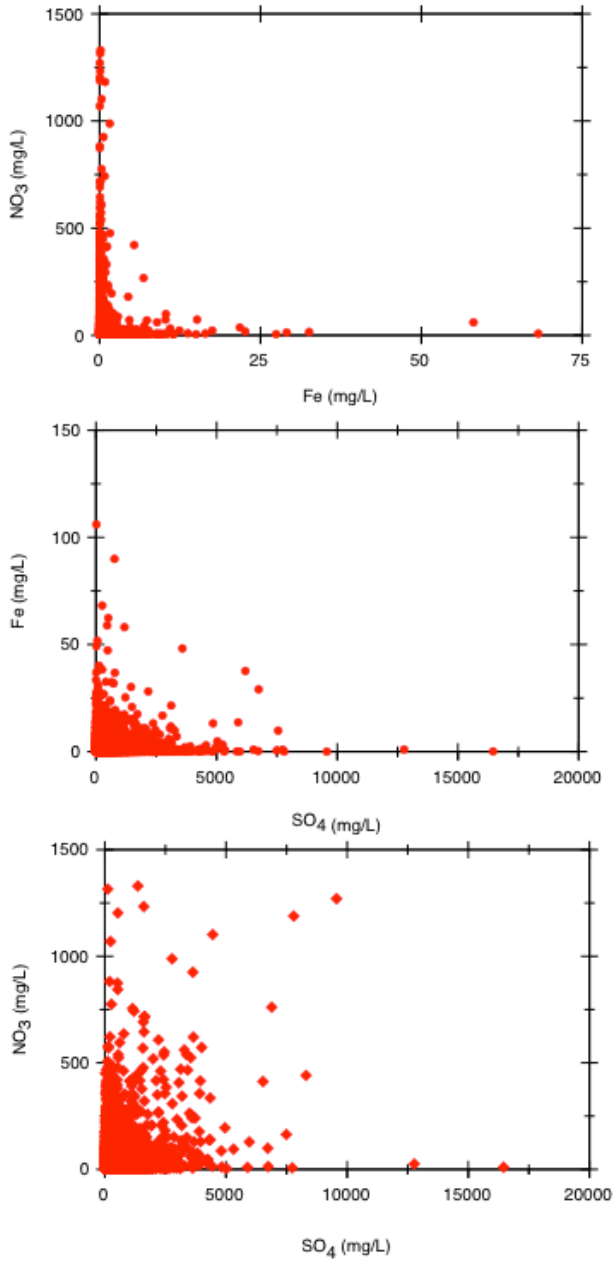

Figure 33: Binary plots showing the relationship between concentrations of NO_3 and Fe and SO_4

Fig. 33 shows binary plots displaying the relationship between concentration of NO_3, Fe and SO_4. Some samples are characterized by elevated NO_3 and SO_4 concentrations especially in groundwater from shallow wells (Fig. 32). Select samples show concentrations of up to, and exceeding, 500 mg/L (8 mM) of NO_3 and 5000 mg/L (50 mM) of SO_4 with the highest concentrations of 1.27 x 10^3 mg/L (20.5 mM) NO_3 and 9.56 x 10^3 mg/L (99.6 mM) SO_4. Groundwater samples with very high Fe and SO_4 concentrations were observed especially in groundwater from shallow wells (Fig. 32). The samples with the highest coupled Fe and SO_4 values had Fe concentrations of 48.2 mg/L (8.62x10^{-1} mM) and 37.6 mg/L (6.74x10^{-1} mM), and SO_4 concentrations of 3.58 x 10^3 mg/L (37.3 mM) and 6.19 x 10^3 mg/L (64.5 mM). The co-occurrence of elevated NO_3 and Fe concentrations was less frequently observed. However, a relationship was observed with concentrations of less than 100 mg/L NO_3 and 5 mg/L Fe. NO_3 concentrations of 2.67 x 10^2 mg/L (4.31 mM) and 421.4 mg/L (6.80 mM), and Fe concentrations of 6.82 mg/L (1.22 x 10^{-1} mM) and 5.36 mg/L (9.60 x 10^{-2} mM) were observed in the samples with the highest coupled NO_3 and Fe concentrations.

Table 14: Redox category classifications for groundwater from aquifers in Alberta.

Criteria used for assigning redox categories to groundwater from Alberta: identifying dominant ongoing redox process(es)				Nitrate	Manganese	Iron	Sulfate
			Threshold [mmol/L]	0.01	0.001	0.005	1
General	**Redox processes favorable #1**	**Redox processes favorable #2**	**Abbreviation**				
Anoxic	NO_3-reducing	Mixed process (NO_3-reducing/sulfate reducing or NO3reducing +pyrite oxidation)	NO_3red or NO_3red-SO_4red	≥	<	<	≥
Anoxic	Mn(IV)-reducing	Mn(IV)-reducing/SO_4reducing (mixed process)	Mn(IV)red or Mn(IV)red-SO4red	<	≥	<	≥
Anoxic	Mn(IV)-reducing	Methanogenesis	Mn(IV)red or CH4fm	<	≥	<	<
Anoxic	Fe(III)-reducing SO_4-reducing	Fe(III)reducing/ SO4reducing (mixed process)	Fe(III)red or Fe(III)red-SO4red	<	<	≥	≥
Anoxic	Fe(III)-reducing SO_4-reducing	Fe(III)-Mn(IV)reducing/ SO4reducing (mixed process)	Mn(IV)red-Fe(III)red-SO_4red	<	≥	≥	≥
Anoxic	SO_4-reducing		SO_4red	<	<	<	≥
Anoxic	Fe(III)-reducing	Methanogenesis (mixed process)	Fe(III)red or CH4fm	<	<	≥	<
Anoxic	Methanogenesis		CH_4fm	<	<	<	<
Anoxic	Methanogenesis	Fe(III)-Mn(IV)reducing	Mn(IV)red-Fe(III)red	<	≥	≥	<
Mixed-Anoxic (Heterogeneity)	Mixed process		NO_3red-Mn(IV)red	≥	≥	<	<
Mixed-Anoxic (Heterogeneity)	Mixed process		NO_3red-Mn(IV)red-SO_4red	≥	≥	<	≥
Mixed-Anoxic (Heterogeneity)	Mixed process		NO_3red-Fe(III)red	≥	<	≥	<
Mixed-Anoxic (Heterogeneity)	Mixed process		NO_3red-Fe(III)red-SO_4red	≥	<	≥	≥
Mixed-Anoxic (Heterogeneity)	Mixed process		NO_3red-Mn(IV)red-Fe(III)red	≥	≥	≥	<

4.2 Development and optimization of redox classification scheme

4.2.1 Definition and objective

As groundwaters evolve from highly oxidized to highly reducing conditions, they undergo a sequence of redox reactions including O_2 consumption, denitrification, Mn- Fe- reduction, bacterial sulfate reduction followed by methanogenesis. Mn(IV)- Fe(III)- reduction entails the potential of elevated Fe(II) and Mn(II) concentrations. To enable the identification of the dominant redox processes in an aquifer, a systematic approach with a classification table has been developed shown in Table 14. The groundwater samples from this study were classified into redox categories depending on the concentration of terminal

electron acceptors (TEAPs) such as O_2, NO_3, Mn, Fe and SO_4 participating in redox reactions. The redox zoning thresholds obtained from BWWT and source D data have been incorporated into the classification approach. This redox category classification has multiple objectives: (1) identify the dominant and ongoing redox processes such as nitrate reduction, manganese and/or iron reduction, bacterial sulfate reduction and methanogenesis; (2) assign a redox state to the groundwater samples based on water-quality parameters that are commonly measured such as NO_3, Mn, Fe and SO_4; (3) evaluate proportions of redox states in the aquifers of Alberta using the redox classes assignments and statistics tools; (4) focus on the identification of methanic redox zones; and (5) predict the potential occurrence of methane in aquifers for sample sets for which gas data are not available.

Table 14 shows the different redox classifications used for the investigated groundwater samples. Using this approach, redox states such as oxic, anoxic or mixed redox conditions were identified, and the predominant redox processes were identified based on the dissolved redox sensitive species concentrations. The redox categories in Table 14 are described as follows:

Nitrate-reduction zone containing nitrate concentrations above the threshold of 0.01 mM and with manganese and iron concentration below their respective thresholds; sulfate concentrations can be below (named NO3red) or above its concentration threshold (named NO3red-SO4red).

Manganese(IV)-reduction zone containing manganese concentrations above its threshold, while nitrate and iron concentrations are below their respective thresholds and sulfate concentrations can be below (named Mn(IV)red) or above its concentration threshold (named Mn(IV)red-SO4red). In the scenario where manganese is the only dissolved constituent above its respective thresholds (named Mn(IV)red), the manganese(IV)reduction zone may contain methane explaining the abbreviation Mn(IV)red or CH4fm.

Iron(III)-reduction zone containing iron concentration above its threshold while nitrate concentrations are below their respective thresholds, manganese (as reduced form) and sulfate concentrations can be below or above its concentration thresholds. Three combinations can be possible; (1) iron and sulfate concentrations are above their concentrations threshold (named Fe(III)red-SO4red), (2) iron, sulfate and manganese concentrations are above their concentrations threshold (named Mn(IV)red-Fe(III)red-SO4red), (3) iron and manganese concentrations are above their threshold concentrations (Mn(IV)red-Fe(III)red). In the scenario where iron is the only dissolved constituent above its respective thresholds (named Fe(III)red), the iron(III)reduction zone may contain methane explaining the abbreviation Fe(III)red or CH4fm.

Bacterial sulfate reduction zone: containing sulfate concentrations above its threshold while nitrate, manganese, and iron concentrations are below their respective thresholds (named SO4red). In addition to sulfate concentration above its threshold and similarly to iron(III), Mn(IV) reduction zones, the presence of iron and/or manganese as reduced form is not incompatible with the sulfate reduction zone (combinations named Fe(III)red-SO4red, Mn(IV)red-SO4red, Mn(IV)red-Fe(III)red-SO4red).

Methanogenesis or methanic zone constrained by concentration of nitrate and sulfate below their respective thresholds. The presence of iron and manganese concentration above their respective thresholds is possible within a methanic zone because the Fe- Mn- reduction could entail elevated Fe(II), Mn(IV) concentrations as mentioned previously and in these cases the redox category are named Mn(IV)red or CH4fm, Fe(III)red or CH4fm,Mn(IV)red-Fe(III)red.

All the other scenarios that do not fit the previous redox zoning description are described as mixed process indicating redox heterogeneity in the studied system.

4.2.2 Calibration and performance metrics of the redox classification model

The explosive level of methane in air is between 5% to 15% by volume (50,000 to 150,000 ppmv). For dissolved methane, Henry's Law relates the dissolved methane concentrations (C_{water}) to gas pressure C_{air} expressed as $C_w=K_H*C_a$. For illustration, at 20°C and one atmosphere pressure (101.325 kPa), using K_H =1.4·10-3 mol.m^{-3}.Pa^{-1}, a dissolved methane concentration of 1.2 mg/L could theoretically generate a lower explosive limit for CH_4 in air of 5% by volume. This scenario would require confined conditions where "an unlimited quantity of aerated water is outgassing into an unventilated chamber" (Edwards, 1991). These conditions are unlikely to be encountered in practice. There are few established guidelines

for dissolved methane concentration in water. The CH_4 risk "action level" was proposed at 10 mg/L by Eltschlager et al. (2011). Other guidelines considered explosion/safety issues related to exsolution of dissolved methane into potentially confined, air-filled spaces. The Colorado Oil & Gas Conservation Commission (COGCC) reported a hazard threshold for dissolved methane concentration > 10 mg/L and a hazard mitigation level of 28 mg/L similar to the US Department of the Interior, Office of Surface Mining (2001). The Quebec Ministry of Environment and the Pennsylvania Department of Environmental Protection both set a threshold value of 7 mg/L for dissolved methane in groundwater. The Ontario Ministry of Environment and Energy proposed a methane volumetric guideline set at 3 L/m^3 corresponding to ~2 mg/L defined in the maximum desirable concentration parameters related to aesthetic quality (source: agrienvarchive.ca). For this study, methane occurrence was characterized according to different groupings related to the explosive range as follows: < 5%; 5%-15%, >15% (Table 15).

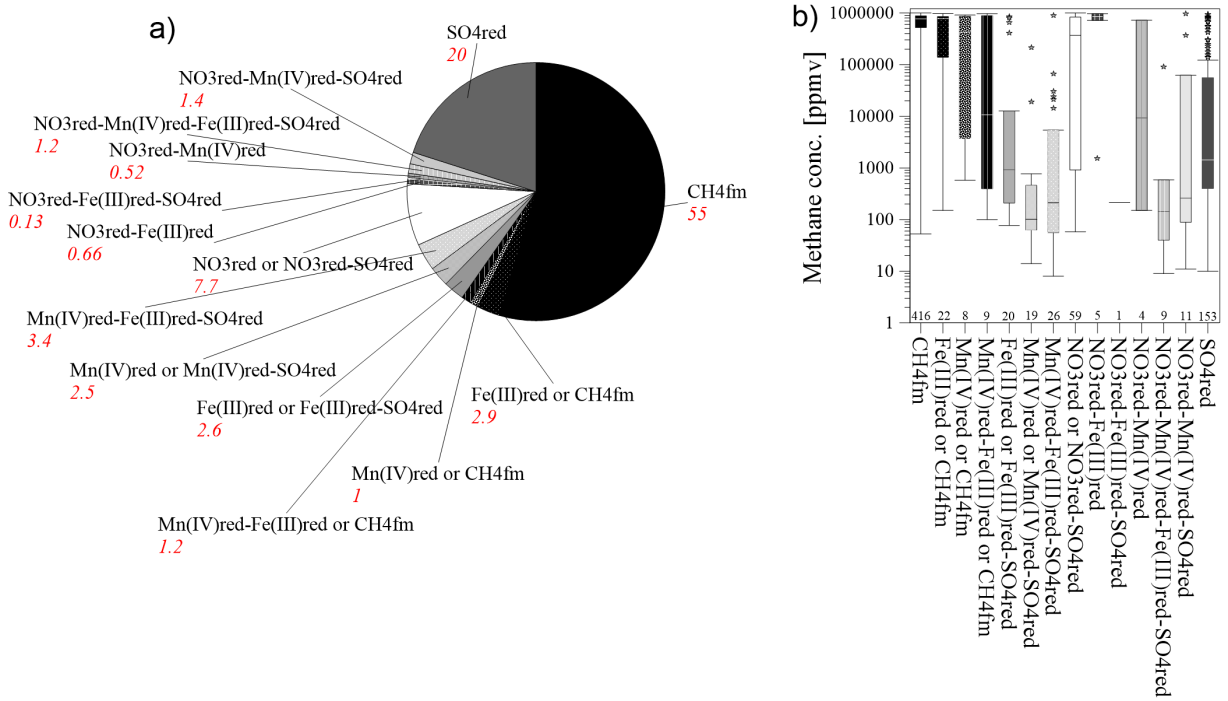

Figure 34: Case study A: Assignment of redox categories applied to samples from the BWWT database a) percentages (red label) of the redox categories represented in a pie chart, b) Box-Whisker plot of the distribution of methane concentrations in each redox category (n represents the number of samples in each redox category).

4.2.2.1 Case study A: Using the 95th percentile redox "thresholds": NO_3 0.01 mM; Fe 0.005 mM; Mn 0.001 mM and SO_4 1 mM

In order to test the efficiency and robustness of this redox category classification, the BWWT dataset with 762 samples was evaluated using this model. The redox sensitive species thresholds calculated from the 95th percentile were used (0.01 mM for NO_3, 0.005 mM for Fe, 0.001 mM for Mn and 1 mM for SO_4). The results are shown in Fig. 34. Over 54 % of the samples (n=416) belong to the methanic zone where NO_3, Mn, Fe and SO_4 are below their respective threshold concentrations (*abbr*. CH4fm). More than 20% of the samples (n=153) belong to a redox zone where sulfate concentrations exceed its threshold indicating that bacterial sulfate reduction is likely ongoing (*abbr*. SO_4red). Over 7 % of the samples belong to the redox zone where NO_3 is present indicating the potential occurrence of NO_3-reduction (NO_3red) and/or a mixed redox zone where SO_4-reduction occurs as well as NO_3-reduction (*abbr*. NO_3red or NO_3red-SO_4red). The remaining samples belong to mixed redox zones where Mn(IV)- reduction (*abbr*. Mn(IV)red or Mn(IV)red-SO_4red), Mn(IV)- reduction/ Fe(III)-reduction (*abbr*. Mn(IV)red-Fe(III)red-SO_4red) are ongoing with presence of dissolved constituents such as Mn, Fe and SO_4 above their respective thresholds or mixed redox zones where NO_3-reduction, NO_3-reduction/Mn(IV) reduction (NO_3red-Mn(IV)red-SO_4red) processes occur (Fig. 34a and Table 14).

Table 15: Assignment of redox categories to BWWT groundwater samples based on the redox sensitive species thresholds (case study A) and distribution of methane concentration in free gas samples in each of the assigned redox category. In orange are the redox classes that are favorable for methane accumulation/formation in green the non-favorable conditions.

Redox class	N	%	CH_4< 50,000 ppmv		50,000 <CH_4< 150,000 ppmv		CH_4> 150,000 ppmv	
			N	%	N	%	N	%
CH4fm	416	54.6	31	7.5	12	2.9	373	**89.7**
Fe(III)red or CH4fm	22	2.9	4	18.2	2	9.1	16	72.7
Mn(IV)red or CH4fm	8	1.0	2	25.0	2	25.0	4	50.0
Mn(IV)red-Fe(III)red or CH4fm	9	1.2	5	55.6	0	0.0	4	44.4
Fe(III)red or Fe(III)red-SO4red	20	2.6	16	80.0	0	0.0	4	20.0
Mn(IV)red or Mn(IV)red-SO4red	19	2.5	18	94.7	0	0.0	1	5.3
Mn(IV)red-Fe(III)red-SO4red	26	3.4	24	92.3	1	3.8	1	3.8
NO3red or NO3red-SO4red	59	7.7	23	39.0	1	1.7	35	59.3
NO3red-Fe(III)red	5	0.7	1	20.0	0	0.0	4	80.0
NO3red-Fe(III)red-SO4red	1	0.1	1	100.0	0	0.0	0	0.0
NO3red-Mn(IV)red	4	0.5	3	75.0	0	0.0	1	25.0
NO3red-Mn(IV)red-Fe(III)red-SO4red	9	1.2	8	88.9	1	11.1	0	0.0
NO3red-Mn(IV)red-SO4red	11	1.4	8	72.7	1	9.1	2	18.2
SO4red	153	20.1	114	74.5	9	5.9	30	19.6
Total	762	100	258		29	68.6	475	

To test the viability of this approach we compared the assigned redox classes described above to the methane concentrations in free gas samples from the BWWT dataset. The results are shown in the Box-Whisker plot in Fig. 34 and summarized in Table 15. Samples containing elevated concentrations of methane (> 150,000 ppmv) were in 89% of the cases associated with redox zones CH4fm. Samples with methane concentrations <50,000 ppmv were predominantly associated with SO4red, and other mixed redox process classes. The SO4red and NO3red zones contain a number of samples having elevated methane concentrations (>150,000 ppmv). This may suggest a co-mingling of waters from different redox zones, or a metastable redox state where methane is potentially migrating into aquifer sections with more oxidizing conditions. This hypothesis is further investigated in section 5 of this report.

This first test of our redox assignment procedure using aqueous geochemistry data revealed that the systematic approach correctly predicts **83%** of the observed methane occurrence (methane presence or absence). A total of 397 of 475 samples or **83.6%** of the samples with elevated methane concentration >150,000 ppmv were correctly classified. A total of 224 of 287 samples or **78%** of the samples with low methane concentration <150,000 ppmv were correctly classified. Evaluating the performance of the model on the lower threshold of 50,000 ppmv for methane gives the following results: a total of 448 of 504 samples or **89%** of the groundwater samples with elevated methane concentration > 50,000 ppmv were correctly classified. A total of 216 of 258 samples or **83.7%** of the groundwater samples with low methane concentration < 50,000 ppmv were correctly classified. These metrics are based on the threshold concentrations of nitrate and sulfate of 0.01 mM and 1 mM respectively. These thresholds have been chosen in order to optimize the classification of methane containing water wells and based on the 95th percentile method. The chosen classification table assigning redox categories appears to be a robust tool with a performance metric of 83% that permits the identification of the predominant redox zones and is a very good predictor of the potential occurrence of methane in groundwater.

4.2.2.2 Case study B: Sensitivity of the redox sensitive species cutoff with: NO_3: 0.1 mM; Fe 0.02 mM; Mn = 0.005 mM and SO_4: 1 mM

This section has the objective to assess the sensitivity of the redox assignment method when thresholds vary as follow NO_3: 0.1 mM; Fe 0.02 mM; Mn = 0.005 mM and SO_4: 1 mM called Case study B. Over 64 % of the samples (n=490) belong to the methanic zone where NO_3, Mn, Fe and SO_4 are below their respective threshold concentrations (*abbr*. CH4fm). More than 30% of the samples (n=232) belonged to a

redox zone where sulfate concentrations exceed its threshold indicating that bacterial sulfate reduction may be ongoing (*abbr*. SO_4red). Only 0.7 % (n=5) of the samples belong to the redox zone where Fe(II) is present indicating the occurrence of Fe(III)-reduction and/or a mixed redox zone where methanogenesis occurs as well as Fe-reduction (*abbr*. Fe(III)red or CH_4fm). The remaining <5% of samples belong to mixed redox zones where Mn(IV)-reduction (*abbr*. Mn(IV)red or Mn(IV)red-SO_4red) or Mn(IV)-reduction/ Fe(III)-reduction (*abbr*. Mn(IV)red-Fe(III)red-SO_4red) are ongoing with the presence of dissolved constituents such as Mn, Fe and SO_4 above their respective thresholds or mixed redox zones where NO_3-reduction, NO_3-reduction/Mn(IV) reduction (NO_3red-Mn(IV)red-SO_4red) occur (Fig. 35 and Table 14).

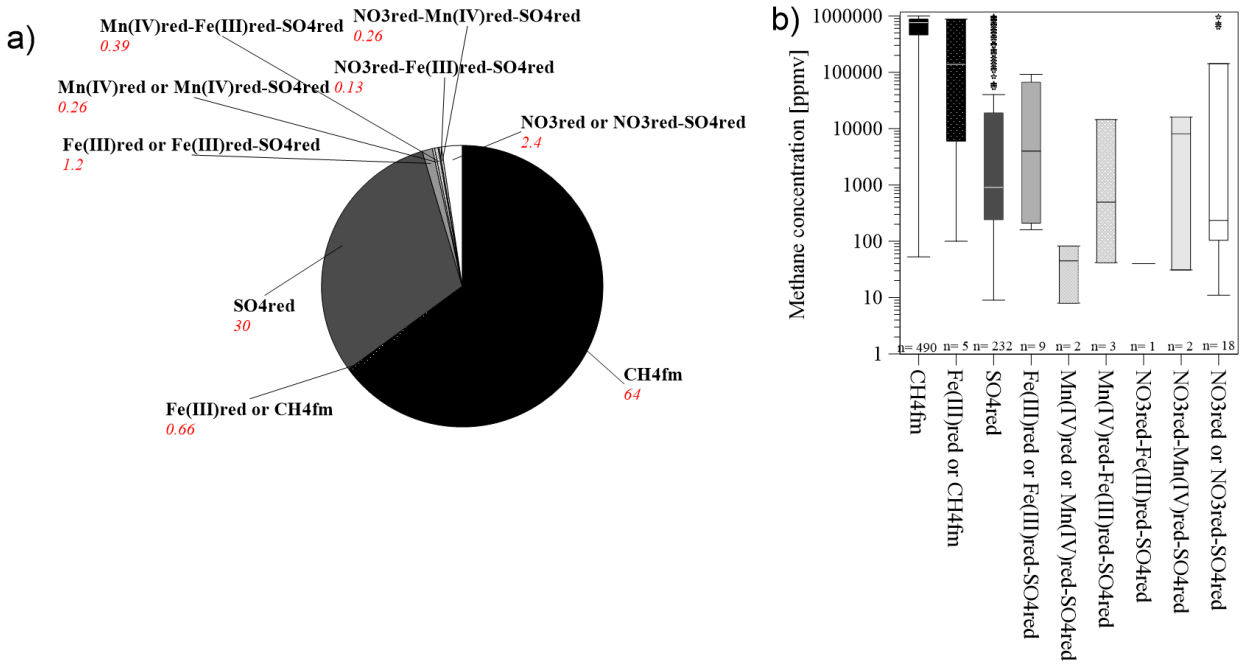

Figure 35: Case study B: Assignment of redox categories applied to samples from the BWWT database a) percentages (red label) of the redox categories represented in a pie chart, b) Box-Whisker plot of the distribution of methane concentrations in each redox category (n represents the number of samples in each redox category).

Table 16: Case study B: Assignment of redox categories to BWWT groundwater samples when changing redox sensitive species thresholds and distribution of methane concentration in free gas samples in each of the assigned redox category.

			CH_4 conc. <50,000 ppmv		CH_4 conc. ≥50,000 ppmv		CH_4conc. <150,000 ppmv		50,000 ≤ CH_4 <150,000 ppmv		CH_4conc. ≥150,000 ppmv	
Redox category [abbreviations]	N	%	N	%	N	%	N	%	N	%	N	%
CH_4fm	490	64.3	45	9	445	91	60	12	15	3	430	88
Fe(III)red or CH_4fm	5	0.7	2	40	3	60	3	60	1	20	2	40
SO_4red	232	30.4	183	79	49	21	193	83	10	4	39	17
Fe(III)red or Fe(III)red-SO_4red	9	1.2	8	78	2	22	9	100	1	11	0	0
Mn(IV)red or Mn(IV)red-SO_4red	2	0.3	2	100	0	0	2	100	0	0	0	0
Mn(IV)red-Fe(III)red-SO_4red	3	0.4	3	100	0	0	3	100	0	0	0	0
NO_3red-Fe(III)red-SO_4red	1	0.1	1	100	0	0	1	100	0	0	0	0
NO_3red-Mn(IV)red-SO_4red	2	0.3	2	100	0	0	2	100	0	0	0	0
NO_3red or NO_3red-SO_4red	18	2.4	13	72	5	28	14	78	1	6	4	22
Total	762	100	258		504		287		28		475	

To test the viability of this approach we compared the assigned redox classes described above to the methane concentrations in free gas samples from the BWWT dataset. The results are shown in the Box-Whisker plot in Fig. 35b and summarized in Table 16. Samples containing elevated concentrations of methane (> 150,000 ppmv) were in >90% of the cases associated with redox zones CH4fm and Fe(III)red or CH4fm. Samples with methane concentrations <150,000 ppmv were predominantly associated with SO4red, and other mixed redox process classes. When taking into account a lower methane concentration threshold from 150,000 ppmv to 50,000 ppmv the results of the calculations are the following: samples containing elevated concentrations of methane (> 50,000 ppmv) were in >89% of the cases associated with redox zones CH4fm and Fe(III)red or CH4fm. Samples with methane concentrations <50,000 ppmv were predominantly associated with SO4red, and other mixed redox process classes (>81%). The SO4red zone contains a number of samples having elevated methane concentrations (>50,000 ppmv and >150,000 ppmv). This may suggest a co-mingling of waters from different redox zones, or a metastable redox state where methane is potentially migrating into aquifer sections with more oxidizing conditions. This hypothesis is further investigated in section 5 of this report.

This first test of our redox assignment procedure using aqueous geochemistry data revealed that the systematic approach correctly predicts **86%** of the observed methane occurrence (methane presence or absence). A total of 432 of 475 samples or **91%** of the groundwater samples with elevated methane concentration >150,000 ppmv were correctly classified. A total of 224 of 287 samples or **78%** of the groundwater samples with low methane concentration <150,000 ppmv were correctly classified. Evaluating the performance of the model on the lower threshold of 50,000 ppmv for methane gives the following results: a total of 448 of 504 samples or **89%** of the groundwater samples with elevated methane concentration >50,000 ppmv were correctly classified. A total of 211 of 258 samples or **82%** of the groundwater samples with low methane concentration <50,000 ppmv were correctly classified. These metrics are based on the threshold concentrations of nitrate and sulfate of 0.01 mM and 1 mM respectively. These thresholds have been chosen in order to optimize the classification of methane containing water wells. The drawback of this approach is that it overestimates the number of groundwater samples that could contain methane. As a result, the predicted number of methane-containing groundwater wells is likely slightly overestimated. Lower thresholds decrease the number of predicted wells containing methane but at the risk of missing samples with elevated methane concentrations (>150,000 ppmv or >50,000 ppmv depending on the threshold chosen). The chosen classification table assigning redox categories appears to be a robust tool that permits the identification of the predominant redox zones and is a very good predictor of the occurrence of methane in groundwater.

4.3 Implication for the redox classification scheme for industrial dataset

The redox class model was applied to the different industrial datasets, which allowed for an investigation of the redox conditions found in selected aquifers of Alberta. Each dataset from the sources A to E were clustered in specific regions of Alberta from southern Alberta, Calgary, Badlands, central, and eastern Alberta regions.

4.3.1 Southern Alberta – Calgary and Badlands regions

The redox class assignment has been applied for the industrial dataset from source A2 including the redox cutoffs for case studies A and B. The distribution shows that the dominant redox classes are: SO_4red, Fe(III)red, and CH_4fm (Table 17). In this region, a high proportion of groundwater samples have elevated nitrate concentrations > 10 mg/L (6.2 mM) up to 5 g/L (0.08 M) especially east of Airdrie and Drumheller.

Table 17: Redox class assignment for source A2 groundwater samples. In orange the methanic and in yellow the non-methanic conditions.

Source A2	Case study A		Case study B	
	n	%	n	%
CH4fm	111	8.53	160	12.30
Fe(III)red or CH4fm	41	3.15	21	1.61
Mn(IV)red or CH4fm	5	0.38	1	0.08
Mn(IV)red-Fe(III)red or CH4fm	15	1.15	1	0.08
Fe(III)red or Fe(III)red-SO4red	245	18.83	182	13.99
Mn(IV)red or Mn(IV)red-SO4red	73	5.61	42	3.23
Mn(IV)red-Fe(III)red-SO4red	235	18.06	41	3.15
NO3red or NO3red-SO4red	111	8.53	89	6.84
NO3red-Fe(III)red	6	0.46	1	0.08
NO3red-Fe(III)red-SO4red	25	1.92	8	0.61
NO3red-Mn(IV)red-Fe(III)red-SO4red	29	2.23	6	0.46
NO3red-Mn(IV)red-SO4red	20	1.54	7	0.54
SO4red	385	29.59	742	57.03
Total	1301		1301	

4.3.2 Central Alberta – Red Deer area

Industrial datasets from sources A3 and a subset of source C and D have groundwater wells in the Red Deer area. The majority of the groundwater samples from source A3 indicate methanic conditions (64% and 84% for the case studies A and B, Table 18). The results from samples from source C show similar patterns with the majority of groundwater samples revealing methanic conditions (>80% in both case study A and B, Table 19).

Table 18: Redox class assignment for source A3 groundwater samples. In orange the methanic and in yellow the non-methanic conditions.

Source A3	Case study A		Case study B	
	n	%	n	%
CH4fm	6	35.29	13	76.47
Mn(IV)red or CH4fm	5	29.41	1	5.88
NO3red or NO3red-SO4red	3	17.65	0	0.00
SO4red	3	17.65	3	17.65
Total	17		17	

Table 19: Redox class assignment for source C groundwater samples. In orange the methanic and in yellow the non-methanic conditions.

Source C (Red Deer)	Case study A		Case study B	
	n	%	n	%
CH4fm	16	72.73	20	90.91
Fe(III)red or CH4fm	0	0.00	1	4.55
Mn(IV)red-Fe(III)red or CH4fm	2	9.09	0	0.00
NO3red or NO3red-SO4red	3	13.64	1	4.55
NO3red-Mn(IV)red-Fe(III)red	1	4.55	0	0.00
Total	22		22	

For groundwater samples represented by sources D1 and D2 the main redox classes also indicated

methanic conditions, while a low number of samples indicated the presence of nitrate and sulfate. In some groundwater systems, dissolved iron and manganese occurred in elevated concentrations (Table 20).

Table 20: Redox class assignment for sources D1 and D2 groundwater samples. In orange the methanic and in yellow the non-methanic conditions.

Source D1	Case study A		Case study B		**Source D2**	Case study A		Case study B	
	n	%	n	%		n	%	n	%
CH4fm	9	29.03	25	80.65	CH4fm	40	36.70	95	87.16
Fe(III)red or CH4fm	3	9.68	1	3.23	Fe(III)red or CH4fm	2	1.83	2	1.83
Mn(IV)red or CH4fm	5	16.13	1	3.23	Mn(IV)red or CH4fm	7	6.42	0	0.00
Mn(IV)red-Fe(III)red or CH4fm	3	9.68	1	3.23	Mn(IV)red-Fe(III)red or CH4fm	5	4.59	0	0.00
NO3red or NO3red-SO4red	10	32.26	3	9.68	NO3red or NO3red-SO4red	45	41.28	9	8.26
NO3red-Mn(IV)red	1	3.23	0	0.00	NO3red-Mn(IV)red	6	5.50	0	0.00
					NO3red-Fe(III)red	1	0.92	0	0.00
					Mn(IV)red or Mn(IV)red-SO4red	1	0.92	1	0.92
					SO4red	2	1.83	2	1.83
Total	31		31		Total	109		109	

Groundwater samples from sources D1 and D2 collected in the Red Deer area contain gas data that can be compared to the assignment of redox classes. Fig. 36 shows that the highest methane concentrations for samples from source D1 are consistent with methanic conditions *i.e.* CH4fm, Fe(III)red or CH4fm, Mn(IV)red or CH4fm for both case studies A and B. For groundwater samples represented in source D2, the highest methane concentrations belong to CH4fm and NO3red-Fe(IV) classes in case study A. The presence of methane at 4.9 mg/L under non-methanic conditions within the NO3red-Fe(IV) redox classes where the nitrate concentration is 1.2 mg/L (0.02 mM) appears to suggest a metastable state of methane in such oxidizing conditions. In case study B, where the redox species concentrations cutoffs are higher, the highest methane concentrations were consistent with CH4fm or methanic conditions.

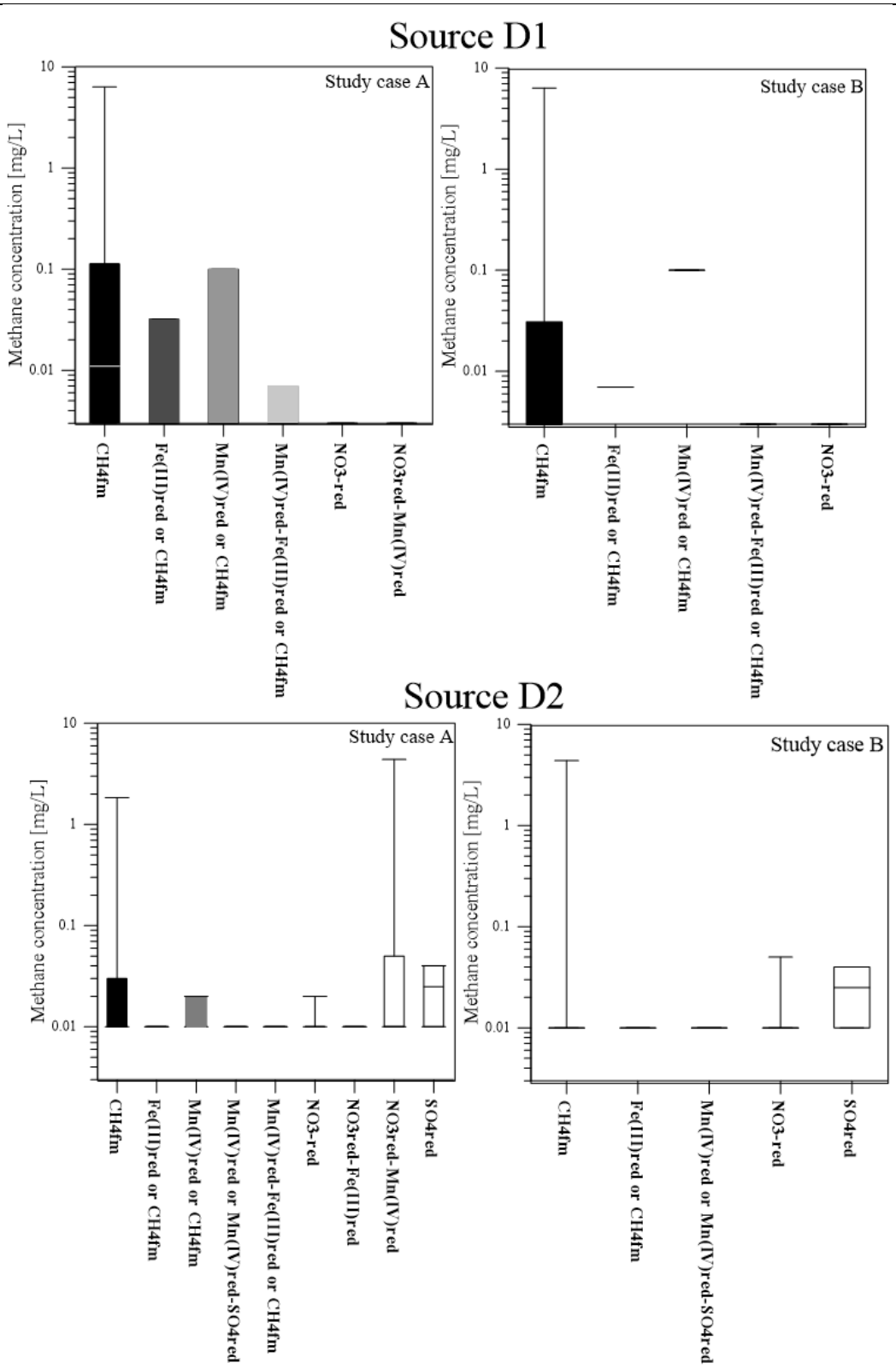

Figure 36: Distribution of methane concentrations versus assigned redox classes for source D1 and D2 for both case studies A and B corresponding to the different redox cutoff scenarios.

4.3.3 Central Alberta – Barrhead area

North of Red Deer, some groundwater wells represented in source C are located around Barrhead. Table 21 summarizes the results of the redox class model assignment and shows that the groundwater samples exhibit conditions not favourable for methane formation or preservation.

Table 21: Redox class assignment for source C groundwater samples. In orange the methanic and in yellow the non-methanic conditions.

Source C (Barrhead)	Case study A		Case study B	
	n	%	n	%
Mn(IV)red or Mn(IV)red-SO4red	1	25.00	0	0.00
SO4red	3	75.00	4	100.00
Total	4		4	

4.3.4 Central Alberta – Edson area

For sources B, E1, and E2 that contain groundwater wells located in the Edson area, the redox class assignment reveals patterns with dominant methanic conditions and groundwater samples with low sulfate concentrations. Manganese and iron concentrations are non-negligible in groundwater of this area (Tables 22 and 23).

Table 22: Redox class assignment for source B groundwater samples. In orange the methanic and in yellow the non-methanic conditions.

Source B	Case study A		Case study B	
	n	%	n	%
CH4fm	5	35.71	13	92.86
Mn(IV)red or CH4fm	3	21.43	0	0.00
Fe(III)red or CH4fm	3	21.43	0	0.00
Fe(III)red or Fe(III)red-SO4red	1	7.14	0	0.00
NO3red or NO3red-SO4red	2	14.29	0	0.00
SO4red	0	0.00	1	7.14
Total	14		14	

Table 23: Redox class assignment for sources E1 and E2 groundwater samples. In orange the methanic and in yellow the non-methanic conditions.

Source E1	Case study A		Case study B		**Source E2**	Case study A		Case study B	
	n	%	n	%		n	%	n	%
CH4fm	1	4.76	17	80.95	CH4fm	10	23.81	30	71.43
Mn(IV)red or CH4fm	7	33.33	0	0.00	Mn(IV)red or CH4fm	8	19.05	1	2.38
Fe(III)red or CH4fm	4	19.05	3	14.29	Fe(III)red or CH4fm	5	11.90	4	9.52
Mn(IV)red-Fe(III)red or CH4fm	6	28.57	0	0.00	Mn(IV)red-Fe(III)red or CH4fm	2	4.76	1	2.38
NO3red or NO3red-SO4red	3	14.29	1	4.76	NO3red or NO3red-SO4red	7	16.67	6	14.29
					NO3red-Fe(III)red	7	16.67	0	0.00
					NO3red-Mn(IV)red-Fe(III)red	3	7.14	0	0.00
Total	21		21		Total	42		42	

4.3.5 Eastern Alberta

A vast number of groundwater wells from source C are located in eastern Alberta in the vicinity of Cold Lake and Vegreville. Results from the redox class assignment model show a wide variety of redox classes suggesting the occurrence of rather complicated groundwater systems. Several samples had non-negligible iron and manganese concentrations that require further investigation in terms of geochemical speciation and origin (Table 24).

Table 24: Redox class assignment for source C groundwater samples. In orange the methanic and in yellow the non-methanic conditions.

Source C (eastern AB)	Case study A		Case study B	
	n	%	n	%
CH4fm	13	8.18	38	23.90
Fe(III)red or CH4fm	0	0.00	15	9.43
Mn(IV)red or CH4fm	16	10.06	13	8.18
Mn(IV)red-Fe(III)red or CH4fm	29	18.24	8	5.03
Fe(III)red or Fe(III)red-SO4red	4	2.52	18	11.32
Mn(IV)red or Mn(IV)red-SO4red	14	8.81	5	3.14
Mn(IV)red-Fe(III)red-SO4red	23	14.47	5	3.14
NO3red or NO3red-SO4red	27	16.98	23	14.47
NO3red-Fe(III)red	1	0.63	0	0.00
NO3red-Mn(IV)red	9	5.66	0	0.00
NO3red-Mn(IV)red-Fe(III)red	2	1.26	0	0.00
NO3red-Fe(III)red-SO4red	0	0.00	0	0.00
NO3red-Mn(IV)red-Fe(III)red-SO4red	0	0.00	0	0.00
NO3red-Mn(IV)red-SO4red	5	3.14	1	0.63
SO4red	16	10.06	33	20.75
Total	159		159	

4.4 Implication for the redox classification scheme for AHS dataset

The same hydrochemical redox zone assignment approach was used for the AHS dataset to determine the likelihood of methane occurrence in the respective aquifers.

4.4.1 Application of redox cutoffs of case study A

For case study A involving the AHS samples, the same TEAP threshold values were used as in the previously described evaluations of the BWWT and industry datasets: 0.01 mM (0.6 mg/L), 0.005 mM (0.3 mg/L), and 1 mM (100 mg/L) for NO_3, Fe, and SO_4, respectively (Table 25).

Table 25: Threshold values from case study A, and number of samples (of 60,435 total samples evaluated) exceeding the threshold, for NO_3, Fe, and SO_4.

	Threshold		N > threshold
	mM	*mg/L*	
NO_3	0.01	0.6	8,487 (14.0%)
Fe	0.005	0.3	13,041 (21.6%)
SO_4	1.0	1.00×10^2	25,380 (42.0%)

Methanic conditions are predominant for the groundwater samples in the AHS database with CH4fm redox class representing 41.2 % of the samples. An additional 5827 groundwater samples belong to the Fe(III)red class, which indicate samples with iron concentration above the threshold. The presence of iron in its reducing form (e.g Fe^{2+} concentration) is compatible within the presence of methane. Both the CH4fm and Fe(III)red classes combined suggest that 30694 groundwater samples are in a potential methanic zone representing 50.8% of all AHS groundwater samples. A large number of groundwater samples belong to SO4red (~25%) or Fe(III) red-SO4 red (> 10%) (Table 26). Groundwater systems with elevated concentrations of iron seem to be frequent and need further investigation regarding its origin and the geochemical speciation.

Table 26: Redox class assignment for groundwater samples from the AHS data source. In orange the methanic and in yellow the non-methanic conditions.

Source AHS	Case study A		Case study B	
	n	%	n	%
CH4fm	24867	41.15	29289	48.46
Fe(III)-red or CH4fm	5827	9.64	2176	3.60
SO4-red	15054	24.91	19344	32.01
NO3-red	3945	6.53	3490	5.77
NO3-SO4-red	3288	5.44	3069	5.08
Fe(III)-SO4-red	6200	10.26	2749	4.55
NO3-Fe(III)-SO4-red	852	1.41	232	0.38
NO3-Fe(III)-red	402	0.67	86	0.14
Total	60435		60435	

4.4.2 Application of redox cutoffs of case study B

In evaluating the concentrations of NO_3, Fe, and SO_4 the following threshold concentrations of the case study B were used: 0.1 mM (6 mg/L), 0.01 mM (1.2 mg/L), and 1 mM (100 mg/L) for NO_3, Fe, and SO_4, respectively. Table 27 lists the threshold values for NO_3, Fe, and SO_4 and the number of samples that exceed the respective threshold values for each TEAP.

Table 27: Threshold values from case study B, and number of samples (of 60,435 total samples evaluated) exceeding the threshold, for NO_3, Fe, and SO_4.

	Threshold		N > threshold
	mM	*mg/L*	
NO_3	0.1	6	6,877 (11.4%)
Fe	0.02	1.2	5,204 (8.6%)
SO_4	1	1.00×10^2	25,380 (42.0%)

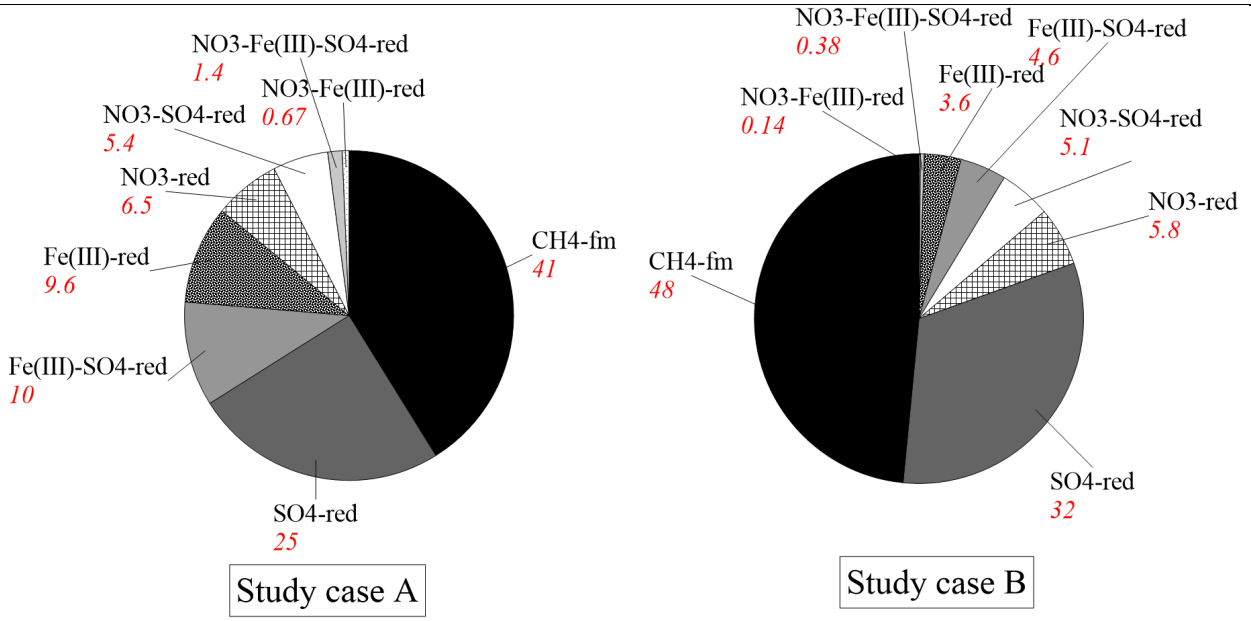

Figure 37: Redox category assignment for AHS groundwater samples based on case studys A and B. Redox category and the number samples per category is listed. In red the percentage of redox class

The redox category classification scheme was applied to the AHS data to determine the redox category for each groundwater sample. The exclusion of Mn and the lack of dissolved oxygen data resulted in fewer redox categories than for the BWWT data. Fig. 37b shows the distribution of redox categories for the AHS groundwater samples. Consistent with the case study A, the largest redox class is the methanic category (CH4-fm) (n= 29289), representing 48.5% of the samples. An additional 2176 groundwater samples belong to the Fe(III)red class, which refers to samples with iron concentrations above the threshold. Both the CH4fm and Fe(III)red classes suggest that 31,465 groundwater samples belong to a potential methanic zone representing 52% of the total groundwater samples. This result is consistent with the findings of BWWT. The sulfate-reducing (SO4-red) category contained 32.0% of the samples and is the second largest (n=19344) redox class. The redox category with the least number of groundwater samples was the nitrate-iron-reducing (NO_3-Fe(III)-red) class (n=86) with 0.1% of the samples. The spatial distribution of redox categories for groundwater samples from the AHS database across Alberta is shown in Fig. 38. A visual evaluation of redox categories reveals that the CH4-fm and SO_4-red redox categories are predominant in groundwater within the Calgary-Edmonton-Corridor. A cluster of Fe(III)-red samples is centered around the Edmonton and Cold Lake regions. In the Cold Lake and Lloydminster regions, Fe(III)-SO_4-red conditions dominate. Samples from the NO3-red redox category are concentrated in the region between Red Deer and south of Calgary.

The resulting AHS redox categories and their percentage distributions are in very good agreement with the BWWT redox results. This agreement allows the prediction of methane occurrence where methane concentrations are not available (i.e. AHS dataset). Based on the systematic approach and redox class assignment, methane could occur in 31,465 groundwater samples classified (CH4-fm or Fe(III)-red). The integration of the 91% success metric of BWWT, that correctly predicted methane occurrence where methane concentrations >150,000 ppmv were observed, implies that ~48% of the groundwater samples in the AHS database are likely favorable for methane presence.

The integration of the 89% success metric of BWWT, that correctly predicted methane occurrence where methane concentrations >50,000 ppmv were observed, suggest that 42% of the groundwater samples in the AHS database are likely favorable for methane presence.

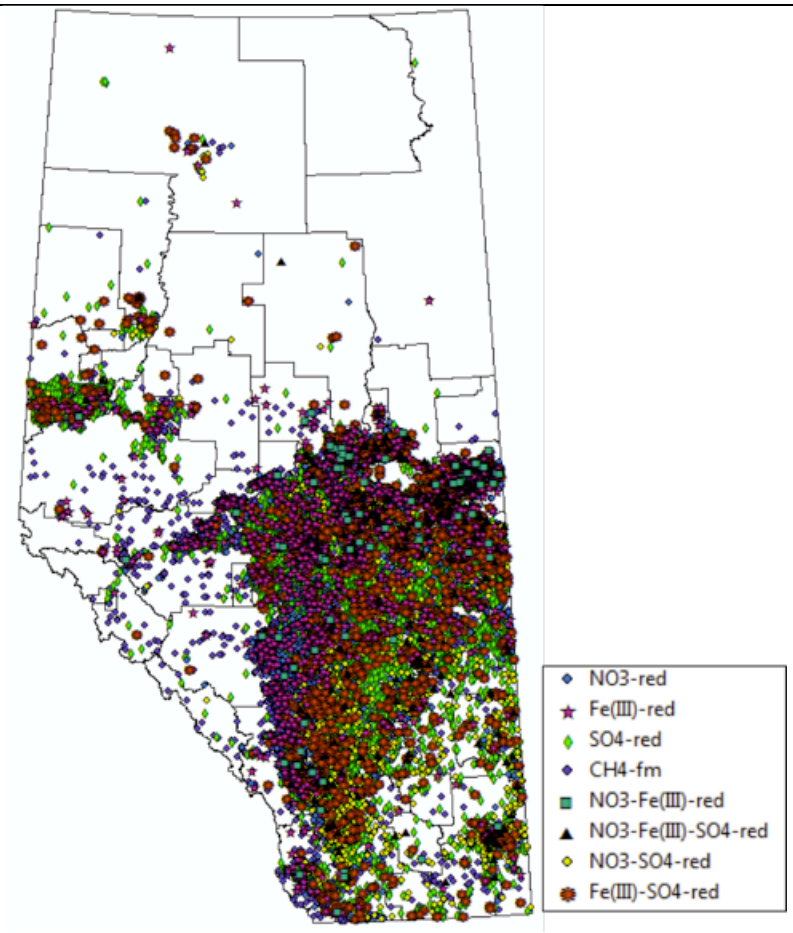

Figure 38: Map showing the spatial distribution of redox categories for AHS groundwater samples based on the parameters cut-off of case study B.

The distribution of redox categories versus the water well depths in Figs. 39 and 40 shows that methanic zones can be encountered at relatively shallow depths. To better understand these observations, additional parameters such as the geological formation in which these water wells are completed would need to be studied and integrated into the systematic approach to further constrain the prediction of methane.

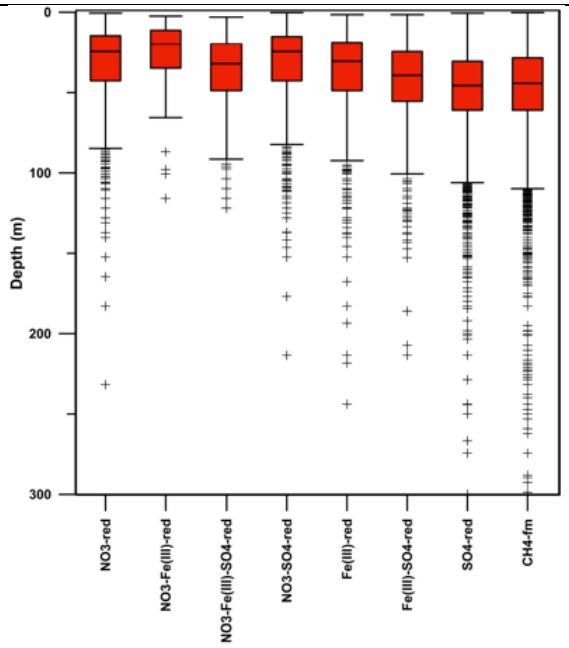

Figure 39: Relationship between redox class assignment and water wells depth for AHS dataset.

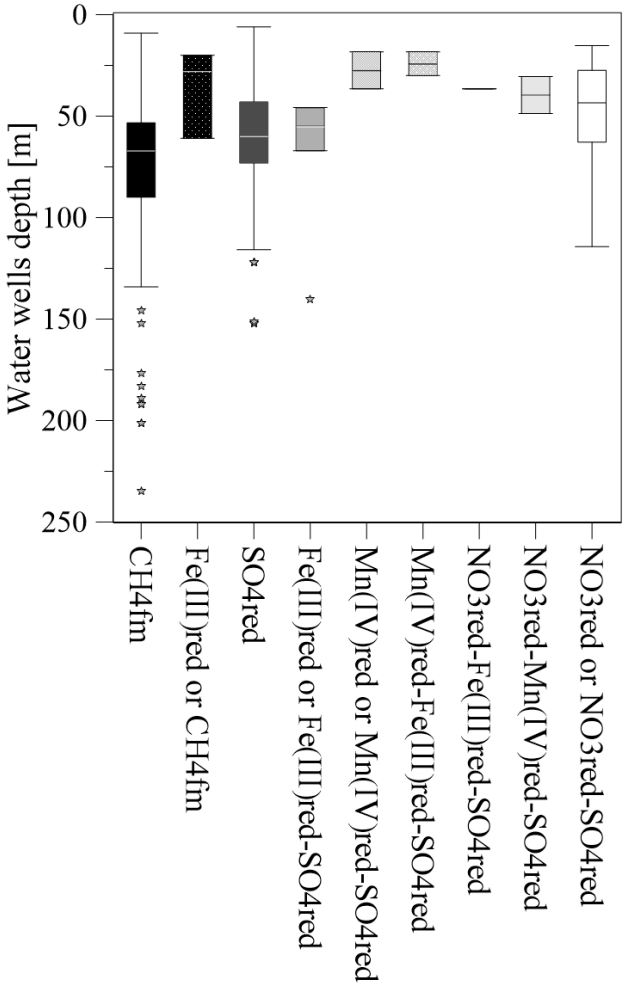

Figure 40: Relationship between redox class assignment and water wells depth for BWWT dataset

4.4.3 Lessons learnt from the large AHS dataset

Access to the large AHS data set provided more than 60,000 routine geochemical analyses of residential groundwater well samples collected between 2002 and 2014. The creation of such a large data set was possible due to the collection and sample submission processes being conducted by residents themselves. The substantial number of AHS sample analyses, integrated with BWWT and industrial datasets, allowed a thorough evaluation of the groundwater geochemistry across Alberta in terms of redox conditions, likelihood of methane presence, and water types.

Although the AHS data are effective scientific data points for demonstrating geochemical trends and for better understanding the status of Alberta's groundwater geochemistry, there are challenges that come with this type of public data. Resolution of the AHS groundwater well sample location was provided to the section (data points plot in the center of one mile by one mile sections) to comply with privacy regulation to ensure resident confidentiality. This can be a limitation when assigning geologic units to well samples in geologically heterogeneous areas where either the geologic unit changes physically (i.e. thickening, pinching out) or chemically (e.g. geochemical heterogeneity in the Paskapoo Fm.) over a short lateral distance. Another limitation was the lack of information on screen interval depths. For this reason, the producing groundwater depth was assumed to be the total well depth in the AHS data set. It is reasonable to assume that a well owner would not want their water well drilled deeper than necessary as costs increase with depth and the driller's time. Using the total depth method, the potential presence of multiple water-bearing units within one water well is not accounted for and thus, the water type assigned to a sample may actually represent mixed waters within its wellbore. When a water well is drilled, the driller may advance the drill bit past the permeable unit into the deeper unit acting as an aquitard to ensure that the entire thickness of the aquifer has been accessed. This means the total depth of the well would suggest completion in an aquitard, which presents a challenge when assigning geologic units based on total depth.

Groundwater wells installed solely for monitoring purposes, such as the GOWN wells, provide precise information on parameters such as screened interval and geologic material at certain depths and are reliable data sources especially in local scale studies. Part of this study was to evaluate the reliability of resident-collected groundwater samples as scientific data points. Validation of the AHS data set comprised of resident-collected groundwater well samples against the scientific monitoring wells within the GOWN and the consultant-collected samples contained in the BWWT data set significantly increases our confidence in the usefulness and application of resident-collected groundwater samples and introduces the potential for inclusion of vast amounts of additional data in similar future studies.

For the BWWT, industry data and AHS databases, milestone 4 has been achieved. Although some of these data sets lack gas data, it is possible to forecast whether or not in-situ methane gas generation may or may not be feasible in the respective aquifers thanks to the systematic approach of redox class assignments. Further steps to improve the systematic approach would be to optimize the TEAPs initial threshold in order to increase methane prediction accuracy. In some cases, the access of the geological models to attribute geological formations for water wells will permit to further constrain the systematic approach.

5 Milestone 5: The use the carbon isotope fingerprints of methane in concert with other indicator parameters to differentiate biogenic and thermogenic gas and cases of microbial oxidation of methane

The investigation of carbon isotope ratios of methane is limited to the BWWT database, since the industry and AHS data do not contain information about carbon isotope ratios of gases.

5.1 Isotope fingerprints of methane and higher alkane chains in groundwater samples

Box-Whisker plots summarizing the carbon isotope ratios of methane, ethane, propane, iso-butane and normal butane expressed in $\delta^{13}C$ values are summarized in Fig. 24b. Methane in free gas samples had median and mean $\delta^{13}C_{CH4}$ values of -67.3 and -64.4 ‰ (n = 518) respectively. The first (Q1) and third quartile (Q3) $\delta^{13}C$ values of methane are -71.1 and -62.9 ‰ (Fig. 24b). Normality test indicated that stable isotope data for methane were not normally distributed ($p<0.05$).

Ethane in free gas samples had median and mean $\delta^{13}C_{CH4}$ values of -49.1 and -49.8 ‰ (n= 395) (Fig. 24b). The first (Q1) and third quartile (Q3) $\delta^{13}C$ values of ethane are -53.3 and -46.1 ‰ (Fig. 16b). Normality test indicated that stable isotope data for ethane were not normally distributed ($p<0.05$).

Propane in free gas samples had median and mean $\delta^{13}C_{CH4}$ values of -32.1 and -34.3 ‰ (n= 20) (Fig. 24b). The first (Q1) and third quartile (Q3) $\delta^{13}C$ values of propane are -38.3 and -27.5 ‰ (Fig. 24b). Normality test indicated that stable isotope data for propane were normally distributed ($p= 0.419$).

Iso-butane in free gas samples had median and mean $\delta^{13}C_{CH4}$ values of -27.5 and -27.9 ‰ (n = 11) (Fig. 24b). The first (Q1) and third quartile (Q3) $\delta^{13}C$ values of iso-butane are -28.4 and -25.6 ‰ (Fig. 24b). Normality test indicated that stable isotope data for iso-butane were normally distributed ($p= 0.106$).

Normal butane in free gas samples had median and mean $\delta^{13}C_{CH4}$ values of -27.0 and -26.9 ‰ (n = 13) (Fig. 24b). The first (Q1) and third quartile (Q3) $\delta^{13}C$ values of normal butane are -28.7 and -25.3 ‰ (Fig. 24b). Normality test indicated that stable isotope data for normal butane were normally distributed ($p= 0.488$).

For the BWWT database, we found that the majority of the methane-containing samples were characterized by $\delta^{13}C$ values of methane < -55 ‰ (n=447; Fig. 41a) while low to negligible concentrations of higher alkane chain components such as ethane resulted in high gas dryness values (D>500) (Fig. 41b). This, together with water chemistry data indicating highly reducing conditions, is indicative of in-situ formation of biogenic methane in the sampled aquifers for the majority of the samples in the database. For a smaller number of samples (n=71), methane with elevated $\delta^{13}C$ values of > -55‰ was identified (Fig. 41a). Group 2a of these samples is characterized by low methane concentrations, which may be consistent with the occurrence of methane oxidation. Group 2b is characterized by high methane concentrations and elevated $\delta^{13}C$ values of methane indicating either the migration of thermogenic gas into shallow aquifers or oxidation of biogenic methane within shallow aquifers resulting in “pseudo-thermogenic” gas samples.

A plot of carbon isotope ratios of methane versus those of CO_2 (Fig. 41d) indicates that biogenic methane is produced via both acetate fermentation and CO_2 reduction pathways while some samples (green colors) showing clear signs of methane oxidation.

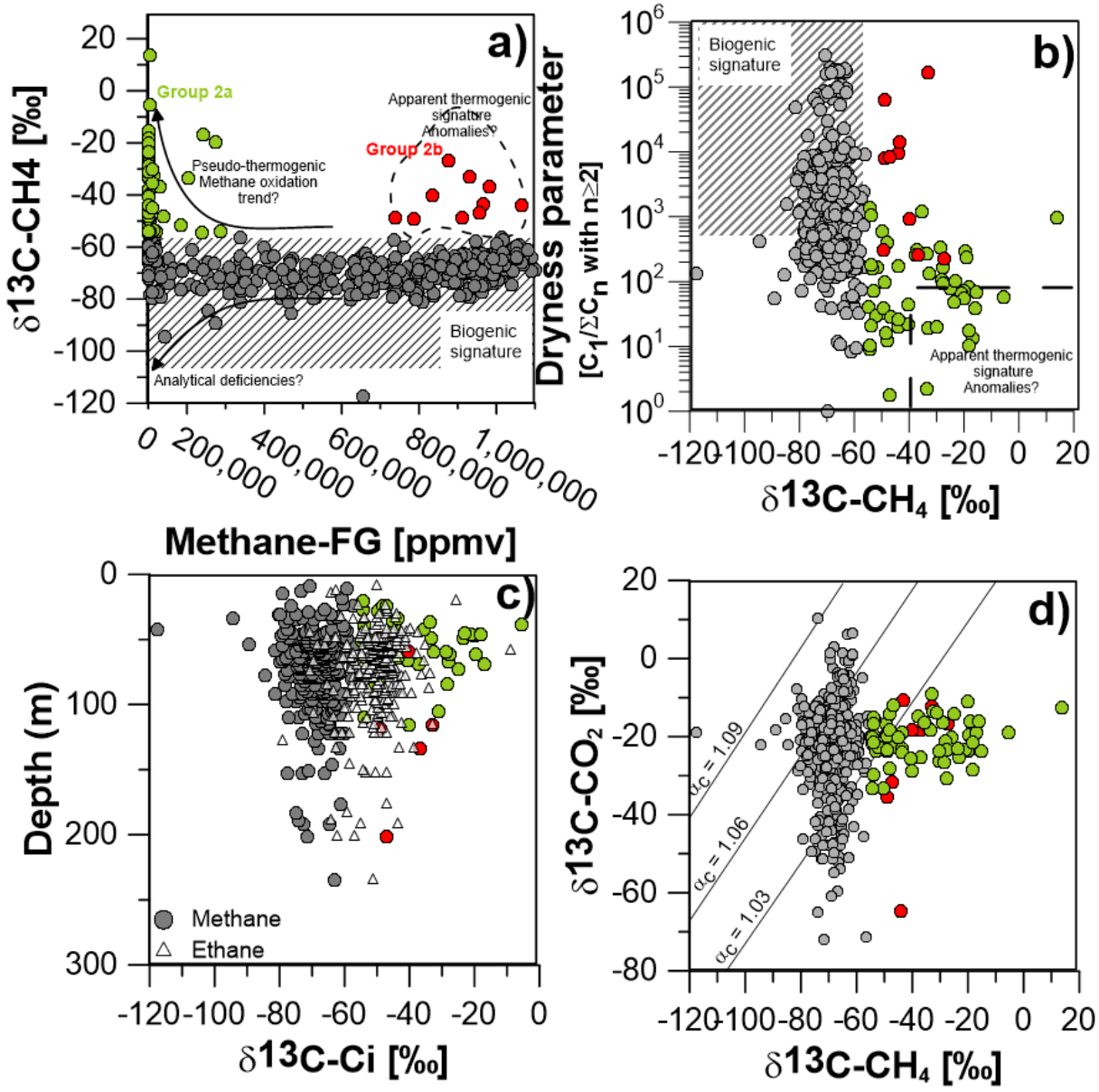

Figure 41: a) δ^{13}C-CH_4 values versus methane concentrations; b) dryness parameter versus δ^{13}C-CH_4 values; c) δ^{13}C-CH_4 values of methane and ethane versus depth; d) δ^{13}C-CH_4 versus δ^{13}C-CO_2 values to assess methane formation pathways.

5.2 Temporal variabilities of methane concentration and isotope composition

Temporal variabilities in methane concentrations were evaluated by comparing repeat analyses of free gas samples obtained from the same wells and results are shown in Fig. 42a. Most of these repeat analyses are from pre-test samples. Based on the QA/QC database, 32 wells contained n-replicate methane concentration samples ($2 \le n \le 3$) over a timeframe of 2005-2013. The coefficients of variation (CV) were calculated and varied from 0.3 % to 129 % with four wells having a CV exceeding 50%. For δ^{13}C values of methane, 21 wells yielded replicate samples (Fig. 42b). The difference between replicated δ^{13}C values is expressed as $\Delta\delta^{13}C_{CH4}$. The $\Delta\delta^{13}C_{CH4}$ varied from $4‰ < \Delta\delta^{13}C_{CH4} < 32‰$.

Three out of 4 wells having repeat groundwater methane concentrations with CV> 50% also yielded carbon isotope data for methane. The difference in C isotope compositions ($\Delta\delta^{13}C_{CH4}$) was large and varied from 11 to 32 ‰ (#11 #12 and #16, Fig. 42) while the highest methane concentration reported was 14,000 ppmv. For sample #16, the $\delta^{13}C_{CH4}$ values increased from -31 ‰ in 2007 to -16 ‰ in 2013, while the methane concentration decreased over time. This trend is due to methane oxidation. In two other cases (#11 and #12), the $\delta^{13}C_{CH4}$ values also increased (#11 from -89 ‰ in 2007 to -56 ‰ in 2011; and #12 from -77 ‰ in 2007 to -66 ‰ in 2009) while the methane concentration increased over time. This case may indicate another source of gas being contributed to the gas mixture.

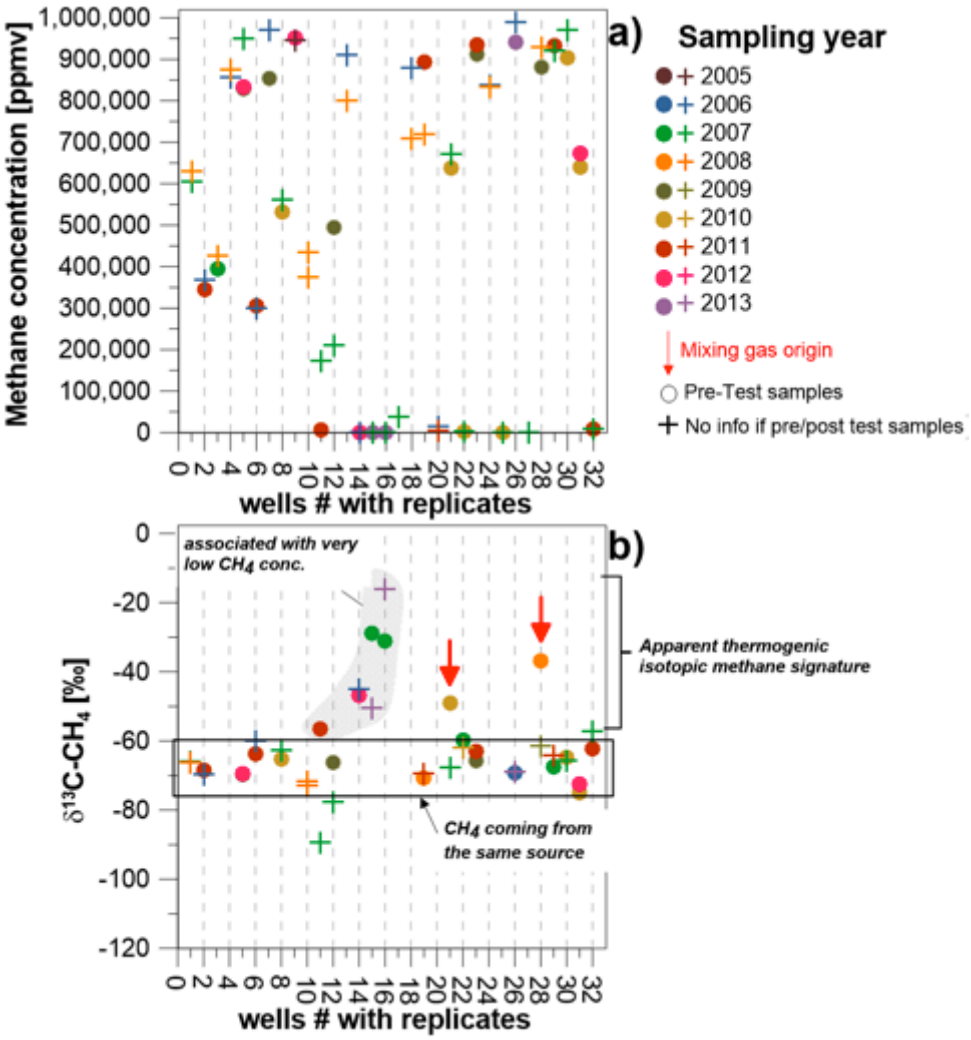

Figure 42: Replicate samples for a) methane concentrations and b) C isotope ratios of methane in free gas for groundwater sampled from wells between 2005 and 2013.

For all the other wells showing groundwater with CV< 50 % in repeat methane concentration analyses, 18 wells have also replicates for the isotopic composition of methane. For 15 of 18 wells, the variation in the repeat $\delta^{13}C$ values for methane is lower than 4 ‰ (Fig 42b). This small isotopic variation indicates that the methane is originating from the same source. For 3 (#15 #21 #28) of 18 wells, the difference in the repeat $\delta^{13}C$ values of methane ($\Delta\delta^{13}C_{CH4}$) varied significantly from 18 to 25 ‰. One of these 3 wells (#15), yielded groundwater with very low concentrations of methane (<200 ppmv) potentially causing elevated isotopic analytical uncertainties ($\delta^{13}C_{CH4}$>-55 ‰). The two other wells (#21 #28) yielded groundwater with elevated concentrations of methane (#21 with CH_4 > 600,000 ppmv and #28 with CH_4 > 850,000 ppmv) making an

analytical cause unlikely. The large isotopic variation for groundwater from these two wells could potentially indicate a mixing of gas of different origins. These occurrences are highlighted by a red arrow in Fig. 42b.

The temporal variability of methane concentrations at some wells may be in part explained by variable sampling conditions (extent of water level drawdown, pumping rate) (Humez et al., 2016) and both natural and anthropogenic causes may explain gas composition variabilities. While methane concentrations are highly variable, gas carbon isotope ratios ($\delta^{13}C$) of methane yielded comparatively constant data suggesting that the origin of methane was derived from the same source in most cases or indicating a mixture of gas sources in others.

To further investigate the thermogenic versus biogenic origin of methane it is crucial to evaluate the aqueous geochemical composition in concert with gas data since this has the potential to reveal the occurrence of gas formation in-situ, gas migration from below, or methane oxidation in the sampled shallow aquifers.

5.3 Aqueous geochemical data

5.3.1 Characterization of water types

The graphical representation of the chemistry of a water samples in a Piper plot shown in Fig. 43 reveals that water types were found to be somewhat variable. Figure 43 represents 762 water samples containing methane and passing all QA/QC tests. It is noteworthy that elevated concentrations of methane (> 280,000 ppmv) in groundwater were found predominantly in Na-type waters e.g. Na-Cl, Na-HCO_3 and Na-HCO_3-Cl types. This observation is consistent with findings by Humez et al. (2016) for samples from dedicated monitoring wells for the province of Alberta.

Figure 44 displays water types versus well depths for this group of samples. The deepest well depths are again associated with groundwater belonging to Na-HCO_3 and other Na-containing water types.

5.3.2 Covariance methane with high Cl content

It is interesting to observe in Fig. 43 that the water samples containing the highest methane concentrations are typically associated with Na HCO_3 and Na-HCO_3-Cl water types.

Thirty-four groundwater samples revealed Cl concentrations higher than 10 mM and the associated methane concentrations are very high with a median value of 918,000 ppmv and minimum/maximum values of 430,000/990,000 ppmv respectively. The $\delta^{13}C_{CH4}$ values vary between -72.6 and -57.4 ‰ (n=27). The water well depth for these samples ranges between 42 and 176 m. Only one sample had an elevated $\delta^{13}C_{CH4}$ value of -36.6 ‰ associated with a Cl concentration of 12.8 mM, a CH_4 concentration of 882,000 ppmv, and a well depth of 134 m.

Sixty-three samples revealed Cl concentrations between 5 and 10 mM and the associated methane concentrations have a median value of 842,500 ppmv and minimum/maximum values of 266,000/971,100 ppmv respectively. The water well depth is on average 68 m. The $\delta^{13}C_{CH4}$ values for these samples vary between -117.6 and -57.8 ‰ (n=53). Two samples with $\delta^{13}C_{CH4}$ values of -48.9 ‰ and -43.4 ‰ were associated with Cl concentrations of 8.7 and 5.2 mM, CH_4 concentrations of 811,800 and 867,000 ppmv, and a depth of 118 m.

It appears that the highest methane concentrations are linked to Na-containing water types either because of mixing with saline water and/or as a result of cation exchange. In contrast, for the lowest methane concentrations, the water samples tend to associate with a Na-SO_4 water type. It is thus possible to identify two end-member types (i) Na-HCO_3-Cl water type associated with the highest methane concentrations and the deepest wells; (ii) Na-SO_4 water type associated with lowest methane concentrations in agreement with the redox ladder concept.

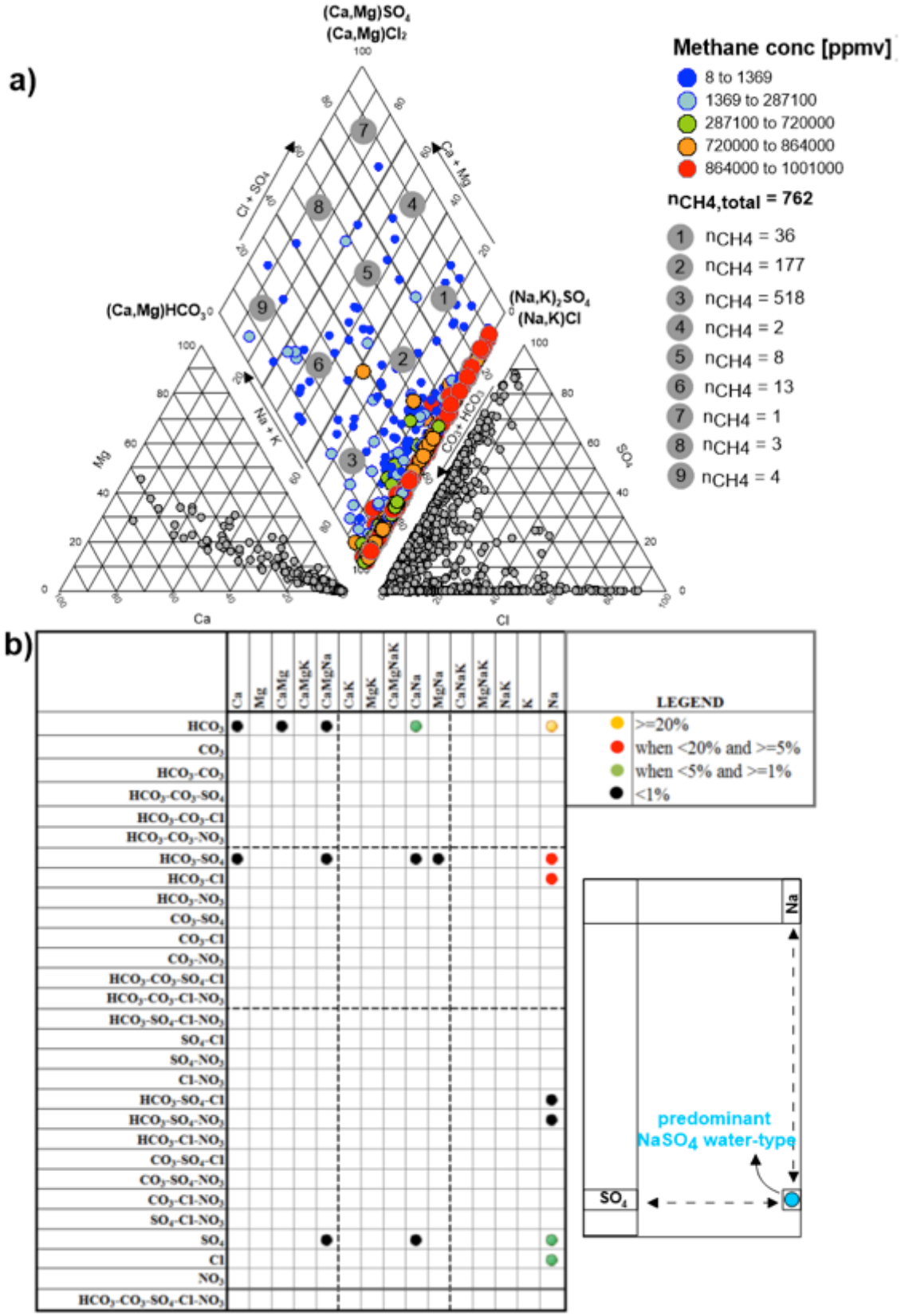

Figure 43: a) Piper plot and b) PHO matrix assigning the different predominant water types combinations. The PHO matrix shows the size (percentage of samples) of the BWWT subset belonging to each water-type.

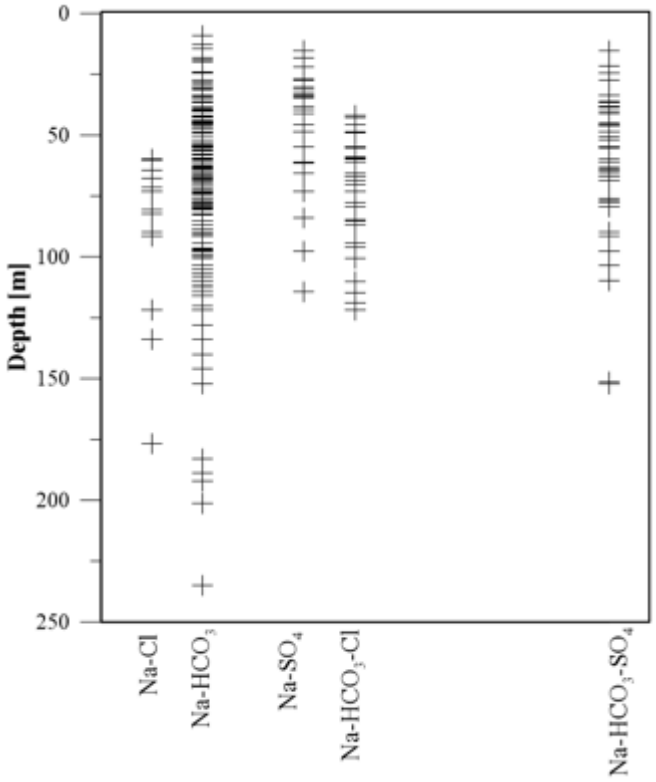

Figure 44: Water well depth versus water types occurrences (n_{total} = 563), only the water type with >20 samples associated with depth information were represented.

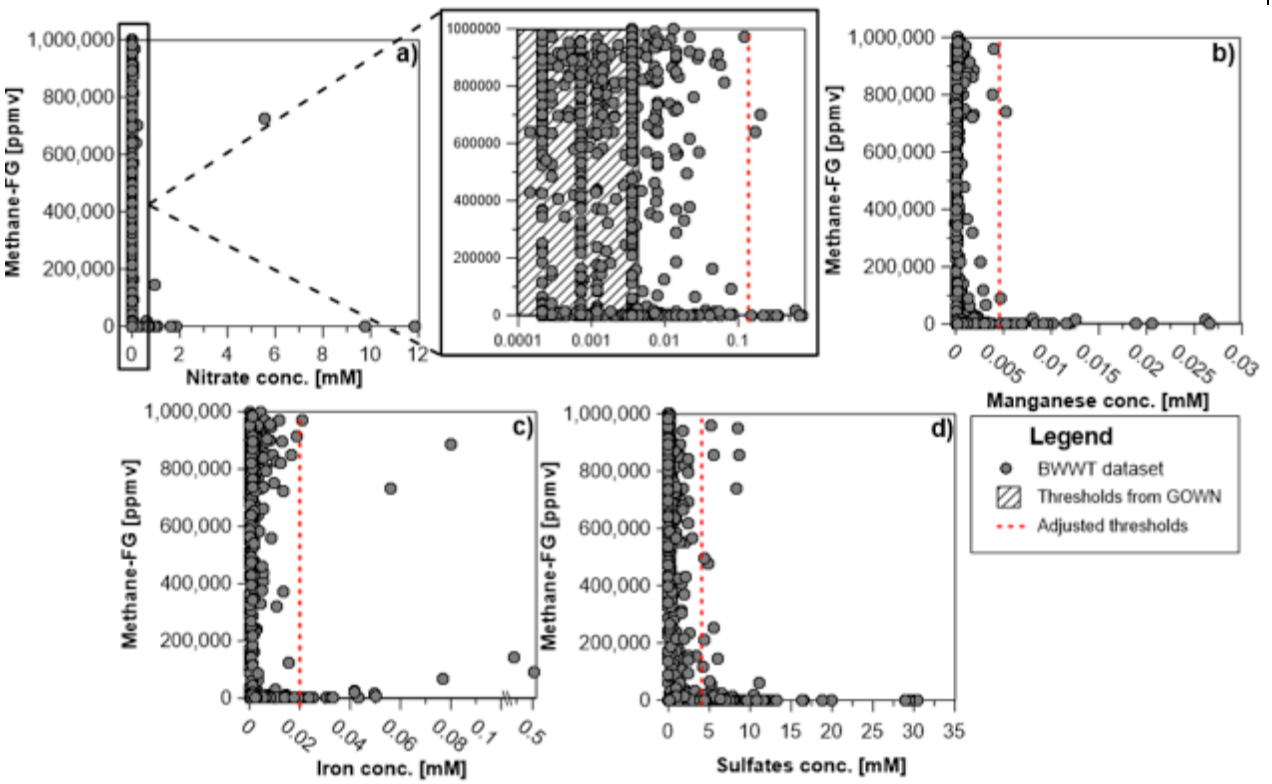

Figure 45: Diagrams showing binary relationship between a) methane/nitrate b) methane/manganese c) methane/iron and d) methane/sulfate concentration in BWWT water samples and identification methane/redox sensitive species thresholds.

5.3.3 Anti-covariance of methane with TEAPs

The redox control on methane in groundwater is further demonstrated in Figs. 45 and 46 showing cross plots of redox sensitive species according to the redox ladder sequence associated with the defined redox ladder thresholds. It is important to note that the highest methane concentrations are associated with the lowest nitrate/manganese, manganese/iron, iron/sulfate concentrations. The distribution of the redox sensitive species versus depth is reported in Fig. 46d and shows the highest methane concentrations for the deepest water wells.

The plots of Figs. 45 and 46 reveal that methane formation does usually not commence while TEAPs are present in non-negligible concentrations. In some cases, methane may have migrated into the groundwater systems containing O_2, NO_3, Mn, Fe and SO_4 thereby creating more reducing conditions. These observations are consistent with the redox ladder concept. Based on samples from dedicated monitoring wells from the GOWN network, Humez et al. (2016) showed that groundwater containing negligible concentrations of nitrate (< 0.006 mM) and moderate to low concentrations of sulfate (<1 mM) contained the vast majority of samples with the highest methane concentrations consistent with favorable redox conditions for in-situ methanogenesis. The threshold concentrations between sulfate/methane and nitrate/methane found in this study are higher than the ones found in the GOWN network. One likely explanation for this is the longer completion screen intervals for these water wells creating mixing effects.

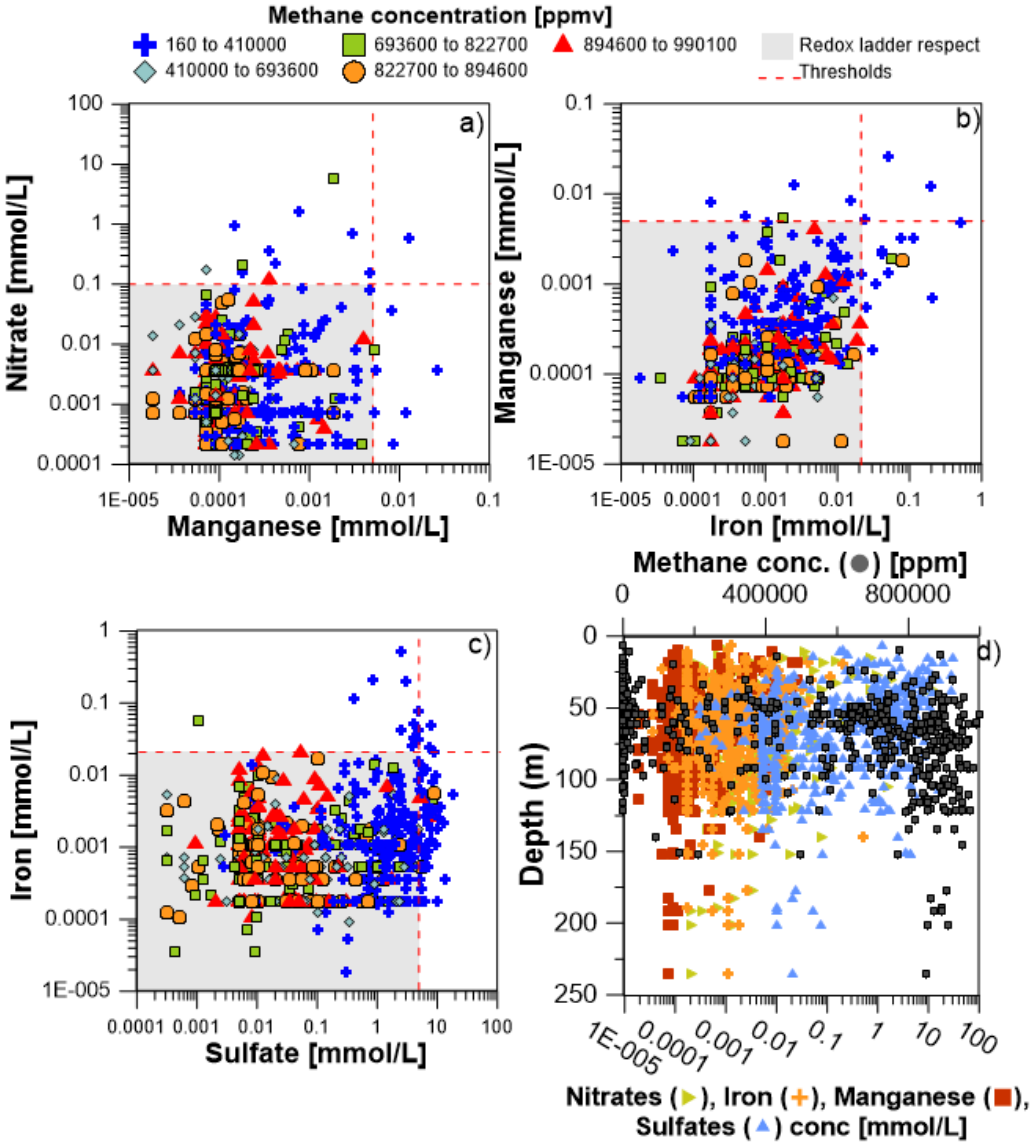

Figure 46: Redox couples plots from the redox ladder concept and depth profile

5.4Evidence for biogenic or thermogenic gases

Combining gas and aqueous geochemistry data provides a stronger indication regarding methane formation, gas migration and fate of methane in shallow aquifers. Combining gas geochemistry of methane, higher alkane component concentrations, dryness parameters, carbon isotopic compositions of methane, and aqueous geochemistry with focus on redox sensitive species, it is possible to assess the methane origin in shallow aquifers following the methodology developed by Humez et al. (2016) (Fig. 47). An assessment for BWWT samples using this approach is provided below.

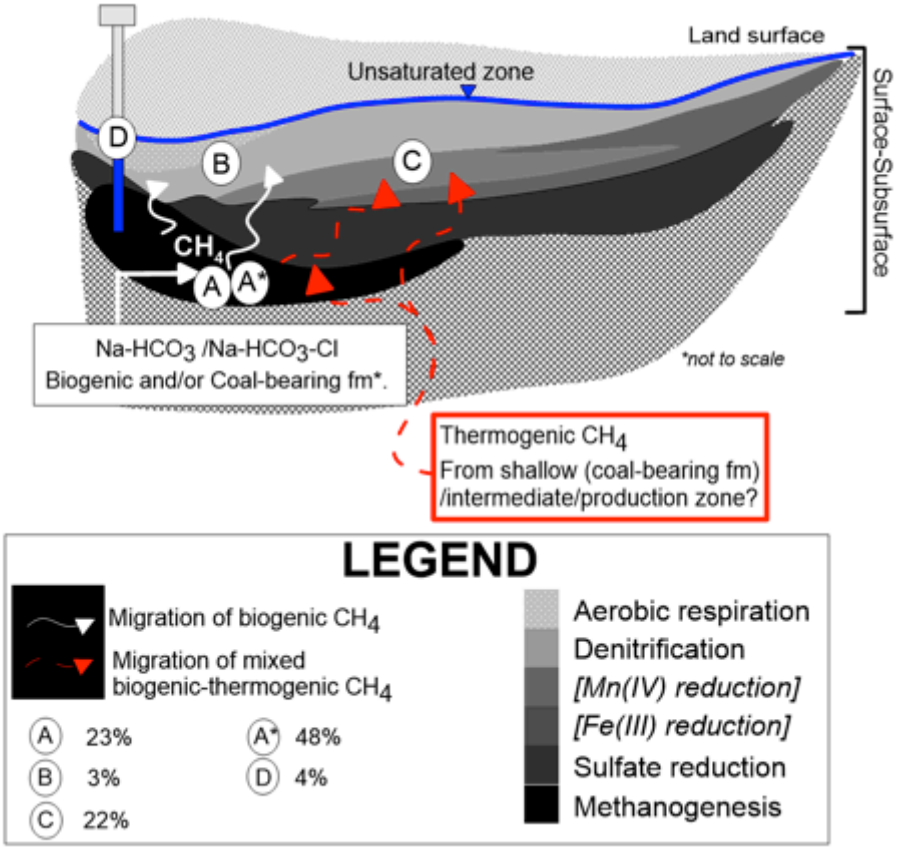

Figure 47: General concept extracted from Humez et al. (2016) on the different types of methane found in groundwater from a study in Alberta using dedicated monitoring wells applied to the BWWT dataset.

a) CH_4-type A: Biogenic methanogenic environment (23%)

For the BWWT database, 55 samples with $\delta^{13}C_{CH4}$ < -55 ‰ and a high dryness parameter > 1000 indicate the formation of biogenic methane. Aqueous geochemistry data were consistent with methanogenic conditions (negligible nitrate, iron, manganese, sulfate concentrations) and no traces of propane were detected. Elevated methane and ethane where found usually with elevated Na concentrations. This category of samples contains 55 of 241 samples (23%) and yields clear evidence that biogenic methane was generated in-situ under methanogenic aquifer conditions. An alternate explanation that also needs to be considered is potential migration of methane into the aquifer that may have triggered removal of TEAPs via redox buffering reactions. These samples are classified as CH_4 type A. The remaining 186 samples that did not fall into CH_4 type A show at least one of the following characteristics:

- Presence of trace of propane (n= 59);
- Dryness parameter <1000 (n=156);
- Elevated methane concentrations (>100,000 ppmv) while concentrations of nitrate (> 0.1 mM) (n=3), iron (> 0.02 mM) (n=2), manganese (>0.005 mM) (n=0), sulfates (> 4 mM) are not negligible (n=11);
- A carbon isotope ratio that may suggest thermogenic methane ($\delta^{13}C_{CH4}$>-55 ‰) (n=16).

b) CH_4-type A*: In-situ biogenic methane (48%)

A total of 115 samples have $\delta^{13}C_{CH4}$ < -55 ‰ and a dryness parameter <1000. Despite a high methane concentration with a median of 746,000 ppmv, the low dryness parameter indicates higher ethane concentrations. Aqueous geochemistry data were consistent with methanogenic conditions (negligible nitrate, iron, manganese, sulfate concentrations) and no traces of propane were detected. The high methane and ethane concentrations could come from a CBM formation with predominantly biogenic methane but also some thermogenic gas component. To test the biogenic or thermogenic origin of ethane requires further investigations. This category of samples contains 115 of 241 samples (48%) and yields evidence that predominantly biogenic methane was generated in-situ under methanogenic aquifer conditions. An alternate explanation that also needs to be considered is potential migration of methane into aquifer that may have triggered removal of TEAPs via redox buffering reactions for the 10 samples with methane concentrations <100,000 ppmv. These samples are classified as CH_4 type A*.

c) CH_4-type B: migration of methane into more oxidizing conditions (3%)

A total of 7 samples have $\delta^{13}C_{CH4}$ < -55 ‰ with a wide range of dryness values from <1000 (n=5) to >1000 (n=2). The methane concentrations vary from 142,400 to 970,000 ppmv and ethane concentrations from 35 to 4820 ppmv and no traces of propane were reported. The high methane concentrations were detected in groundwater either with non-negligible nitrate concentrations (> 0.1 mM), iron concentrations (> 0.02 mM), manganese concentrations (>0.005 mM) or sulfate concentrations (> 4 mM). These conditions are not consistent with favorable in-situ conditions of methanogenesis. Therefore it is postulated that biogenic methane had migrated from more reducing sections of the aquifers into more oxidizing conditions but has not yet been fully oxidized.

d) CH_4-type C: Mixed thermogenic-biogenic gas origin (22%)

A total of 48 samples have $\delta^{13}C_{CH4}$ < -55 ‰ associated with dryness parameters varying from 1 to >20,000. Methane and ethane concentrations vary widely from <100,000 to > 900,000 ppmv and 40 to 3870 ppmv respectively and all samples contain traces of propane indicating a mixed gas origin. Additional information on the stratigraphic unit and lithology would be desirable to assess if these samples were collected from wells completed in CBM formations where the presence of higher alkane chain components has been demonstrated such as in the Horseshoe Canyon formation (Cheung et al., 2009; Humez et al., 2016). These samples are currently classified as mixed gas origin.

Four samples have $\delta^{13}C_{CH4}$ > -55 ‰ and a low dryness parameter <1000. These samples are associated with high methane concentrations, elevated ethane concentrations and no traces of propane. Aqueous geochemistry data were consistent with redox ladder concept conditions (low nitrate, iron, manganese, sulfate concentrations). In addition, three samples have $\delta^{13}C_{CH4}$ > -55 ‰ and a high dryness parameter >1000. These samples show relatively high methane concentration >800,000 ppmv, presence of ethane in low concentration (<100 ppmv) and traces of propane (<180 ppmv) explaining the high dryness (i.e. ratio) parameter. Aqueous geochemistry data were consistent with redox methanogenic conditions (nitrate, iron, manganese, sulfate concentrations). These seven samples yielded free gas with low $\delta^{13}C_{CO2}$ values (-31.7‰ to -10.8‰) and high $\delta^{13}C_{CH4}$ > -55 ‰ values and plot into the methane oxidation field (Whiticar, 1999). However, considering the high methane concentration and elevated ethane content the hypothesis of methane oxidation seems not consistent and these samples are currently classified as mixed gas origin.

e) CH_4-type D: Apparent or pseudo-thermogenic methane in shallow aquifers (4 %)

A total of 9 samples have $\delta^{13}C_{CH4}$ > -55 ‰ with a low dryness parameter <1000 (n=6). The methane and ethane concentrations are low <175,000 ppmv and <600 ppmv and these samples show traces of propane explaining the low dryness parameters. Aqueous geochemistry data were consistent with methanogenic redox conditions (negligible nitrate, iron, manganese, sulfate concentrations). The carbon isotopic fingerprint of methane as well as the presence of propane would suggest a mixed thermogenic and biogenic gas. However, the $\delta^{13}C_{CH4}$ (> -55‰) versus $\delta^{13}C_{CO2}$ values (-29.8 to -13.5 ‰) of these 9 samples plot in the methane oxidation field and may indicate a false pseudo-thermogenic signature of the samples.

Some concentration data for ethane and higher alkanes in the BWWT database appear somewhat suspect, and if confirmed, would result in too low dryness ratio data, affecting the interpretation provided above.

Milestone 5 has been achieved using results from the BWWT database.

6 Milestone 6: Data housing and display

It is important that the results of this study will be made accessible to the stakeholder community. We suggest to achieve this initially by distribution of this detailed report to the industrial stakeholders thereby delivering on milestone 6. In addition, we are ready to make the results available to PTAC for data housing and display potentially facilitated and coordinated by Troy Jones at CAPP. We are prepared to make all data available and will follow his recommendations for database design so that the results can be effectively archived and displayed by CAPP making the study findings permanently accessible through GIS based tools.

7 Milestone 7: Scientific assessment of baseline aqueous and gas geochemistry data for Alberta groundwater in areas of past, current and future energy resource development and communication of results

The key deliverable of this project is the highly scientific assessment of baseline aqueous and gas geochemistry data for Alberta groundwater in areas of past, current and future energy resource development that is summarized in this report. This scientific evaluation is complemented by a simplified summary scheme for water quality data that may be understandable to non-experts and the public at large. Figure 48 is an example of a simplified summary of the redox ladder concept that could provide a guideline for well owners to interpret their water quality data with the occurrence of methane in mind. A further simplification could be a basic traffic light protocol that subdivides groundwater samples from methanogenic aquifers with high potential for occurrence of elevated concentrations of methane (red light) from groundwater samples obtained from aquifers with less reducing redox states and a low risk of methane occurrence (green light). The orange traffic light would represent aquifer conditions with bacterial sulfate reduction representing groundwater samples where occurrence of methane predominantly with concentrations < 150,000 ppmv in the free gas phase is feasible. After received feedback on the final report, we remain available for developing a communication plan for interested stakeholders in close consultation with the funding agency. In addition, we are in the process of developing manuscripts for publishing selected results in the peer-reviewed scientific literature after consultation and approval by the funding organization, thereby delivering on milestone 7.

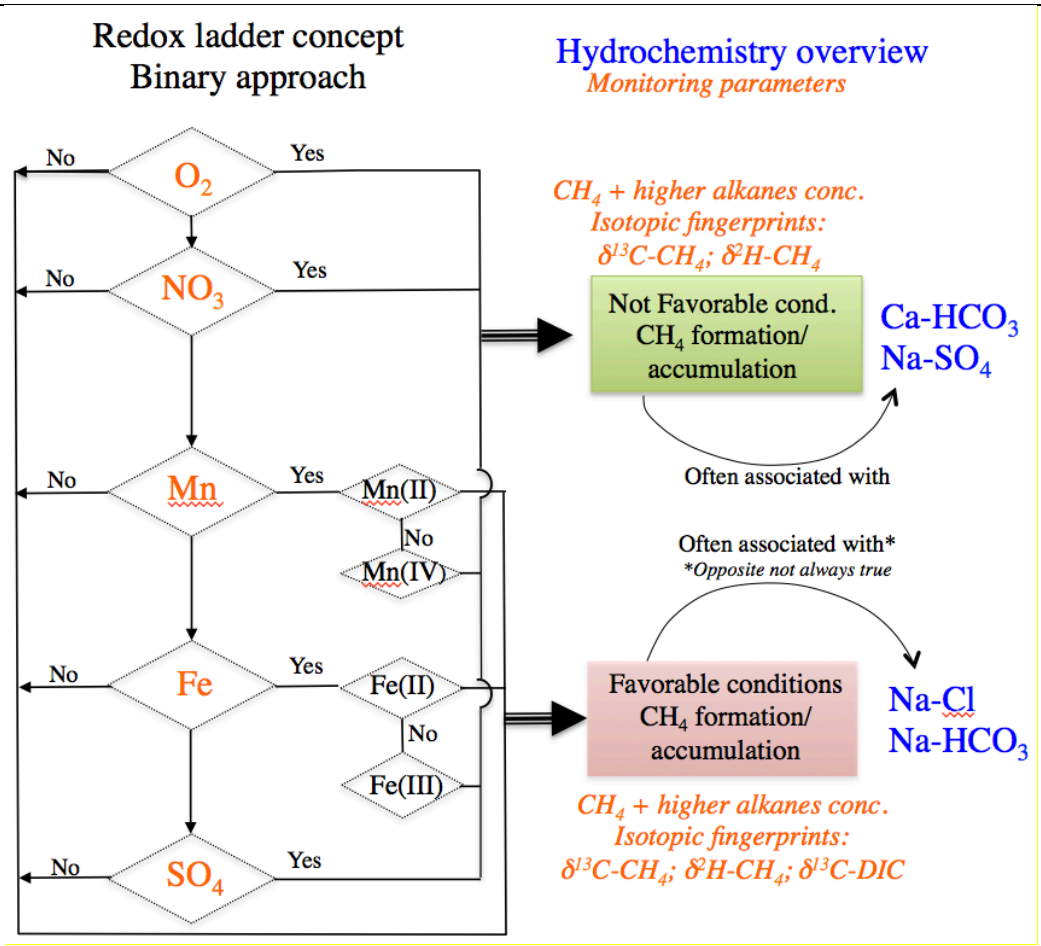

Figure 48: Example of a simplified summary of the redox ladder concept that could provide a guideline for well owners to interpret their water quality data with the occurrence of methane in mind.